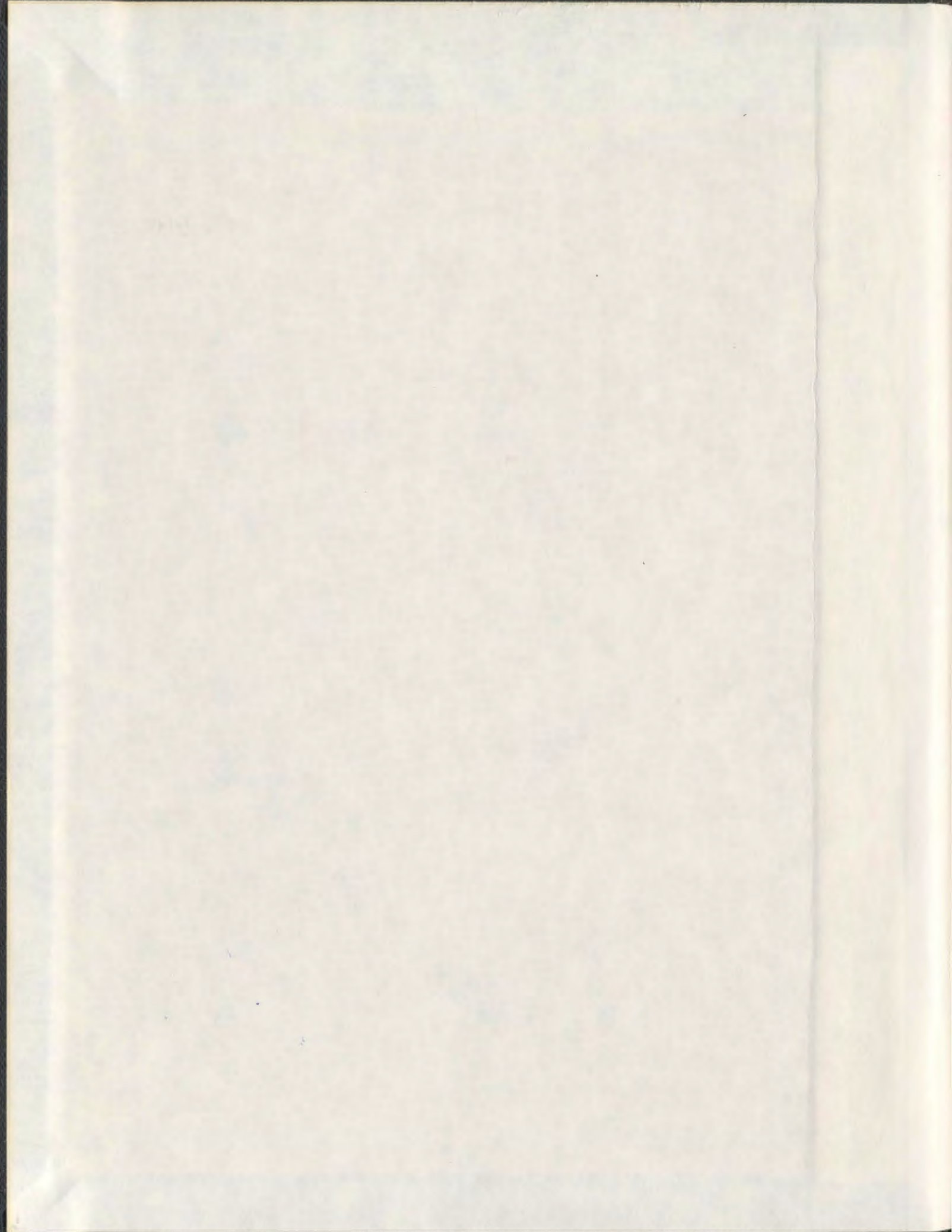


SURFACTANT-MEDIATED MATRIX-ASSISTED LASER  
DESORPTION/IONIZATION TIME-OF-FLIGHT MASS  
SPECTROMETRY IN THE ANALYSIS OF SMALL  
BIOLOGICAL MOLECULES

DAVID CHARLES GRANT



001311



**Surfactant-Mediated Matrix-Assisted Laser Desorption/Ionization  
Time-of-Flight Mass Spectrometry in the Analysis of Small Biological Molecules**

David Charles Grant, B.Sc. (Honours)

A thesis submitted to the School of Graduate Studies  
in partial fulfillment of the requirements  
for the degree of Doctor of Philosophy

Department of Chemistry  
Memorial University of Newfoundland  
March, 2010

St. John's

Newfoundland

## ABSTRACT

As an analytical method, matrix-assisted laser desorption/ionization (MALDI) has been used primarily for the analysis of large biomolecules. However, its applications to small molecules have been limited. To try to circumvent this limitation, a variety of surfactants have been tested as matrix ion suppressors for the analysis of small molecules by matrix-assisted laser desorption/ionization time-of flight mass spectrometry (MALDI-TOF-MS). Their addition to the common matrix  $\alpha$ -cyano-4-hydroxycinnamic acid (CHCA) greatly reduces the presence of matrix-related ions when added at the appropriate mole ratio of CHCA/surfactant while still allowing the analyte signals to be observed. A range of cationic quaternary ammonium surfactants as well as a neutral and an anionic surfactant were tested for the analysis of phenolics, phenolic acids, peptides and caffeine. It was found that cationic surfactants, particularly cetyltrimethylammonium bromide (CTAB), were suitable for the analysis of acidic analytes. The anionic surfactant, sodium dodecylsulfate, showed promise for peptide analysis. The matrix:surfactant mole ratio was a critical parameter for suitable matrix ion suppression while allowing for an acceptable intensity of analyte signal. Of notable significance when using surfactants is that the resulting mass resolution of most analytes was improved by 25-75 %. No other study has observed this.

Additional experiments were conducted to examine the homogeneity of the matrix:surfactant:analyte dried spots or order to explain the surfactant suppression phenomenon. Depth profiling of sample spots, by varying the number of laser shots, revealed that the surfactants tend to migrate toward the top of the droplet during dried

droplet crystallization. It is likely that the analyte is also enriched in this surface region. This would lead to higher analyte/surfactant concentrations and reduced matrix-matrix interactions (known to be a major source of matrix-derived ions).

Surfactant-mediated MALDI-TOF-MS has been successfully used for the identification and quantitation of flavonoids from three berry extracts: lowbush blueberry (*Vaccinium angustifolium*), lingonberry (*Vaccinium vitis-idaea*), and blackberry (*Rubus armeniacus*). The use of the matrix CHCA led to extensive fragmentation of the sugar moiety of the glycosides, whereas 2,4,6-trihydroxyacetophenone (THAP) allowed for the intact glycoside molecule to be observed. The flavonoids were also analyzed by LC-UV-ESI-MS for comparison. The intact flavonoids could be quantified with RSD values of less than 10% and are comparable to LC. However, the use of MALDI greatly reduces the analysis time compared to traditional LC-MS methods.

In a second application, surfactant-mediated matrix-assisted laser desorption/ionization time-of-flight mass spectrometry (MALDI-TOF-MS) was successfully used in the analysis of caffeine and the vitamins riboflavin, nicotinamide and pyridoxine found in energy drinks. Of five common MALDI matrices tested, CHCA was found to be most suitable for the analysis of high sugar-containing energy drinks. Cetyltrimethylammonium bromide (CTAB) surfactant was suitable as a matrix-ion suppressor at a matrix:surfactant mole ratio of approximately 500:1. For comparative purposes, LC-ESI-MS with UV detection was used. The calibration curves showed substantial improvement when the surfactant-mediated method was used compared to traditional MALDI, where correlation coefficients of 0.989 (nicotinamide), 0.991 (pyridoxine), 0.983 (caffeine) and 0.987 (riboflavin) were attained. Reproducibility

experiments gave RSD values ranging from 9.7 to 18.1% and quantitative results were comparable to LC-MS.

## **DEDICATION**

This thesis is dedicated to my daughter Hannah. I hope and pray that my years spent away from you writing this thesis will now bring benefits for us.

## ACKNOWLEDGEMENTS

First of all I would like to thank my family for their understanding and moral support during the years it took to complete this research and write the thesis/manuscripts.

I would like to acknowledge the Chemistry Department, and in particular, my supervisory committee members, Dr. Christina Bottaro and Dr. Erika Merschrod.

Ms. Linda Windsor, from the Center for Chemical Analysis and Research Training (C-CART) is acknowledged for my initial training on MALDI and LC-MS instruments as well as her advice over the years. As well, Mr. Glenn Piercey from the Micro Analysis Facility Inco Innovation Center is thanked for his help in running the SIMS.

I would like to thank all past and present members of the Analytical Chemistry Group for their friendship and help over the past years, particularly, Dr. Samuel Mugo, Dr. Geert Van Biesen, and Ms. Sandra Estevez.

Finally, I would like to thank my supervisor, Dr. Robert (Bob) Helleur for his great encouragement, support, and mentoring over the past five years.

## TABLE OF CONTENTS

Title.....	i
Abstract.....	ii
Dedication.....	v
Acknowledgements.....	vi
Table of Contents.....	vi
List of Figures.....	xi
List of Tables.....	xiii
List of Abbreviations.....	xviii
<b>Chapter 1 – Introduction and Overview.....</b>	<b>1</b>
1.1 Introduction.....	2
1.1.1 A Brief History of MALDI.....	2
1.1.2 Instrumental Components of MALDI.....	5
1.1.3 Matrix Selection.....	10
1.1.4 MALDI Experimental Sample Preparation.....	13
1.2 Analysis of small molecules by MALDI-TOF-MS.....	18
1.2.1 Overview.....	18
1.2.2 Small Molecule Classes.....	19
1.2.3 Inherent difficulties.....	21
1.2.4 Solutions to Small Molecule Analysis.....	22
1.3 Ion Suppression in MALDI.....	25

1.3.1 Overview of Ion Suppression.....	25
1.3.2 Matrix Suppression Effect: Optimum Matrix/Analyte ratio .....	27
1.3.3 Analyte Suppression Effect: Excessive Matrix/Analyte ratio.....	31
1.3.4 Surfactant-Mediated Matrix Suppression.....	31
1.4 Surfactants.....	36
1.4.1 Overview of Surfactants.....	36
1.4.2 Surfactant Properties and Applications.....	37
1.5 Thesis objectives.....	39
1.6 Co-authorship statement.....	39
1.7 References.....	41

**Chapter 2 – Surfactant Mediated Matrix-Assisted Laser Desorption/Ionization**

<b>Time-of-Flight of Small Molecules.....</b>	<b>46</b>
Abstract.....	47
2.1 Introduction.....	48
2.2 Experimental.....	50
2.2.1 Chemicals.....	50
2.2.2 Sample Preparation.....	51
2.2.3 Instrumentation.....	54
2.3 Results and Discussion.....	54
2.3.1 Influence of Various Surfactants.....	54
2.3.2 Effect of Concentration of Surfactant.....	66
2.3.3 Heterogeneity of Surfactant-Containing Sample Spots.....	68

2.4 Conclusions.....	76
2.5 References.....	77

**Chapter 3 – Rapid Screening of Anthocyanins in Berry Samples by Surfactant-Mediated Matrix-Assisted Laser Desorption/Ionization Time-of-Flight Mass**

<b>Spectrometry.....</b>	<b>79</b>
3.1 Introduction.....	80
3.2 Experimental.....	82
3.2.1 Chemicals.....	82
3.2.2 Sample Preparation.....	83
3.2.3 MALDI-TOF-MS Instrumentation.....	83
3.2.4 LC-UV-ESI-MS.....	84
3.2.5 Extraction Method.....	85
3.3 Results and Discussion.....	86
3.3.1 Identification and Quantification of Flavonoids by LC-UV-ESI-MS.....	86
3.3.2 MALDI-MS versus Surfactant-Mediated MALDI-MS of Flavonoid Standards.....	90
3.3.3 Analysis of Berry Extracts by MALDI-MS and Surfactant-Mediated MALDI-MS.....	93
3.3.4 Quantification by Surfactant-Mediated MALDI-TOF-MS.....	98
3.4 Conclusions.....	102
3.5 References.....	103
3.6 Addendum.....	105

<b>Chapter 4 – Simultaneous Analysis of Vitamins and Caffeine in Energy Drinks by Surfactant-Mediated Matrix-Assisted Laser Desorption/Ionization Time-of-Flight Mass Spectrometry</b> .....	119
4.1 Introduction.....	120
4.2 Experimental.....	122
4.2.1 Chemicals.....	122
4.2.2 Standard Preparation.....	123
4.2.3 Energy Drink Preparation.....	124
4.2.4 MALDI Preparation.....	124
4.2.5 MALDI-TOF Analyses .....	125
4.2.6 LC Analyses.....	125
4.3 Results and Discussion.....	126
4.3.1 Identification and Quantification by LC-MS.....	126
4.3.2 Identification by Surfactant-Mediated MALDI-TOF-MS.....	129
4.3.3 Quantification by MALDI.....	133
4.4 Conclusion.....	136
4.5 References.....	137
4.6 Addendum.....	139
<b>Chapter 5 – Conclusions and Future Research</b> .....	152
References.....	163

## LIST OF TABLES

### Chapter 1

Table 1.1: Laser sources used for MALDI.....	6
Table 1.2: Matrix compounds used in MALDI-TOF-MS.....	11
Table 1.3: A summary of the physical properties and their applications among surfactant classes.....	38

### Chapter 2

Table 2.1: Common CHCA-fragment ions and adducts observed in mass spectra using a 337 nm N <sub>2</sub> laser.....	56
Table 2.2: Analysis of analytes with each individual surfactant demonstrating the level of matrix ion suppression.....	61

### Chapter 3

Table 3.1: Summary of chromatographic peaks and mass spectrometry information obtained by LC-ESI-MS of berry samples and quantification by UV detection.....	87
Table 3.2: Flavonoids detected in berries using MALDI-TOF-MS with CHCA or THAP matrix.....	95
Table 3.3: Results from quantitation by MALDI-TOF-MS analysis of anthocyanins in blackberry and lingonberry extract.....	100

### Chapter 4

Table 4.1 Analyte concentrations determined by LC-UV and surfactant-mediated MALDI-TOF-MS in four energy drinks (sample codes BF, FT, RS and SB; n=10	
---	--

replicates). The percentage of discrepancy (%disc) illustrates the difference in  
quantification between the two methods.....128

Table 4.2 Relative standard deviation (RSD) values among analyte concentrations in  
energy drinks as determined by surfactant-mediated MALDI-TOF-MS.....135

## **Chapter 5**

nil

## LIST OF FIGURES

### Chapter 1

Figure 1.1: MALDI-TOF-MS instrument design.....	3
Figure 1.2: Mechanism of ion desorption.....	4
Figure 1.3: Principle of a time-of-flight mass spectrometer.....	7
Figure 1.4: Summary of delayed-extraction with laser desorption/ionization.....	9
Figure 1.5: Typical MALDI matrices.....	12
Figure 1.6: MALDI-TOF-MS spectra of bradykinin.....	14
Figure 1.7: Analysis of substance P by DHB matrix using (a) matrix : analyte mole ratio of 1000:1 and (b) matrix : analyte mole ratio of 100:1.....	26
Figure 1.8 Mass spectra of CHCA and suppressed matrix of CHCA with CTAB surfactant [72]. (a) CHCA matrix at 0.1 mol/L (b) suppressed CHCA with CTAB ratio of 1000:1 and keeping CHCA concentration the same.....	33

### Chapter 2

Figure 2.1: Molecular structure of analytes (top) and surfactants used (bottom).....	53
Figure 2.2: (a) MALDI mass spectra of CHCA matrix only. Resulting spectra of CHCA matrix /HTAB surfactant at mole ratio of (b) 1000:1, (c) 1000:0.01 and (d) 1000:0.0001.....	55
Figure 2.3: (a) MALDI mass spectra of CHCA/ <i>p</i> -coumaric acid (A) at mole ratio of 1000:5, (b) mass spectra of CHCA/ <i>p</i> -coumaric acid /CTAB at mole ratio of 1000:5:0.1.....	58
Figure 2.4: MALDI mass spectra of CHCA/chrysin(A)/HTAB at mole ratio of	

1000:5:0.001.....	59
Figure 2.5: MALDI mass spectra of CHCA/trialanine(A)/TBAB at mole ratio of	
1000:5:0.001.....	63
Figure 2.6: (a) MALDI mass spectra of CHCA/trialanine(A)/SDS at mole ratio of	
1000:5:0.1, (b) MALDI mass spectra of CHCA/trialanine(A)/SDS when analyte is diluted	
1000- fold.....	65
Figure 2.7: Molar concentration profile displaying the effect of Brij <sup>®</sup> concentration on	
[trialanine + Na] <sup>+</sup> , <i>m/z</i> 254 signal. The mole ratio of CHCA/trialanine held constant at	
1000:5 (n = 5).....	67
Figure 2.8: Monitoring the change in MALDI mass spectra of CHCA/caffeine (mole	
ratio 1000:5) as number of laser shots varied; (a) 5 shots, (b) 10 shots, (c) 30 shots. A=	
analyte; *=matrix ions.....	70
Figure 2.9: Monitoring the change in MALDI mass spectra of CHCA/caffeine/ CTAB	
(mole ratio 1000:5:1) as number of laser shots varied; (a) 5 shots, (b) 10 shots, (c) 30	
shots. A=analyte; S= surfactant.....	71
Figure 2.10: Monitoring the change in MALDI mass spectra of CHCA/caffeine/CTAB	
(mole ratio 1000:5:0.1) as number of laser shots varied; (a) 5 shots, (b) 10 shots, (c) 30	
shots. A=analyte; S=surfactant; *=matrix ions.....	72
Figure 2.11: Monitoring the change in average ion intensity of selected ions as the	
number of laser shots is increased on individual spots (n=10); (a) Ion profile of	
CHCA/caffeine, (b) of CHCA/ caffeine/CTAB where mole ratio is 1000:5:1, (c) of	
CHCA/caffeine/CTAB where mole ratio is 1000:5:0.1. %RSD values range	

from 6-10%.....74

### **Chapter 3**

Figure 3.1: Structures of flavonols and anthocyanins.....88

Figure 3.2. UV chromatographic profile of anthocyanins (520 nm) in extracts from (a) blueberry, (b) lingonberry, (c) blackberry, and (d) UV detection (360 nm) of blackberry flavonols.....89

Figure 3.3: Positive ion mode MALDI-TOF-MS mass spectra of flavonoid standards obtained with the addition of (a) CHCA, (b) THAP, (c) CHCA/CTAB, and (d) THAP/CTAB.....91

Figure 3.4: Positive ion mode MALDI-TOF-MS mass spectra of blackberry extract obtained with the addition of (a) CHCA, (b) THAP, (c) CHCA/CTAB, and (d) THAP/CTAB.....94

Figure 3.5. Positive ion mode MALDI-TOF-MS mass spectra obtained when THAP/CTAB was used for the analysis of (a) lingonberry extract, and (b) blueberry extract.....97

Figure 3.6: MALDI-TOF-MS calibration curves of cyanidin 3-glucoside standard by analysis with (a) THAP and (b) THAP/CTAB.....99

Figure 3.7. Electrospray ionization mass spectra of anthocyanins.....106

Figure 3.8. Electrospray ionization mass spectra of flavonols.....113

Figure 3.9. LC results UV detection (360 nm) of (a) blueberry extract, (b) lingonberry extract and (c) blackberry extract. ....116

Figure 3.10. Scanning electron microscope images of (a) standard with CHCA matrix

and (b) standard with THAP matrix.....117

Figure 3.11. Calibration curves produced by LC analysis for (a) anthocyanins and (b) flavonols.....118

#### **Chapter 4**

Figure 4.1: Structures of analytes and surfactants used.....123

Figure 4.2: LC chromatograms of standard mixture with UV detection at 261 nm and (b) 290 nm, with (c) ESI (+)TIC. The identity of labeled peaks are indicated in Figure 1.....127

Figure 4.3: Selection of suitable matrix; MALDI-TOF-MS mass spectra of 4-component energy drink standard mixture when analyzed by (a) CHCA, (b) sinapinic acid, (c) DHB, (d) CHCA/CTAB, (e) sinapinic acid/CTAB, and (f) DHB/CTAB. Assigned labels are N (nicotinamide), P (pyridoxine), C (caffeine), R (riboflavin) and CTAB (cetyltrimethylammonium bromide).....130

Figure 4.4: MALDI-TOF-MS mass spectra of CHCA/CTAB used for the analysis of energy drinks (a) BF, (b) FT, (c) RS, and (d) SB.....132

Figure 4.5: MALDI-TOF-MS calibration curves for standards using (a) CHCA and (b) CHCA with CTAB surfactant for the analysis of nicotinamide, pyridoxine, caffeine, and riboflavin.....134

Figure 4.6. LC-ESI-MS mass spectra of standards of (a) nicotinamide, (b) pyridoxine, (c) caffeine, and (d) riboflavin.....140

Figure 4.7. HPLC calibration curves of standards of standards of (a) nicotinamide, (b) pyridoxine, (c) caffeine, and (d) riboflavin.....141

Figure 4.8. SEM image of sugar drink/CHCA/CTAB.....	142
Figure 4.9. SEM image of sugar drink/sinapinic acid/CTAB.....	143
Figure 4.10. SEM image of sugar drink/dithranol/CTAB.....	144
Figure 4.11. SEM image of sugar drink/DHB/CTAB.....	145
Figure 4.12. SEM image of sugar drink/THAP/CTAB.....	146
Figure 4.13. SEM image of non-sugar drink/CHCA/CTAB.....	147
Figure 4.14. SEM image of non-sugar drink/sinapinic acid/CTAB.....	148
Figure 4.15. SEM image of non-sugar drink/dithranol/CTAB.....	149
Figure 4.16. SEM image of non-sugar drink/DHB/CTAB.....	150
Figure 4.17. SEM image of non-sugar drink/THAP/CTAB.....	151
 <b>Chapter 5</b>	
Figure 5.1: Structure of hypericin.....	155
Figure 5.2: MALDI mass spectra of hypericin with CHCA matrix.....	156
Figure 5.3: Surfactant-mediated MALDI mass spectra of hypericin with CHCA and surfactant CTAB.....	156
Figure 5.4: MALDI mass spectrum obtained from urine analysis after coffee consumption with use of CHCA matrix.....	158
Figure 5.5: Surfactant-mediated MALDI mass spectrum obtained when urine sample was analyzed with CHCA matrix and CTAB surfactant.....	159
Figure 5.6: SIMS mass spectrum obtained during a survey scan of caffeine standard.....	160
Figure 5.7: SIMS depth profile obtained by monitoring ions for caffeine, CHCA, and CTAB at <i>m/z</i> 96, 100 and 225, respectively.....	161

## LIST OF ABBREVIATIONS

- 9-AA - 9-aminoacridine
- ACN - acetonitrile
- AMP - adenosine-5'-monophosphate
- ANP - 2-amino-5-nitropyridine
- API - atmospheric pressure ionization
- ASE - analyte suppression effect
- CE - capillary electrophoresis
- CHCA -  $\alpha$ -cyano-4-hydroxycinnamic acid
- CMC - critical micelle concentration
- CNT - carbon nanotubes
- CTAB - cetyltrimethylammonium bromide
- Da - dalton
- DDTAB - dodecyltrimethylammonium bromide
- DHB - 2,5-dihydroxybenzoic acid
- DL - detection limit
- DMB - decamethonium bromide
- DNPH - 2,4-dinitrophenylhydrazine
- EI - electron ionization
- ESI - electrospray ionization
- ESI-MS - electrospray ionization mass spectrometry
- eV - electron volt

FAB - fast atom bombardment

GC-MS - gas chromatography mass spectrometry

HPLC - high performance liquid chromatography

HTAB - hexyltrimethylammonium bromide

IR - infra red

LC - liquid chromatography

LC-MS - liquid chromatography mass spectrometry

LDI - laser desorption/ionization

LTOF - linear time-of-flight

MALDI - matrix-assisted laser desorption/ionization

MALDI-TOFMS – matrix-assisted laser desorption/ionization time of flight mass spectrometry

MS - mass spectrometry

MSE - matrix suppression effect

MSLDI - matrix-suppressed laser desorption/ionization

MW- molecular weight

m/z - mass-to-charge ratio

PEG - polyethylene glycol

PMMA - poly(methyl methacrylate)

ppb - parts per billion

PSD – post source decay

PVDF - polyvinylidene fluoride

RP - reversed phase  
RSD - relative standard deviation  
SALDI - surface-assisted laser desorption/ionization  
SDS - sodium dodecyl sulfate  
SEM - scanning electron microscopy  
SIMS - secondary-ion mass spectrometry  
S/N - signal to noise ratio  
TBAB - tetrabutylammonium bromide  
TFA - trifluoroacetic acid  
THAP - 2,4,6-trihydroxyacetophenone  
TIC - total ion chromatogram  
TOF - time-of-flight  
UV - ultraviolet

## **CHAPTER 1**

### **INTRODUCTION AND OVERVIEW**

## **1.1 INTRODUCTION**

### **1.1.1 A Brief History of MALDI**

Matrix-assisted laser desorption/ionization (MALDI) is a relatively new technique which was first described by two independent groups, one German and one Japanese, nearly simultaneously in the late 1980's. The German group was lead by Hillenkamp and Karas [1] who coined the MALDI term using an organic matrix; the Japanese by Tanaka [2] using a Co powder in glycerol matrix. MALDI developed from similar desorption/ionization methods such as fast atom bombardment (FAB) and laser desorption/ionization mass spectrometry (LDI-MS). It has been found useful in the analysis of macromolecules such as proteins, nucleic acids and synthetic polymers [3, 4, 5]. Its distinguishing feature is that the analyte is embedded in a molar excess of chemical matrix (ca. 100-50 000 x) [6].

MALDI-TOF-MS (matrix-assisted laser desorption/ionization time-of-flight mass-spectrometry) is a laser-based soft ionization method, i.e., laser energy is used as the desorption/ionization source, but it excites the matrix molecules, rather than degrading and decomposing the analyte. The matrix has a key role here because it absorbs the laser energy and causes a small amount of the analyte to vapourize. Once vapourized, the charged analyte molecules can be electrostatically transferred to a mass analyzer for separation and detection. A schematic of MALDI-TOF-MS can be seen in Figure 1.1 [7].

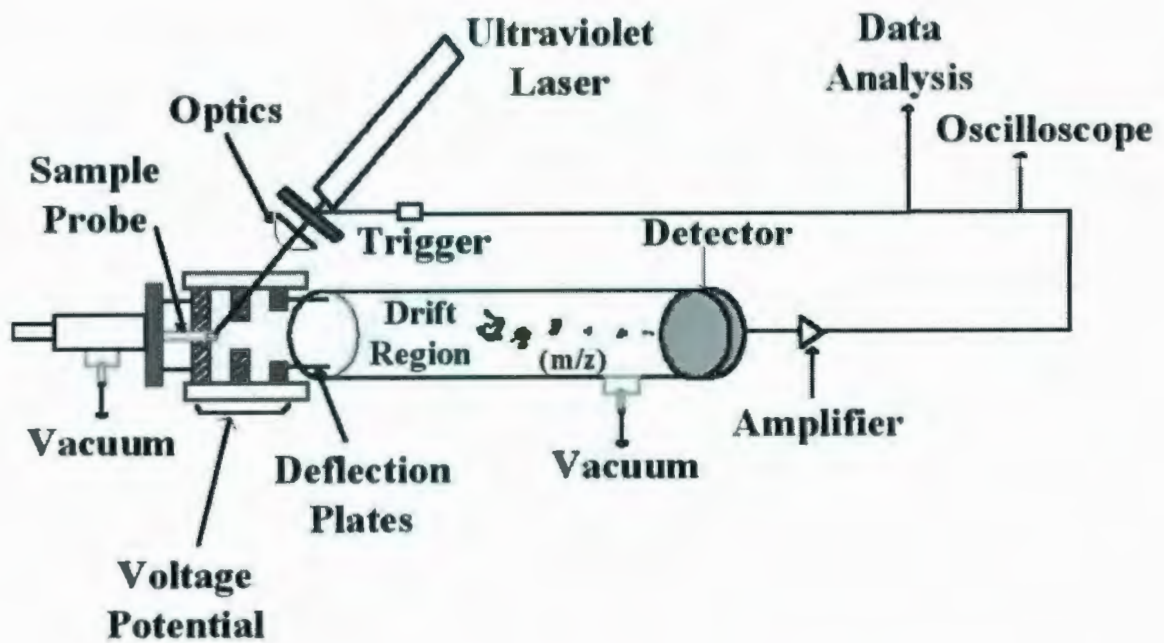


Figure 1.1. MALDI-TOF-MS instrument design. Adapted from [7].

The mechanism of ion desorption is often disagreed upon, but most models agree with some basic principles that are represented in Figure 1.2 [8]. It consists of three stages: 1) the formation of a 'solid solution', 2) matrix excitation, and 3) analyte ionization.

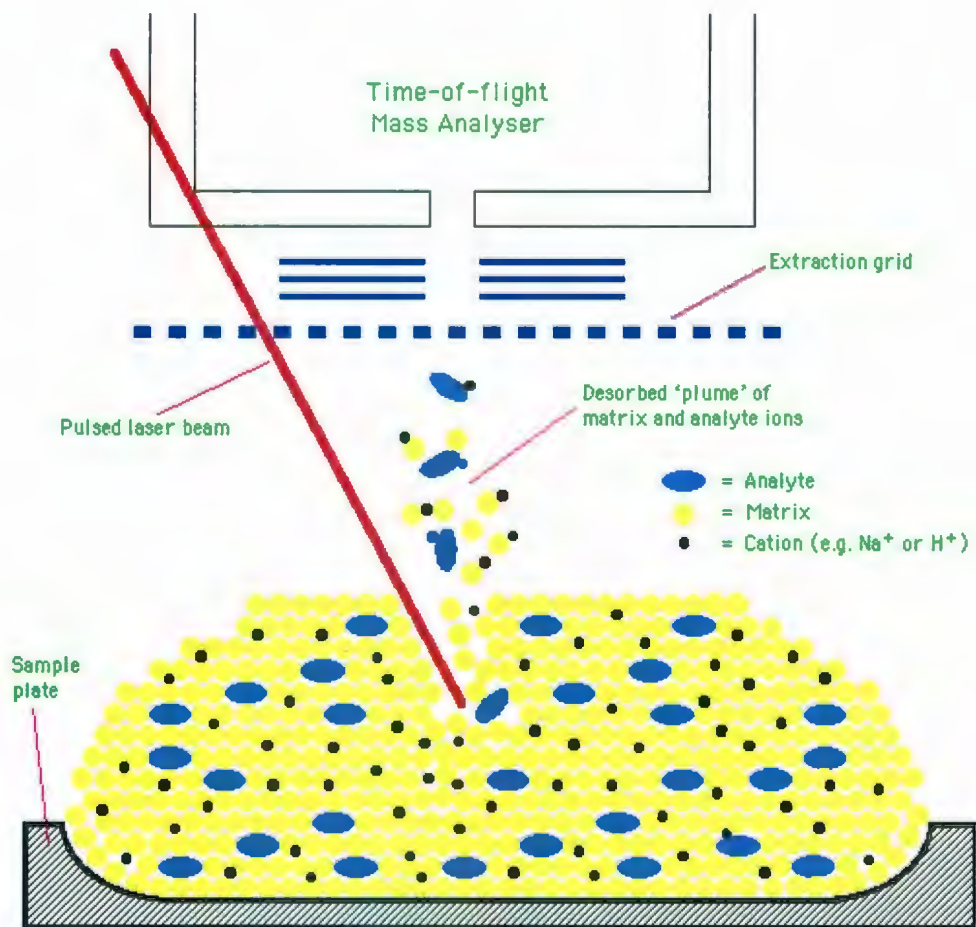


Figure 1.2. Mechanism of ion desorption. Adapted from [8].

In stage 1, the analyte molecules are distributed throughout the matrix (ie. co-crystallization) so that they are isolated from one another. This allows the matrix and analyte to form a homogeneous “solid solution”; any liquid solvents used in the preparation are removed prior to analysis as the mixture dries and crystallizes. Then laser

energy is absorbed by the matrix, causing rapid vibrational excitation and bringing about localized disintegration of the solid solution. Clusters, which are made up of an analyte molecule that is surrounded by both neutral and excited matrix molecules, then form. The matrix molecules evaporate away or decompose to leave the excited analyte molecule. Finally, analyte molecules can be ionized by simple protonation or cationization by the excited matrix, which leads to typical  $[M+X]^+$  type species (where X = H, Li, Na, K, etc.). In addition, multiply charged species, dimers, and trimers of the same analyte may also form. Negative ions are formed from reactions involving deprotonation of the analyte by the matrix to yield  $[M-H]^-$  and from interactions with photoelectrons to form the  $[M]^\ominus$  radical molecular ions. Anions such as  $Cl^-$  and  $Br^-$  can add to molecules to lead to the formation of parent ions as well.

### **1.1.2 Instrumental Components of MALDI**

MALDI laser sources emit radiation in either the UV or IR portion of the spectrum with UV lasers being the most common. These are readily available and cheaper than their IR counterparts. The most common is the nitrogen laser which emits at 337 nm and these are found in most commercial instruments [9]. Alternatively, frequency tripled Nd:YAG lasers at 355 nm may be used. In the IR range, the main laser is the Er:YAG laser which emits at 2.94  $\mu m$ . These are much more expensive than nitrogen lasers. IR-MALDI is offered because it has the advantage of being a softer technique which aids in the analysis of fragile compounds like oligonucleotides and other non-covalently bound complexes. Its disadvantages are that there are few IR-MALDI matrices to choose from, the lower sensitivity compared to UV-MALDI, and the larger

penetration depth of radiation into the sample (shorter lifetime of sample). A summary of lasers used in MALDI is presented in Table 1.1 [adapted from 9].

Table 1.1 Laser sources used for MALDI [9].

Laser	Wavelength	Photon Energy (kcal/mol)	Photon Energy (eV)	Pulse Width
Nitrogen	337 nm	85	3.68	< 1 ns – few ns
Nd:YAG $\mu$ 3	355 nm	80	3.49	5 ns
Nd:YAG $\mu$ 4	266 nm	107	4.66	5 ns
Excimer (XeCl)	308 nm	93	4.02	25 ns
Excimer (KrF)	248 nm	115	5.00	25 ns
Excimer (ArF)	193 nm	148	6.42	15 ns
Er:YAG	2.94 $\mu$ m	9.7	0.42	85 ns
CO <sub>2</sub>	10.6 $\mu$ m	2.7	0.12	100 ns + 1 $\mu$ s tail

MALDI is often coupled with time-of-flight (TOF) mass analyzers due to their practically unlimited mass range. Although it is not common, other mass analyzers have been coupled with MALDI; hence, matrix-assisted laser desorption/ionization time-of-flight mass spectrometry (MALDI-TOF-MS) has become a primary mode of analysis for large molecules.

In a time-of-flight instrument, ions are accelerated by an electric pulse of  $10^3$ - $10^4$  V that has the same frequency as the ionization pulse, but lags behind it. These accelerated particles pass through a field-free drift tube which is approximately 1 m in length. The total flight time that an ion takes from ion formation to impacting a detector is then measured. Since all the ions entering the tube ideally have the same kinetic energy, their velocities must vary inversely with their masses. This means that lighter particles spend less time in the tube than heavier particles as illustrated in Figure 1.3 [10].

Typical flight times are 1-30  $\mu\text{s}$  [11]. By calibration of the ions' flight times through the instrument with standards, a mass spectrum can be obtained.

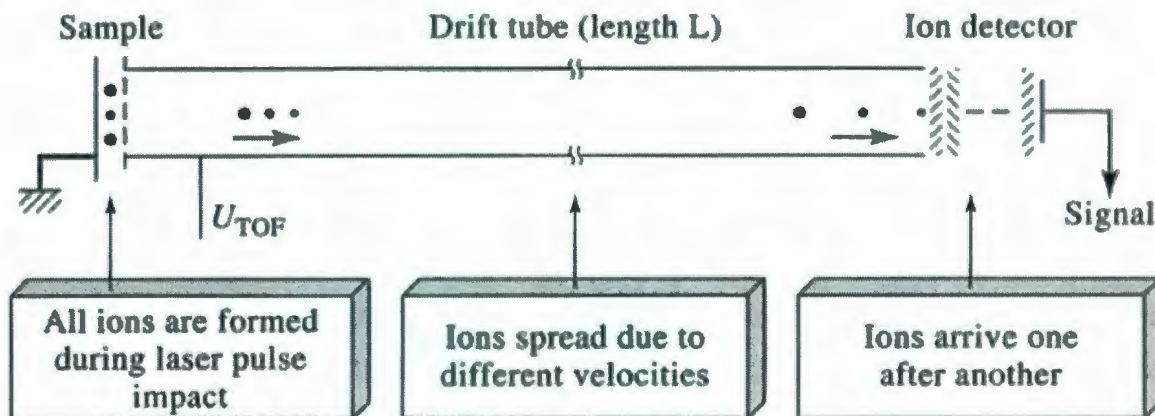


Figure 1.3. Principle of a time-of-flight mass spectrometer [10].

An ion's flight time (in seconds) is proportional to the square root of the mass to charge ratio ( $m/z$ ), as given in equation 1 [12]:

$$t = [m L / (2zeV_{\text{acc}})]^{1/2} \quad (1)$$

where  $t$  is the flight time in seconds,  $m$  is the mass of the ion in kilograms,  $z$  is the charge on the ion,  $e$  is the elementary charge ( $1.6 \times 10^{-19}$  C),  $V_{\text{acc}}$  is the accelerating voltage in volts, and  $L$  is the length of the flight path in meters.

Instruments that use time-of-flight mass spectrometers have poorer resolution and reproducibility than those that employ magnetic or quadrupole analyzers. These disadvantages are predominant in the linear time-of-flight mode (LTOF). However, the advantages of TOF include instrument simplicity and ruggedness, ease of accessibility to the ion source, and practically unlimited mass range.

The resolution between two ions,  $m_1$  and  $m_2$ , is proportional to the ions flight time divided by twice the time interval of ion arrival at the detector, as seen in equation 2:

$$R = m/\Delta m = t/2\Delta t \quad (2)$$

Longer flight paths result in higher resolution than do shorter paths.

One method used to improve the resolution of ions in most modern MALDI-TOF-MS instruments is the use of delayed extraction [13,14]. In this method, the accelerating voltage is not applied until after a short time delay following the laser pulse. This extraction delay can provide some compensation for the spread of energies given to molecules and lead to an increase in resolution. The mass resolution is improved because of the correlation between the velocity and position of ions subsequent to those that are produced in the ion source. Ions with a greater kinetic energy end up yielding higher velocities and move closer to the extraction electrode before the accelerating voltage is applied. Any ions with less kinetic energy stay closer to the surface of the target electrode. Thus, they begin being accelerated at a greater potential than the other ions that are farther from the target electrode. This results in the slower ions receiving more energy to catch up to the faster ions, and then ions with the same  $m/z$  should reach the detector simultaneously. This process is illustrated in Figure 1.4 [15].

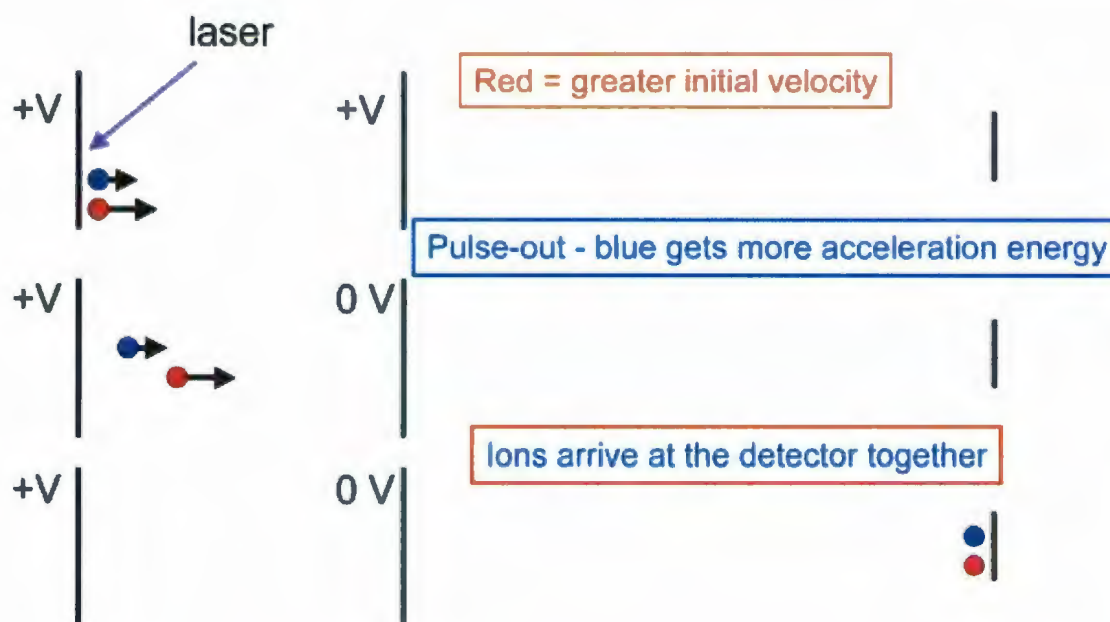


Figure 1.4 Summary of delayed-extraction with laser desorption/ionization [15].

Another method to improve mass resolution, one that can be used to increase the flight path and addresses a higher order ion focusing problem, is the addition of an electrostatic mirror (i.e. constant electrostatic field) at the end of the flight tube. This reverses the ions direction and refocuses it toward the detector. These reflectron TOF (re-TOF) mass analyzers double the flight pathlength, yielding longer flight times and higher mass resolution [3,16-18]. This also corrects the kinetic energy distribution of the ions by ensuring that ions with a greater kinetic energy spend more time in the reflectron and those with less energy spend less time. Thus, all ions of the same  $m/z$  leave the reflectron at the same time.

### 1.1.3 Matrix Selection

The use of a matrix serves two main purposes. First, it absorbs the energy of the laser light, preventing analyte decomposition. Secondly, it isolates analyte molecules which prevents analyte/analyte association. A MALDI matrix must meet several requirements; it must embed and isolate analyte molecules, be soluble in solvents that are compatible with the analyte, be vacuum stable, absorb light energy at the laser wavelength, cause co-desorption of the analyte upon laser irradiation, lead to formation of crystals, and promote analyte ionization [3,12,19].

Carboxylic acids are very good matrices in the positive ion mode because they have labile protons which can protonate neutral analytes in the excitation plume. Since acidic environments are sometimes undesirable (possible denaturation of the tertiary structure of biomolecules, some non-acidic matrices are used [3]. For compounds that are not easily protonated, they may be cationized by doping the sample with a salt (sodium or potassium chloride, copper or silver nitrate) [12]. In contrast, easily deprotonated analytes may be analyzed using the negative ion mode.

The choice of a matrix is likely the most important part in designing a MALDI experiment. It is typically a small organic compound which has one or more acidic functional groups. Matrices should have a high molar absorptivity ( $\epsilon_\lambda$ ) at the wavelength of the particular laser source being used. Most matrices have  $\epsilon_\lambda$  values that range from  $1 \times 10^3$  to  $1 \times 10^5 \text{ M}^{-1}\text{cm}^{-1}$  [12]. The matrix should not modify or react with the analyte prior to laser radiation. It should also be soluble in similar solvent systems as the analytes to ensure proper mixing and co-crystallization of the pair. Common mixing

mole ratios of matrix to analyte range from 100:1 to 50 000:1. The matrix/analyte mixture is then dried as a small droplet on a stainless steel probe or plate.

The matrix is important because it is required to absorb the energy from the laser and simultaneously protect the analyte from excessive energy which would lead to analyte fragmentation. Secondly, it enhances ion generation from analyte molecules by excitation or ionization via the matrix molecules. This is followed by proton transfer to the analyte molecule in the case of acidic matrices. Thirdly, sample dilution by the matrix minimizes any possible association of analyte molecules [20].

Hundreds of potential matrices have been tested over the years in an empirical fashion. Some of the more common ones have been summarized in Table 1.2.

Table 1.2. Matrix compounds used in MALDI-TOF-MS [adapted from 3,12,19,20].

Name	Abbreviation	Form	$\lambda$ (nm)	Applications
Nicotinic acid	NA	Solid	266	Proteins
Glycerol	-	Liquid	337	Polymers, proteins
Sinapinic acid	SA	Solid	337	Peptides, proteins
Ferulic acid	FA	Solid	337	Peptides, proteins
Succinic acid	CA	Solid	337	Proteins
			2.94 $\mu$ m	
2,5-dihydroxybenzoic acid	DHB	Solid	337	Proteins, carbohydrates
$\alpha$ -cyano-4-hydroxycinnamic acid	CHCA	Solid	337	Peptides, proteins
3-hydroxypicolinic acid	3-HPA	Solid	337	Oligonucleotides
Harmaline	-	Solid	337	Oligosaccharides
3-aminoquinilone	3-AQ	Liquid	337	Peptides, proteins
Dithranol	-	Solid	337	Proteins, lipids

When optimizing an experiment, the selection of a suitable matrix is usually the first step considered. The possibility of matrix-analyte interactions are not always easy to predict, and multiple matrices should be tested for an analyte (trial and error method) before further method optimization is considered. Typically, proteins with a mass of greater than 10 000 Da are suitably analyzed with a matrix of  $\alpha$ -cyano-4-hydroxycinnamic acid (CHCA), while those less than 10 000 Da are best analyzed with sinapinic acid matrix. Oligonucleotides usually require a matrix of 3-hydroxypicolinic acid and dithranol works well for lipid analyses. Synthetic polymers are sometimes identified using 2,5-dihydroxybenzoic acid (DHB). Structures of some of the most common MALDI matrices have been provided in Figure 1.5.

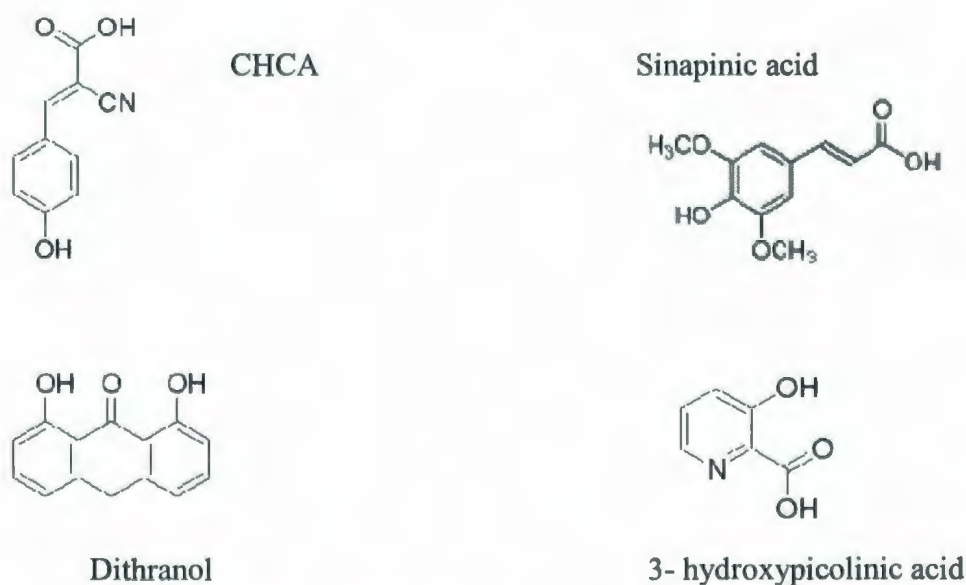


Figure 1.5. Typical MALDI matrices.

#### 1.1.4 MALDI Experimental Sample Preparation

Analysis via MALDI consists of two main processes: the first step is sample preparation and the second is desorption of the solid sample via a laser pulse.

Sample preparation involves mixing the sample with a large molar excess (ex. 100-2000) of matrix. The original procedure which has been used for over two decades is called the “dried-droplet” method. It was originally described by this statement [1]: “An aqueous solution of the matrix compound is mixed with analyte solution. A tiny droplet of this solution is then dried resulting in a solid deposit of analyte-doped matrix crystals that is introduced into the mass spectrometer for analysis.”

MALDI works best when analyte concentrations are between 1-10 pmol/ $\mu$ L. After the solvent evaporates the matrix/analyte crystals may be washed with water to remove impurities. Since MALDI is a very sensitive technique care must be taken to reduce the number of potential sample contaminant steps. However, MALDI is more forgiving of sample impurities than its complementary method, electrospray ionization-mass spectrometry (ESI-MS).

Matrix solutions should be used within a week of preparation; otherwise they start to degrade [21]. It is advantageous to prepare fresh solutions of both analyte and matrix daily.

Once the matrix/analyte mixture has been spotted (0.5-1.0  $\mu$ L) on the MALDI plate and thoroughly dried, it is loaded into the mass spectrometer. The loading process is fully automated in current MALDI-TOF-MS instruments. However, parameters such as mass range scanned, order of samples analyzed and laser intensity can be varied.

To minimize the variation in shot-to-shot reproducibility several laser scans (10-100) are averaged to provide a good signal-to-noise ratio. This increases the accuracy of the molar mass determination. Both heterogeneous analyte incorporation into the matrix crystal structure and variation of the analyte/matrix ratio within the dried crystallized spot lead to the poor reproducibility.

A typical MALDI mass spectrum of a peptide is illustrated in Figure 1.6 [22].

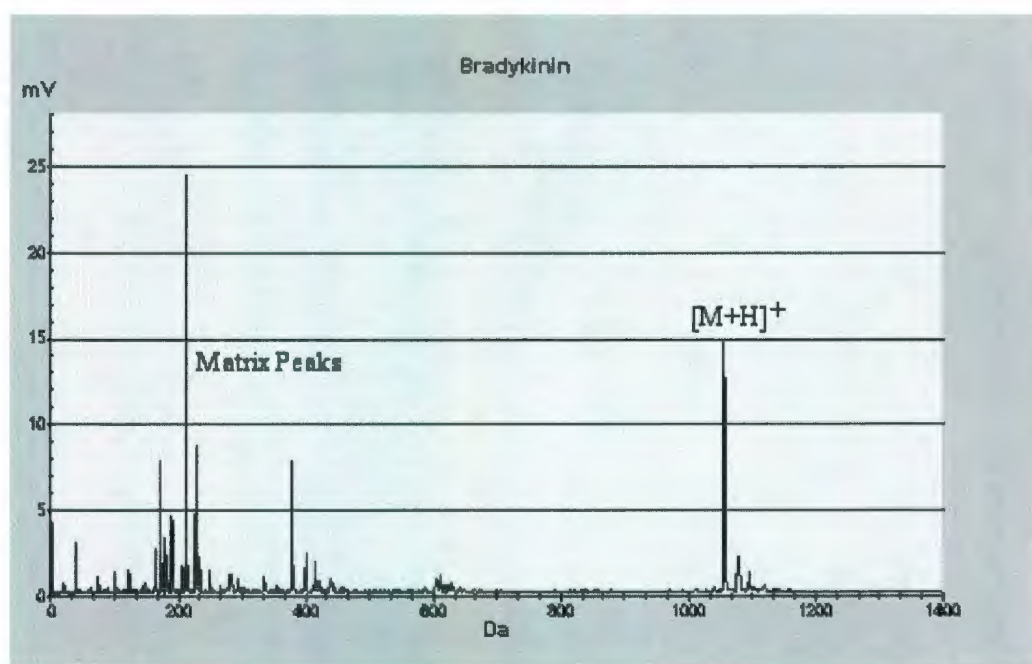


Figure 1.6 MALDI-TOF-MS spectra of bradykinin [22].

The protonated analyte signal can be seen with a mass of approximately 1060 Da. In the lower mass end of the spectrum many peaks can be seen due to the fragmentation and various reactions of the associated matrix. This can lead to difficulty in identifying analyte signals if the analyte has a low mass that falls in this region.

MALDI-TOF-MS is mainly based on laser desorption of solid matrix-analyte deposits. There are inherent difficulties such as low shot-to-shot reproducibility, short sample life and a strong dependence on the sample preparation method being used. Several groups have investigated the potential for the use of liquid matrices to hopefully address these aforementioned disadvantages [23-25]. The liquid matrix methods include the use of chemical liquids, particle-doped liquids (two-phase) and chemical-doped liquids [9]. But the solid state methods are far more common and will be discussed briefly. These include the dried-droplet method, vacuum-drying, fast-evaporation, overlayer, sandwich, electrospray, quick and dirty, and matrix-precoated targets.

The dried-droplet method is the original preparation method used by Hillenkamp and Karas [1]. This is still one of the most effective and widely used MALDI sample preparation schemes. It involves adding a drop of aqueous matrix solution to a drop of analyte solution, mixing the two and then spotting (approximately 1  $\mu$ L) and drying on the sample target. The sample is left to dry slowly, resulting in a solid deposition of the analyte-doped matrix crystal. It is possible to wash the crystals to remove impurities such as non-volatile compounds. This method has been reported to tolerate the presence of salts and buffers well. It is an excellent choice for samples that contain more than one protein or peptide.

Vacuum-drying is a variation of the dried-droplet technique where the final matrix/analyte mixture is dried very rapidly in a vacuum chamber [26]. This helps to reduce the size of crystals and can lead to increased homogeneity. Some of the

advantages are the decreased need to look for “sweet-spots”, thinner samples, and increased mass accuracy and resolution.

The fast evaporation method can result in improved resolution and mass accuracy [12]. The matrix and analyte are spotted one after the other. The matrix solution is first spotted and allowed to dry. Then the analyte solution is spotted on top of it and its solvent is allowed to evaporate.

The overlayer method uses the fast evaporation technique to form the first layer of matrix crystals. However, in the second layer, a combination of the matrix and analyte is spotted. Some researchers found that the addition of matrix into the second step provided better results, particularly for proteins and peptides [9].

The sandwich method involves first spotting a layer of matrix, allowing it to dry, and then depositing a layer of analyte. A final layer of matrix is then deposited so that the analyte is “sandwiched” between two layers of matrix.

In the electrospray method, a small amount of the analyte mixture is electrosprayed from a high voltage stainless steel or glass capillary onto a grounded metal plate [27,28]. This plate is mounted 1 to 3 cm away from the capillary tip. With this method of sample deposition a homogenous layer of equally sized microcrystals is achieved and the analyte molecules are evenly distributed. The method is fast and minimizes the effects of sample segregation.

In the quick and dirty method, a drop of matrix solution is spotted on top of a drop of analyte solution (ca. 0.1-10 mM). Both solutions are mixed with a pipette tip before the mixture is dried under air or N<sub>2</sub>. It can be used for analyzing in-plate protein digests.

It is simple to add an internal standard using this method. However, it is the method having the least control out of all sample preparation methods.

The matrix-precoated target method is very simple, fast and sensitive. It involves adding a single drop of undiluted analyte to a precoated target spot. It can be used to interface MALDI sample preparation to liquid chromatography (LC) and capillary electrophoresis (CE) [29,30]. Some of the common, commercially-available precoated target substrates consist of nylon, PVDF, nitrocellulose or anion- and cation-modified cellulose.

## **1.2 ANALYSIS OF SMALL MOLECULES BY MALDI-TOF-MS**

### **1.2.1 Overview**

MALDI was developed as a soft ionization tool for the analysis of large molecules, particularly biomolecules. The technique was developed and built around the fundamental problems which must be solved when dealing with large molecules and this is why some of the features of MALDI were ascertained; ie. small molecule organic matrix fragments in the spectra are not a problem when analyzing large molecular weights and very high matrix:analyte mixing ratios were required to adequately desorb large molecules into the gas phase. However, over the past decade, there has been a growing interest in the possibility of using MALDI to analyze smaller compounds [31-36].

MALDI-TOF-MS has historically been used minimally for small molecule analysis, particularly for quantitative studies. There are a number of reasons behind this. For one, scientists have thought that the potential differences between the ionization efficiency of internal standards and analytes and the lack of homogenous sample spots limit the ability to obtain reproducible results [37]. In terms of the acquisition of MALDI spectra, the problem with saturated matrix-related ions and the fact that software can not reject them means that when they are combined with peaks that are not saturated the respective peak areas or heights are not suitable for quantitation.

Analysis of small molecules by MALDI was also hindered by the low resolution of the initial MALDI-TOF instruments. The inherent common problem of matrix-ion interference complexity in the low-mass region of spectra for low molecular weight

analyte analysis seemed insurmountable. More importantly, competition from electrospray ionization (ESI) and atmospheric pressure ionization (API) mass spectrometry techniques limited the amount of research carried out on small molecules by MALDI. Many mass spectrometrists consider MALDI inappropriate for small molecule analysis [12].

In the past decade, improvements in TOF mass analyzers have resulted in better mass resolution. There is an increased demand placed on high-throughput capabilities (mainly chromatography) from the biotechnology and drug discovery markets. Chemists who analyze highly complex samples, containing salts and buffers are beginning to turn towards MALDI due to its tolerance for these contaminants.

### **1.2.2 Small Molecule Classes**

Peptides are perhaps the most analyzed small molecule by MALDI-TOF-MS. Many peptides (< 1500 Da) have been analyzed using CHCA but other matrices have worked. Several small peptides such as angiotensin and substance P are now utilized as standards when technicians verify instrumental performance [38, 39]. Other analyte classes include saccharides [35, 40-42], drugs [43-48] and lipids [49-51]. Although there are many more examples of small molecule analyte classes relevant to MALDI, a complete review is outside the scope of this thesis and only the more common will be mentioned in brief.

Saccharides and the mechanisms involved in their MALDI analysis have been studied by a few authors [40,41]. Perreault *et al.* [41] made phenylhydrazone derivatives

of various oligosaccharides which were characterized by both ESI and MALDI. Hao *et al.* [40] demonstrated that for oligosaccharides, cationized species were the dominant ions under positive-ion mode MALDI. Negative ions were not formed to any significant extent. However, it was concluded that the key processes involved were related to analyte mass. For low molecular weight oligosaccharides, matrix-assisted ionization was critical, while for high molecular weight analytes (ie. > 20000 Da), matrix-assisted desorption was crucial. The differences in these processes led to differences in their MALDI mass spectra.

For several classes of drugs, the classical approach involves derivatization of these analytes to make them amenable to MALDI [44,45]. For example, neutral steroid species are not easily ionized under MALDI conditions but derivatization to their Girard P hydrazones (a derivative of a quaternary ammonium ion, where the quaternary nitrogen is part of a pyridine ring) makes them more easily protonated [45]. Volmer *et al.* [46] researched some of the underlying physical and technical aspects of dealing with drug molecule analysis by MALDI. They employed a specially made instrument with a very high-repetition laser (1 kHz). This led to successful determination of drugs such as quinidine, danofloxacin, ramipril and nadolol.

Lipid analysis by MALDI-TOF-MS was successfully done by Jackson *et al.* [49] who studied phospholipids from rat brain tissue. Very interesting direct tissue samples were probed in a MALDI instrument and imaged as well. Molecular ions due to phosphatidcholines, phosphatidylethanolamines and sphingomyelin were recorded.

### 1.2.3 Inherent Difficulties

There are several major difficulties when dealing with a MALDI experiment for small mass analytes [3,9,12]. One problem is the matrix-ion signals interfering with those of the analyte in the low-mass region of a mass spectrum. The multitude of matrix-related ions are caused by degradation and decomposition of the organic matrix under highly energetic conditions. Second, there is the issue of requiring the sample and matrix to co-crystallize, which stems from possible solubility differences between matrices and analytes. Third, it is difficult to obtain adequate mass resolution of the target analytes in order to distinguish them from matrix-ions. Finally, contamination in samples can be an issue, leading to the formation of cationized species as well as protonated ones.

Larger analytes induce matrix ion suppression at higher mixing ratios because of their higher molecular weight. They require more of the matrix to cause desorption from the sample target. It has been found that this effect should scale roughly to the surface area of an analyte or its mass to the  $2/3$  power [52], assuming they are generally spherical in shape. But it was also realized that smaller molecules have non-spherical shapes and deviations from the proposed theory will exist.

The ideal situation would be when there was significant matrix ion suppression (MSE) resulting in a low abundance of matrix-related ions in the spectra. One of the reasons for not observing the matrix suppression effect (MSE, discussed in section 1.3) is due to problems attaining matrix/analyte co-crystallization. For MSE to occur, a matrix and analyte should be soluble in similar solvents. Otherwise, poor crystallization results as was observed between PEGs [Poly(ethylene glycol)] in DHB and AMP (adenosine-5'-

monophosphate monohydrate) in sinapinic acid [52]. For samples such as these, alternative deposition methods need to be employed.

#### 1.2.4 Some Solutions to Small Molecule Analysis

Due to the solubility differences between salts and matrices, particularly CHCA, salts tend to crystallize around the outer surface of matrix crystals, whereas analyte molecules are more evenly distributed. However, this can create a problem for heterogeneous samples with a high salt content. Washing the dried sample spot with deionized water prior to analysis can improve the quality of mass spectra. This is fast and easy and utilizes the low water solubility of CHCA. However, it is likely that there is some sample loss during this step. Even when a solution is relatively clean, alkali metals lead to formation of matrix clusters. Ammonium salt buffer solutions have been tested as an alternative washing agent [53].

Addition of ammonium salts have been tested as co-matrices for MALDI of small oligonucleotides. Chan *et al.* [54] have found that ammonium halides cause a dramatic enhancement when added to the matrix ANP (2-amino-5-nitropyridine) in the analysis of oligonucleotides. In this study, fourteen ammonium salts were tested as co-matrices for negative ion MALDI analysis of oligonucleotides using various matrices. The authors found that  $\text{NH}_4\text{F}$  and  $(\text{NH}_4)\text{HF}_2$  yielded the greatest signal enhancement.

One method that aids in the analysis of small molecules by MALDI has been the use of a binary matrix. For example, Guo *et al.* [55] recently demonstrated that a mixture of CHCA and 9-aminoacridine (9-AA), two matrices with very different proton affinities

can suppress matrix clusters showing up in the mass spectrum in both positive and negative ion mode. Essentially, it has already been established that the mixing ratio is very important to limit matrix-related ions. However, for analysis of biological samples, this is not always possible as the analytes are present in unknown concentrations. One example is to use amino compounds as co-matrices to aid in oligonucleotide detection [56-58]. Smirnov *et al.* [53] used ammonium salts of CHCA to reduce formation of matrix clusters.

In the above study, CHCA ( $pK_a = 1.2$ ) was recognized as an acidic matrix that was commonly used to produce positive analyte ions, whereas 9-AA ( $pK_a = 10.2$ ) is a basic matrix that is used to yield negatively charged analytes [55]. Thus, the thermodynamic competition produced mainly the  $[CHCA-H]^-$  and  $[9AA + H]^+$  ions. Mixing these matrices at nearly equimolar ratios resulted in minimal matrix-related ions, and aided in identification of low-mass analytes that were initially swamped with matrix peaks. This method is particularly useful for samples that can yield analyte ions of interest in either polarity from the same sample preparation for confirmation purposes.

The suppression effect caused by the use of co-matrices is believed to be due to two effects; “directional” proton transfer and a reduced laser fluence threshold [55]. First, any MALDI experiment results in collisions between excited matrix molecules (ex.  $M_a^*$ ), which leads to matrix ions and clusters, such as  $[M_a+H]^+$ ,  $M_a^+$ ,  $[2M+Na]^+$ ,  $[M-H]^-$ ,  $M_a^-$ , etc. In the case of a species at similar concentration but of higher proton affinity, proton donation from  $M_a^*$  is favored. The two-step model provided by Knochenmuss *et al.* [59] explains analyte-assisted matrix suppression when multiple analytes of different

proton affinities are mixed at approximately the same matrix : analyte ratio. This model also explains how there is a dominant presence of  $[M_b+H]^+$  in positive polarity and  $[M_a-H]^-$  in negative polarity. This is because of “directional” proton transfer to  $M_b$  from  $M_a$  during ionization.

The second cause is related to the laser fluence threshold, the minimum amount of laser power required to effectively desorb a given matrix and yield ions, of the respective matrices. The CHCA requires much less energy to cause sublimation than 9-AA. Since the two matrices are mixed, the one with the lower threshold is desorbed first and provides the “kick” to get both matrices and the analytes off of the targets’ surface. It was found that a laser fluence 63% less was sufficient to ionize both the matrices and the analyte, as opposed to when only 9-AA was used as a matrix [55]. This decreased laser power results in less energetic intermolecular collisions, and thus less of a matrix background is present.

One of the biggest limitations of this method is that it is not applicable to all analytes; it is selective for those with pKa values very different from either of the matrices. For compounds of basicity higher than 9-AA, its presence reduced CHCA fragment ions without affecting analyte protonation. If the analytes were more acidic than 9-AA, no analyte ions were detected, however, as the protons were lost to 9-AA. In positive polarity, only analytes with a proton affinity higher than 9-AA were improved. Thus, a binary matrix mixture is only effective for analytes with pKa values outside the bracketed range of those of the matrices.

## 1.3 ION SUPPRESSION IN MALDI

### 1.3.1 Overview of Ion Suppression

Suppression of matrix ions has been reported by several researchers [60-62] as resulting from matrix-analyte reactions, but until a two-step ion generation model was suggested, the phenomenon was not fully understood. This is now known to be a result of secondary reactions [63-65]. Essentially, at the appropriate matrix : analyte ratios, the matrix-related ions can be completely suppressed from the resulting mass spectra. This has been referred to as the matrix suppression effect (MSE). During suppression, the matrix ions are completely suppressed through contact with an analyte ion. This encompasses all types of matrix ions (protonated, cationized, radical cation). Thus, if a basic analyte is able to deprotonate primary matrix ions, then depletion of other matrix ions must occur via interconversion.

As an example to demonstrate the matrix suppression effect, Figure 1.7 [63] illustrates the analysis of substance P in DHB matrix by positive-ion mode MALDI. In (a), the matrix to analyte ratio was 1000:1 and several corresponding matrix peaks were observed. However, in (b) the mixing ratio was reduced to 100:1, and subsequently, substance P was detected as its molecular ion with negligible matrix background noise.

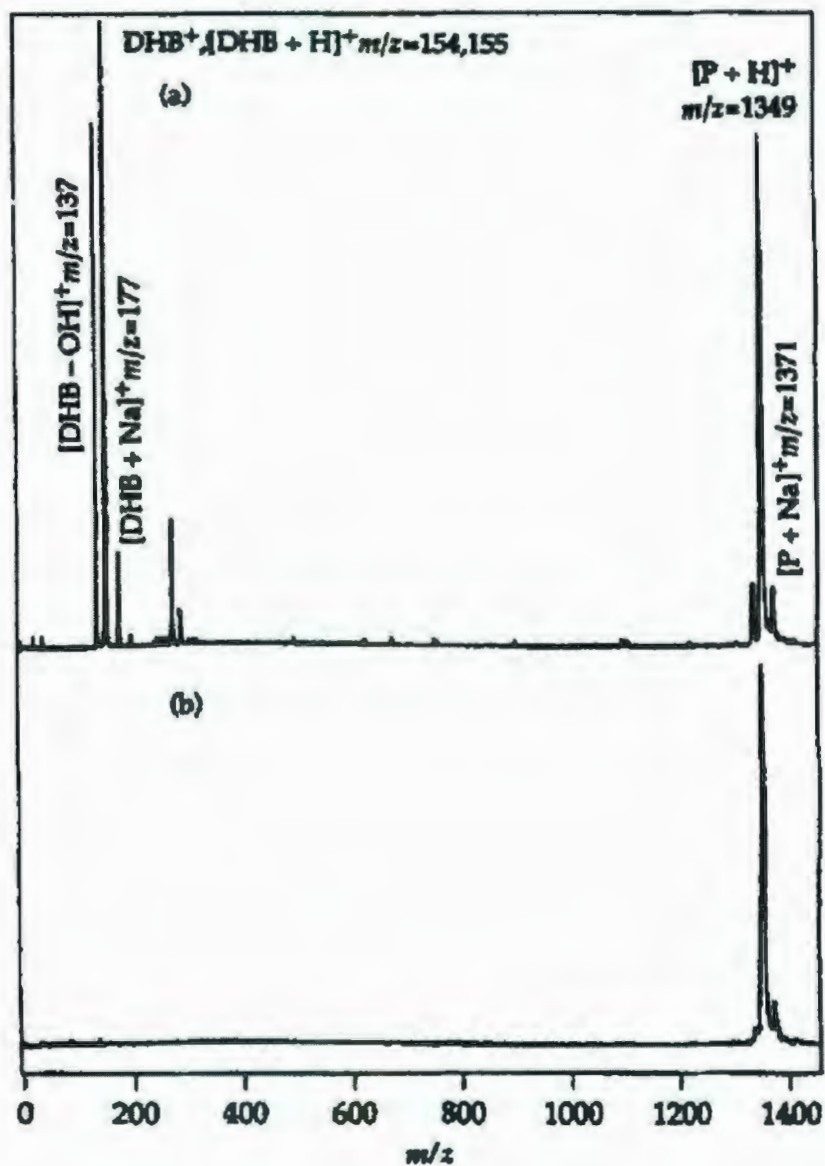


Figure 1.7 Analysis of substance P by DHB matrix using (a) matrix : analyte ratio of 1000:1 and (b) matrix : analyte ratio of 100:1 [63].

The preformed/cluster model is a model which assumes that analyte molecules are already separated from each other and are in ionic form, just waiting to be desorbed [66]. However this model is not able to explain the matrix suppression effect. Although this

model demonstrates that preformed matrix ions may donate their charge to analytes within the same cluster, attaining MSE would still require that there could never be more charges than analyte molecules in any cluster, which is statistically impossible. This is particularly true since the analyte ions are not uniformly distributed in many MALDI samples [67,68]. However, mobility is much higher in the gas phase and mixing is improved, which decreases inhomogeneities in sample distribution. This fact, combined with interconversion reactions, can explain the MSE.

If an analyte reacts efficiently with matrix ions of one polarity, then it is unlikely that a reaction in the opposite polarity would occur to any great extent. Thus, MSE usually only occurs and is observed in one polarity. This polarity can often be easily predicted. For example, a basic analyte depleting a protonated matrix will illustrate matrix-ion suppression in positive mode. It should be noted that predictions must use gas-phase properties instead of solution-phase.

For full suppression, it is required that enough analyte be present to react with all the primary matrix ions. Thus, the MSE is highly dependant on concentration, as well as laser fluence, which determines the concentration of primary ions.

### **1.3.2 Matrix Suppression Effect: Optimum Matrix/Analyte ratio**

It has been reported that when analytes less than 20 000 Da are mixed with common matrices at relatively high molar ratio (10:1 to 2000:1 matrix to analyte ratio), all positive matrix-related ions can be suppressed. This has been observed in positive polarity with several matrices such as nicotinic acid, CHCA and DHB [62,63,69]. As previously stated, since matrix suppression involves all types of ions, this has ruled out competition

models of the effect, and suggests that multiply excited aggregates of the matrix are the primary ion generators.



Since matrix ions may also form in the absence of analyte, a similar pathway must lead to the production of matrix ions as well



The experimental data have been found to be well represented by equations 1 and 2 and are consistent. However, the first experiments were only applied to positive ion matrices. A matrix can react amphoterically with analytes. In parallel to scheme 1, an equation can be proposed for deprotonation



If all of the excited matrix is utilized, then matrix-ion suppression should be observed, while matrix signals will be observed in the positive mode. The observed polarity of matrix ion suppression is determined by thermodynamics and the kinetics of reaction pathways, however, it must be mentioned that this suppression is a property of the analyte/matrix pair, and not due to the matrix alone.

In the aforementioned study [52], the authors chose matrices with a basic or neutral tendency to study negative ion suppression; 2-amino-3-hydroxypyridine (AHP) (pKa 7.2) and 3-aminoquinoline (3AQ)(pKa 8.8). The analytes studied included 3-morpholino-propane-sulfonic acid (MOPS) and 4-(2-hydroxyethyl)-piperazine-1-ethansulfonic acid (HEPES). When using the 3AQ, a matrix to analyte ratio of approximately 10:1 was used, and it was found that full matrix-ion suppression occurred

in negative polarity, in the same analysis, there were many strong matrix signals in the positive ion polarity mode. However, when using a neutral, or even an acidic matrix, suppression was not observed in either mode.

Matrix suppression requires that an analyte be thoroughly mixed with the matrix, and that a matrix form no more than a bilayer during crystallization. Otherwise, as an analyte becomes diluted, not all excited matrix molecules will be able to react with an analyte molecule. Knochenmuss *et al.* [52] tested the matrix suppression effect by monitoring the M:A ratio for the pair of 3AP with MOPS and were able to plot a curve with three distinct regions. At a high M:A molar ratio the curve is linear, however, from M:A of 700-1000, there was a decrease in matrix signal, indicating that suppression had occurred. Finally, between M:A of 50-700, a plateau exists where increasing the concentration of analyte has almost no effect on signal observed, and thus, at lower mixing ratios, only was the full MSE observed. This structured curve was found to be comparable between several analytes, including valinomycin, adenosine monophosphate, insulin and cytochrome C.

Hao *et al.* studied the resulting positive and negative ion mode MALDI mass spectra of various saccharides [40]. Although the mechanism has been studied and proposed for peptides and proteins, until this study, little investigation of saccharides occurred. The authors tested the matrices of sinapinic acid (SA), 2,5-dihydroxybenzoic acid (DHB) and CHCA [40]. DHB was found to be the best matrix for the saccharides tested; raffinose, stachyose, and dextran. A matrix to analyte mole ratio of about 2000 to 1 was employed. It was found that in positive mode, the main ions were due to the

sodiated and potassiated adducts of the saccharides, while in negative mode only minor analyte ions  $[M-H]^-$  were observed. The matrix ions of DHB were almost totally suppressed in positive polarity mode, but were abundant in negative mode.

Unfortunately, no matrix suppression was observed when the CHCA or SA matrices were used instead. Here, cationized oligosaccharides were observed, but large matrix peaks were present as well, and adjustments of laser fluence and M:A ratios were not reported to induce MSE. The authors propose that for oligosaccharides, the matrix-assisted ionization is more important than the matrix-assisted desorption [40]. Thus, saccharides do not behave amphoterically as peptides do, and they prefer to form cationized (i.e. metal adducts) species in positive polarity mode. They do not easily form protonated or deprotonated ions because they lack the functional groups necessary to stabilize these states. However, alkali ions can easily coordinate with the oxygen atoms that are present.

For analysis of polysaccharides such as dextran T40 and T70, no matrix suppression was observed in either polarity, and it was demonstrated that the spectra relied more on the crystallization of the sample and a higher matrix-to-analyte ratio [40]. Thus, as opposed to MALDI spectra of oligosaccharides, there was virtually no difference between the spectra of polysaccharides in either polarity mode. It is possible that these are ionized by a different mechanism, and the matrix assisted desorption is the key feature instead of ionization. Thus, the key processes in MALDI of a sample seem related directly to their molecular weight.

### 1.3.3 Analyte Suppression Effect: Excessive Matrix/Analyte ratio

The matrix signal in the presence of an analyte, or the intensities of multiple analytes can be modified by secondary reactions [70]. For two analytes, A and B, reactions can take place with the matrix ions (M) and with each other:



Thus, there are two pathways for analyte suppression. If analyte B reacts more readily with  $M^{++}$  than A, then  $A^{++}$  would not yield a dominant ion, as opposed to being readily apparent in the lack of B. As well, charge transfer reactions between analytes may occur. The analyte suppression effect (ASE) implies that sufficient analyte be present to deplete the matrix (otherwise both eqns 1 and 2 may occur), so ASE is accompanied by MSE.

The analyte suppression effect illustrates an extreme example of a general problem in MALDI; varying sensitivity factors of analytes depending on the mixture being studied. From the secondary ionization model, the parameters important to control these effects are the reaction exothermicities, charge transfer reactions, and the relative concentrations of reactants [71].

### 1.3.4 Surfactant-Mediated Matrix Suppression

Guo *et al.* [72] described a technique where the surfactant cetyltrimethylammonium bromide (CTAB) was used as a co-additive to the typical CHCA matrix for MALDI-MS analysis of various small molecules (MW < 500 daltons). This method was found to

suppress the matrix-related ions, and the mass resolution of low-mass analyte ions was also improved. The analytes studied included amino acids, peptides, small nitrogen-containing drugs, cyclodextrins, and mixtures of these. In the experimental design, a matrix : analyte : surfactant ratio (M:A:S) of 100 000: 1 : 10-100 was used. Thus, this is a fairly large molar excess of matrix, even by MALDI standards, for small molecule analysis.

The above methodology demonstrated that at a mixing ratio of about 1000 : 1 of CHCA to surfactant, CTAB, the matrix-related ions could be mostly suppressed, while still retaining the particular desired analyte signals. Although the analyte signals were also partially suppressed, they were better resolved and had a similar signal-to-noise (S/N) ratio. However, for some standard peptides, it was found that the detection limit was drastically worsened to about 90 fmol from 4 fmol for a typical analysis.

The surfactant CTAB was shown to function purely as a co-additive (as a suppressor) and the matrix is still required to absorb the UV energy and to allow the MALDI process to occur. The authors propose that the mechanism given by Knochenmuss [73] (ie. MSE) can explain this phenomenon. Excited matrix species act as precursors for both protonated and cationized ions. During desorption/ionization, analytes abstract a relevant ion from matrix carriers to yield analyte ions. The matrix-related ions are formed from interactions amongst the excited matrix molecules. For matrix suppression to occur, all excited matrices should react with analyte molecules so that the interaction between matrix molecules should be reduced as much as possible. Thus, this sets a strict limit on the matrix : analyte mixing ratios and all matrix molecules should be near at least one

molecule of the analyte. The authors hypothesized that the CTAB could function as an analyte during the desorption/ionization. This would result in less excited matrix species being present, and would decrease the formation of matrix-related ions. Figure 1.8 illustrates the suppression effect that CTAB had on CHCA matrix at a mole ratio of 1000:1 matrix/surfactant [72].

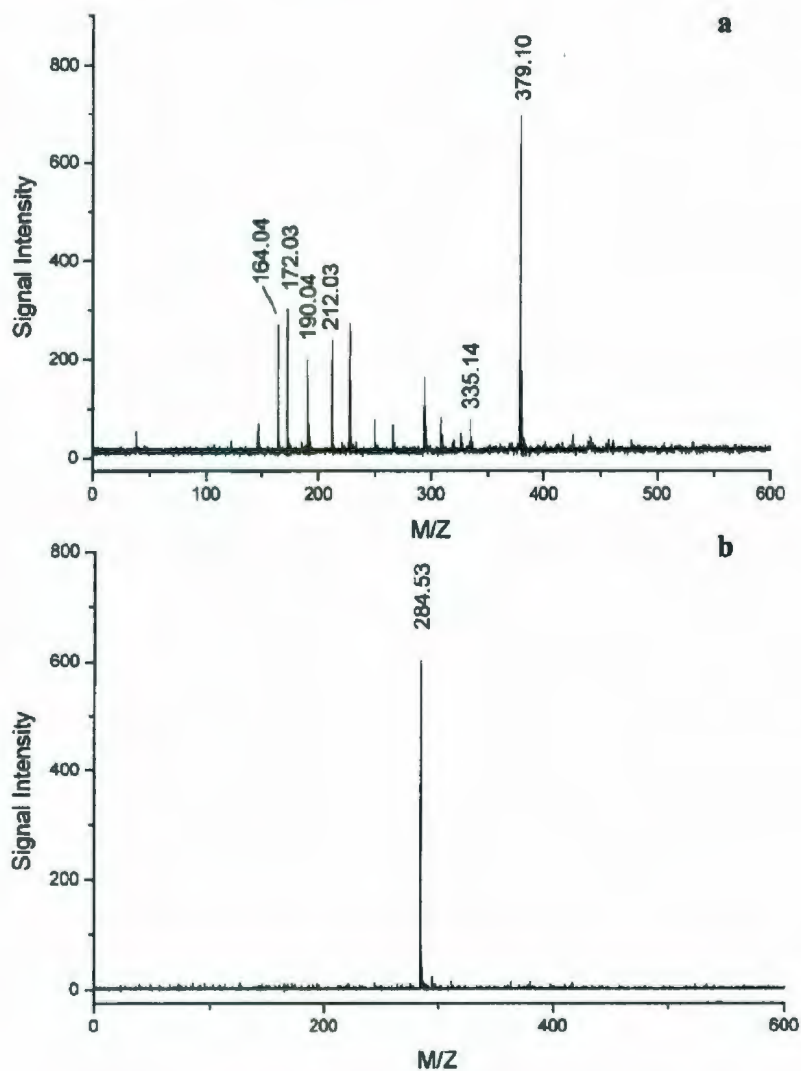


Figure 1.8 Mass spectra of CHCA and suppressed matrix of CHCA with CTAB surfactant [72]. (a) CHCA matrix at 0.1 mol/L (b) suppressed CHCA with CTAB ratio of 1000:1 and keeping CHCA concentration the same.

In one of the few other studies using surfactants in MALDI analysis, Rajnarayanan *et al.* [74] used alkylammonium ion-pairing reagents, including cetyltrimethylammonium bromide, to test as a possible means of recovering peptide/protein MALDI signals from sodium dodecyl sulfate-contaminated mixtures. The (SDS) is a commonly used and powerful solubilizing agent for proteins, peptides, and other biomolecules, and is routinely used in electrophoretic and chromatographic methods [75]. Unfortunately, SDS follows the trend of other surfactants; in trace amounts, it suppresses analyte signals during MALDI analysis and thus has a negative impact on the final analysis. There are various methods to remove SDS during sample clean-up, including a staining/destaining step during gel electrophoresis, precipitation with cold acetone [76], extraction with chloroform-water-methanol [77], size separation by dialysis [78], and gel filtration [79]. However, all of these methods leave residual SDS and this still affects the signals.

In the above study, ion-pairing reagents, such as long-chain alkylammonium salts have a cationic group which interacts electrostatically with the anionic sulfate group of SDS or other anionic surfactants to form neutral and amphipathic ion pairs [74]. The authors used a two-layer sample preparation method with a matrix-ion-pairing reagent on the bottom layer, and a top layer of the analyte (SDS, a buffer, and protein). In these experiments, a very high matrix to analyte ratio of 20 000 : 1 was used to dilute the effects of buffers and salts.

A series of ammonium and tetraalkylammonium salts were tested. They were monitored for their ability to enhance MALDI-MS signals from SDS-containing proteins in water and buffer solutions. In their method, a 0.1 % CTAB solution was added to a

0.1% SDS solution of the analyte. For the analysis, it was found that the two-layer method produced better results than the dried-droplet. The authors calculated the recovery ratio, which was the ratio of the signal achieved with SDS plus the ion pair reagent to the signal achieved with only SDS.

Overall, alkylammonium reagents were found to be more effective than non-alkylammonium salts. Within the alkylammonium salts, the order of recovery was CTAB > tetrahexylammonium bromide (THAB) > tetrapentylammonium bromide (TPAB) > tetramethylammonium bromide (TMAB). This indicates that longer alkyl groups in tetraalkylammonium salts give rise to greater recovery of analyte signals. The observation that CTAB yielded better results than TMAB indicates that a single unbranched chain is more favourable than four shorter chains (four hexyl groups in THAB) with a higher number of carbon atoms. The enhancement ratio for those samples with CTAB ranged from 1.4 to 11.6. A significant effect was also observed to be due to the buffer.

The information and results pertaining to the use of various long chain and branched tetraalkylammonium salts, as described above, will lead to a further study within this thesis (Chapter 2) as potential surfactants in surfactant-mediated MALDI experiments.

## 1.4 SURFACTANTS

Surfactant-mediated MALDI-TOF-MS was researched as a possible avenue for minimizing the problems dealing with adequate resolution of low-mass molecules while still maintaining the traditional small organic matrices. This method was seen to have the potential to be powerful, simple, and is not yet heavily researched. Except for the use of surfactants such as SDS in the clean-up process for peptides, these molecules were typically avoided in the mass spectrometer as they are well known to be ion-suppressors.

### 1.4.1 Overview of Surfactants

Surfactants are organic compounds composed of a hydrophobic body (the “tail”) and a hydrophilic portion (the “head”). Thus, they are amphiphilic.

Surfactants are classified by the groups contained in their “head”. They typically fall into the category of being cationic, anionic, nonionic, or zwitterionic. Cationic surfactants have positively charged end groups, and some examples are cetylpyridinium chloride (CPC), cetyltrimethylammonium bromide (CTAB) and benzalkonium chloride (BAC). Anionic surfactants have a net negative charge on their “head”. These are often based on sulfate, sulfonate, or carboxylate anions. Zwitterionic surfactants are amphoteric. They are essentially a single particle salt acting as both an anion and a cation. They can often have a base coupled to an acid within the surfactant molecule. Nonionic surfactants have no net charge. Some examples include alkyl poly(ethylene oxide), fatty alcohols (ex. cetyl alcohol), and copolymers of poly(ethylene oxide) and poly(propylene oxide).

### **1.4.2 Surfactant Properties and Applications**

Both cationic and anionic surfactants have powerful properties that are pH-sensitive, as well as being sensitive to ionic strength and their counterion. Cationic surfactants are often used in the purification of DNA, in disinfecting methods, and in drug/vaccine delivery systems. Anionic surfactants are typically used for their ability to disrupt cell membranes and fully denature proteins. Zwitterionic surfactants, being electrically neutral, are useful in protecting the native conformation of proteins. They are also used as an alternative choice to non-ionic surfactants in applications such as ion-exchange, electrophoresis, and isoelectric focusing. The nonionic surfactants are more gentle detergents. They have been used for applications such as solubilizing proteins. In doing so, they do not readily destroy the protein and can conserve the enzymatic activity and functions.

A brief summary of the classifications of surfactants, with specific examples and their properties and uses is given in Table 1.3. The surfactants illustrated have their critical micelle concentration (CMC) listed. Above their CMC, micelles begin to form. Essentially this is the upper limit at which monomers exist. At higher CMC's, the surfactants bind weaker and are removed more easily by dialysis or other methods. The aggregation number is the numerical average of monomers in a micelle.

Table 1.3. A summary of the physical properties and their applications among surfactant classes. Note: CTAB = cetyltrimethylammonium bromide; TTAB = trimethylammonium bromide; SDS = sodium dodecyl sulfate; NaCo = sodium cholate; CHAPS = 3-[(3-Cholamidopropyl)dimethylammonio]-1-propanesulfonate; SB3-16 = 3-(N,N-dimethylpalmitylammonio) propanesulfonate. Adapted from [80].

Category	Cationic		Anionic		Nonionic		Zwitterionic	
	CTAB	TTAB	SDS	NaCo	Brij 35	Triton X-100	CHAPS	SB3-16
Molecular Weight	365	337	289	431	1200	625	615	392
CMC (mM)	1	4-5	7-10	9-15	0.05-0.1	0.2-0.9	6	0.01-0.06
Aggregation Number	170	80	62	39509	20-40	100-155	10	155
Average micellular weight	62000	27000	18000	900-1300	48000	80000	6150	60700
Diagnostic applications	✓	✓	✓	✓	✓	✓	✓	✓
Molecular Biology			✓	✓		✓		
Cell Culture								
Electrophoresis/Chromatography			✓	✓	✓	✓	✓	✓
Membrane Protein Solubilization			✓	✓	✓	✓	✓	✓
Enzymology	✓		✓	✓	✓	✓	✓	✓
Antigen/Vaccine Preparation	✓		✓	✓			✓	
Drug delivery/liposomes	✓		✓	✓	✓		✓	

## **1.5 THESIS OBJECTIVES**

This thesis began with the initial objective of testing various common surfactants as possible matrix-ion suppressors in MALDI-TOF-MS. The objectives were later developed into this specific list:

1. Test a representative group of cationic surfactants based on the CTAB derivative, and observe if they have the ability to induce matrix-ion suppression.
2. Test several different anionic surfactants as matrix-ion suppressors.
3. Test several neutral surfactants as matrix-ion suppressors.
4. Observe the degree of suppression in positive- and negative-ion mode.
5. Investigate the possibility of using surfactants to suppress matrix-ion signals to aid in the analysis of antioxidants found in berries.
6. Test this method for the analysis of vitamins and caffeine present in energy drinks.

## **1.6 CO-AUTHORSHIP STATEMENT**

Chapters 2, 3 and 4 were published in peer-reviewed journals with D. Grant as the principal author and Dr. R.J. Helleur as the author of correspondence. It is appropriate to clarify both authors' contributions to these papers.

The principal author proposed the research of using surfactants for the analysis of the small molecules in Chapter 2.

All experimental work was performed by the principal author. This includes all flavonoid extractions from berry samples as well as chemical workup prior to instrumental analysis, including MALDI and LC-MS. The principal author also performed all data analysis with advice from Dr. Helleur about the interpretation of mass spectra and chromatograms.

The principal author also drafted all manuscripts and replied to comments of peer reviewers. Some editing was undertaken by Dr. Helleur.

## 1.7 REFERENCES

1. Karas M, Bachmann D, Hillenkamp F. *Anal. Chem.* 1985; **57**: 2935.
2. Tanaka K, Waki H, Ido Y, Akita S, Yoshida Y, Yoshida T. *Rapid Commun. Mass Spectrom.* 1988; **2**: 151.
3. Karas M, Bahr U, Ingendoh A, Nordhoff E, Stahl B, Strupat K, Hillenkamp F. *Analytica Chimica Acta.* 1990; **241**:175.
4. Distler AM, Allison J. *Anal. Chem.* 2001; **73**: 5000.
5. Bahr U, Deppe A, Karas M, Hillenkamp F. *Anal. Chem.* 1992; **64**: 2866.
6. Weidner S, Kuhn G, Friedrich J. *Rapid Commun. Mass Spectrom.* 1998; **12**: 1373.
7. Young S. MALDI-TOF mass spectrometry. Mauritz Group Research Page. (2003). <http://www.psrc.usm.edu/mauritz/maldi.html>
8. Gates P. Matrix-assisted laser desorption ionization (MALDI). Mass Spectrometry www Server. (1997). <http://www-methods.ch.cam.ac.uk/meth/ms/theory/maldi.html>
9. Sigma-Aldrich. MALDI-Mass Spectrometry. Analytix: Advances in Analytical Chemistry, 6 (2001).
10. Verbueken AH, Bruynseels FJ, Van Grieken R, Adams F. *Inorganic Mass Spectrometry.* 1988: 186.
11. Delgass WN, Cook RG. *Science.* 1987; **235**: 545.
12. Limback P.A. *Spectroscopy.* 1998; **13**: 16.
13. Brown RS and Lennon JJ. *Analytical Chemistry.* 1995; **67**: 1998.
14. Colby SM. *Rapid Communications in Mass Spectrometry.* 1994; **8**: 865.
15. Delayed Extraction. Wikipedia. Obtained June 2009. [http://en.wikipedia.org/wiki/File:Delayed\\_extraction.gif](http://en.wikipedia.org/wiki/File:Delayed_extraction.gif)
16. Cornish TJ. *Rapid Communications in Mass Spectrometry.* 1993; **7**: 1037.
17. Flensburg J. *Journal of Biochemical and Biophysical Methods.* 2004; **60**: 319.

18. Wang TI. *Review of Scientific Instruments*. 1994; **65**: 1585.
19. Matrix materials for matrix-assisted laser desorption ionization-time of flight (MALDI-TOF): Guidelines for selection. Application Note, Applied Biosystems.
20. Hillenkamp F, Karas M, Beavis RC, Chait BT. *Analytical Chemistry*. 1991; **63**: 1193A.
21. Owen S.J., Meier F.S., Brombacher S. and Volmer D.A. *Rapid Communications in Mass Spectrometry*. 2003; **17**, 2439.
22. MALDI in the lab. Stanford Research Systems. (2003). Obtained December 2003. <http://www.srsmaldi.com/Maldi/Lab.html>
23. Li Y, Zhang LK, Gross ML. *Proceedings 50<sup>th</sup> ASMS Conference on Mass Spectrometry and Allied Topics*. 2002; 583.
24. Li Y, Gross ML. *Journal of the American Society for Mass Spectrometry*. 2004; **15**: 1833.
25. Towers M, Cramer R. *Spectroscopy*. 2007; **22**: 29.
26. Chapman JR. *Methods in Molecular Biology*. Humana Press, Totowa, NJ. 1996; **61**.
27. Wei H, Nolkranz K, Powell DH, Woods JH, Ko MC, Kennedy RT. *Rapid Communications in Mass Spectrometry*. 2004; **18**: 1193.
28. Hanton SD, Hyder IZ, Stets JR, Owens KG, Blair WR, Guttman CM, Giuseppetti AA. *Journal of the American Society for Mass Spectrometry*. 2004; **15**: 168.
29. Momcilovic D, Wahlund KG, Wittgren B, Brinkmalm G. *Rapid Communications in Mass Spectrometry*. 2005; **19**: 947.
30. Zhang H, Caprioli RM. *Journal of Mass Spectrometry*. 1996; **31**: 1039.
31. Olaf Bornsen K. *Analytical Methods and Instrumentation*. 1995; **2**: 202.
32. Cohen LH, Gusev AI. *Analytical and Bioanalytical Chemistry*. 2002; **373**: 571.
33. Kraj A, Dylag T, Gorecka-Drzazga A, Bargiel S, Dzibuban J, Silberring J. *Acta Biochimica Polonica*. 2003; **50**: 783.
34. Lee PJ, Chen W, Gebler JC. *Analytical Chemistry*. 2004; **76**: 4888.

35. McCombie G, Knochenmuss R. *Analytical Chemistry*. 2004; **76**: 4990.
36. Guo Z, He L. *Analytical and Bioanalytical Chemistry*. 2007; **387**: 1939.
37. Applied Biosystems; Application Note; Small-Molecule Quantitation Using Automated Single-Shot Averaging MALDI-TOF Mass Spectrometry; 2002.
38. Falkner JA, Kachman M, Veine DM, Walker A, Strahler JR, Andrews PC. *Journal of the American Society for Mass Spectrometry*. 2007; **18**: 850.
39. Wang Y, Schneider BB, Covey TR, Pawliszyn J. *Analytical Chemistry*. 2005; **77**: 8095.
40. Hao C., Ma X., Fang S., Liu Z., Liu S., Song F., and Liu J. *Rapid Communications in Mass Spectrometry*. 1998; **12**, 345.
41. Lattova E, Perreault H. *Proceedings 50<sup>th</sup> ASMS Conference on Mass Spectrometry and Allied Topics*. 2002: 439.
42. Sturiale L., Garozzo D., Silipo A., Lanzetta R., Parrilla M. and Molinaro A. *Rapid Communications in Mass Spectrometry*. 2005; **19**, 1829.
43. Andalo C., Bocchini P., Pozzi R. and Galletti G.C. *Rapid Communications in Mass Spectrometry*. 2001; **15**, 665.
44. Tholey A., Wittmann C., Kang M.J., Bungert D., Hollemeyer K. and Heinzie E. *Journal of Mass Spectrometry*. 2002; **37**: 963.
45. Griffiths W.J. Liu S., Alvelius G. and Sjovall J. *Rapid Communications in Mass Spectrometry*. 2003; **17**, 924.
46. Sleno L. and Volmer D.A. *Rapid Communications in Mass Spectrometry*. 2005; **19**, 1928.
47. Su A.K., Liu J.T., Lin C.H. *Analytical Chimica Acta*. 2005; **546**, 193.
48. Su A.K., Liu J.T. and Lin C.H. *Talanta*. 2005; **67**, 718.
49. Jackson S.N., Wang H.Y.J., Woods A.S., Ugarov M., Egan T. and Schultz J.A. *Journal of the American Society for Mass Spectrometry*. 2005; **16**, 133.
50. Jones J.J., Stump M.J., Fleming R.C., Lay J.O., Wilkins C.L. *Journal of the American Society for Mass Spectrometry*. 2004; **15**, 1665.

51. Touboul D., Piednoel H., Voisin V., De La Porte S., Brunelle A., Halgand F. and Laprevote O. *European Journal of Mass Spectrometry*. 2004; **10**, 657.
52. Knochenmuss R., Karbach V., Wiesli U., Breuker K. and Zenobi R. *Rapid Communications in Mass Spectrometry*. 1998; **12**, 529.
53. Smirnov IP, Zhu X, Taylor T, Huang Y, Ross P, Papayanopoulos IA, Martin SA, Pappin DJ. *Analytical Chemistry*. 2004; **76**: 2958.
54. Leo Y.C. Cheng S. and Chan T.W.D. *Rapid Communications in Mass Spectrometry*. 1998; **12**, 993.
55. Guo Z. and He L. *Analytical Bioanalytical Chemistry*. 2007; **387**, 1939.
56. Cheng SW, Chan TWD. *Rapid Communications in Mass Spectrometry*. 1996; **10**: 907.
57. Asara JM, Allison J. *Analytical Chemistry*. 1999; **71**: 2866.
58. Simmons TA, Limbach PA. *Rapid Communications in Mass Spectrometry*. 1997; **11**: 567.
59. Knochenmuss R. *Journal of Mass Spectrometry*. 2002; **37**: 867.
60. Bokelmann V, Spengler B, Kaufmann R. *European Journal of Mass Spectrometry*. 1995; **1**: 81.
61. Chan TWD, Colburn AW, Derrick PJ. *Organic Mass Spectrometry*. 1992; **27**: 53.
62. Chan TWD, Colburn AW, Derrick PJ. *Organic Mass Spectrometry*. 1991; **26**: 342.
63. Knochenmuss R, Dubois F, Dale MJ, Zenobi R. *Rapid Communications in Mass Spectrometry*. 1996; **10**: 871.
64. Knochenmuss R, Karbach V, Wiesli U, Breuker K, Zenobi R. *Rapid Communications in Mass Spectrometry*. 1998; **12**: 529.
65. Knochenmuss R. *Analytical Chemistry*. 2003; **75**: 2199.
66. Gluckmann M, Pfenninger A, Kruger R, Thierolf M, Karasa M, Horneffer V, Hillenkamp F, Strupat K. *International Journal of Mass Spectrometry*. 2001; **210**:121.

67. Dai Y, Whittal RM, Li L. *Analytical Chemistry*. 1996; **68**: 2494.
68. Horneffer V, Forsmann A, Strupat K, Hillenkamp F, Kubitscheck U. *Analytical Chemistry*. 2001; **73**: 1016.
69. Juhasz P, Wang BH, Biemann K. *Proceedings 40<sup>th</sup> Annual ASMS Conference in Mass Spectrometry*. 1992: 372.
70. Knochenmuss R. *The Analyst*. 2006; **131**: 966.
71. Knochenmuss R, Stortelder A, Breuker K, Zenobi R. *Journal of Mass Spectrometry*. 2000; **35**: 1237.
72. Guo Z., Zhang Q., Zou H., Guo B. and Ni J. *Analytical Chemistry*. 2002; **74**: 1637.
73. Knochenmuss R, Dubois F, Dale M, Zenobi R. *Rapid Communications in Mass Spectrometry*. 1996; **10**: 871.
74. Rajanarayanan R.V. and Wang K. *Journal of Mass Spectrometry*. 2004; **39**, 79.
75. Maizel JV. *Trends in Biochemical Science*. 2000; **25**: 590.
76. Ehring H, Stromberg S, Tjernberg A, Noren B. *Rapid Communications in Mass Spectrometry*. 1997; **11**: 1867.
77. Puchades M, Westman A, Blennow K, Davidsson P. *Rapid Communications in Mass Spectrometry*. 1999; **13**: 344.
78. Swiderek KM, Klein ML, Hefta SA, Shively JE. *Techniques in Protein Chemistry 6*. 1995: 267.
79. Amons R, Schrier PI. *Analytical and Bioanalytical Chemistry*. 1981; **116**: 439.
80. Detergent Properties and Applications. Sigma-Aldrich. 2006. Obtained June 2006. [http://www.sigmaaldrich.com/etc/medialib/docs/Sigma/Instructions/detergent\\_selection\\_table.Par.0001.File.tmp/detergent\\_selection\\_table.pdf](http://www.sigmaaldrich.com/etc/medialib/docs/Sigma/Instructions/detergent_selection_table.Par.0001.File.tmp/detergent_selection_table.pdf)

## Chapter 2

# **SURFACTANT-MEDIATED MATRIX-ASSISTED LASER DESORPTION/IONIZATION TIME-OF-FLIGHT MASS SPECTROMETRY OF SMALL MOLECULES**

A version of this chapter has been published. Grant DC and Helleur RJ. Surfactant-mediated matrix-assisted laser desorption/ionization time-of-flight mass spectrometry of small molecules. *Rapid Commun. Mass Spectrom* 2007; **21**: 837-845.

## ABSTRACT

A variety of surfactants have been tested as matrix ion suppressors for the analysis of small molecules by matrix-assisted laser desorption/ionization time-of flight mass spectrometry. Their addition to the common matrix  $\alpha$ -cyano-4-hydroxycinnamic acid (CHCA) greatly reduces the presence of matrix-related ions when added at the appropriate mole ratio of CHCA/surfactant, while still allowing the analyte signal to be observed. A range of cationic quaternary ammonium surfactants, as well as a neutral and an anionic surfactant, were tested for the analysis of phenolics, phenolic acids, peptides and caffeine. It was found that the cationic surfactants, particularly cetyltrimethylammonium bromide (CTAB), were suitable for the analysis of acidic analytes. The anionic surfactant, sodium dodecylsulfate, showed promise for peptide analysis. For trialanine, the detection limit was observed to be in the 100 femtomole range. The final matrix:surfactant mole ratio was a critical parameter for matrix ion suppression and resulting intensity of analyte signal. It was also found that the mass resolution of analytes was improved by 25-75 %. Depth profiling of sample spots, by varying the number of laser shots, revealed that the surfactants tend to migrate toward the top of the droplet during crystallization, and that it is likely that the analyte is also enriched in this surface region. Here, higher analyte/surfactant concentration would reduce matrix-matrix interactions (known to be a source of matrix-derived ions).

## 2.1 INTRODUCTION

Matrix-assisted laser desorption/ionization (MALDI) is a powerful technique which was first described by two independent groups, a German group led by Hillenkamp and Karas and Tanaka's Japanese group, nearly simultaneously in the late 1980s [1,2]. MALDI evolved from similar desorption/ionization methods such as fast atom bombardment (FAB) and laser desorption/ionization (LDI) mass spectrometry and it has been found to be useful in the analysis of macromolecules, such as proteins, oligonucleotides, and synthetic polymers [1-6]. Its distinguishing feature is that the analyte is embedded in a molar excess of chemical matrix.

Although MALDI time-of-flight mass spectrometry (MALDI-TOFMS) has proven to be innovative in the analysis of macromolecules, its applications to small molecules (< 500 Da) has yet to be fully exploited. One of the fundamental reasons for this has been the abundance of matrix-related ions, due to the decomposition and various reactions of the associated matrix in the low mass range of spectra.

There have been several methods studied to improve matrix ion interference. These include using fullerenes [7,8], inorganic compounds [2,9-12] and high-mass molecules [13,14]. Carbon nanotubes were first investigated as a potential matrix for MALDI by Xu *et al.* [15] and there have been studies that looked at derivatizing nanotubes and using them as a matrix for cyclodextrins, peptides, carbohydrates, and small molecules [16-19]. Although these methods work well, they have limited application, do not incorporate the conventional, well-established organic matrices, and many of the above materials are not commercially available. Thus, when using

commercial organic matrices, techniques for suppression of matrix-ion signals are still desired to improve MALDI analysis of small molecules.

Ion suppression was first reported by Chan *et al.* [20] who observed an absence of matrix peaks when an optimal molar ratio of nicotinic acid to insulin was used.

Knochenmuss *et al.* further investigated the mole ratio dependent matrix suppression effect (MSE) for small to medium sized analytes (1000 – 20 000 Da) and found that at appropriate matrix/analyte mixing ratios, the positively charged matrix-related ions could be fully suppressed [21]. This was found to be true regardless of the analyte form, whether it be a radical cation, protonated molecule or alkali-metal adduct. This approach has also been the focus of other studies [22,23]. Using conventional matrixes such as DHB (2,5-dihydroxybenzoic acid) and CHCA ( $\alpha$ -cyano-4-hydroxycinnamic acid), a matrix/analyte mole ratio of < 200: 1 was efficient for large molecule analysis, while for smaller molecules ratios of < 10:1 were selected. It is believed that under these conditions neutral analytes can deplete primary matrix ions by secondary ion-molecule reactions and when enough analyte is present to react with all excited matrix ions, matrix-matrix reactions will be minimized. A further requirement was that enough analyte must be present and the laser intensity should not be too high above the intensity threshold.

Another method used to achieve matrix-ion suppression was reported by Guo *et al* [24]. They found that the surfactant cetyltrimethylammonium bromide (CTAB) suppressed CHCA-related signals for the analysis of various peptides, cyclodextrin derivatives, and small drug molecules using a matrix/CTAB mole ratio of 1000:1. To our knowledge, they were the first to term this technique “matrix-suppressed laser

desorption/ionization" (MSLDI). This is interesting as surfactants are often avoided in mass spectrometry as they are known to be analyte ion suppressors; however, in this study, the amount of surfactant used was very low. Recently, Su *et al.* used this technique to analyze clandestine tablets for drugs, such as amphetamines and related compounds [25].

This research presents a more thorough exploration of the use of CTAB as a matrix-suppressor. As well, a variety of other surfactants were examined to determine if they also induce matrix-ion suppression. In addition, a wider class of small molecule analytes has been investigated with respect to their suitability for analysis by surfactant-mediated MALDI-TOFMS, including for the first time, acidic organics such as phenolics and phenolic acids. The optimum ratio of matrix/surfactant has been found for each analyte/surfactant group. Depth profile analysis within a given spot sheds some light on the mechanism of matrix-ion suppression and the properties of the surfactant.

## **2.2 EXPERIMENTAL**

### **2.2.1 Chemicals**

The  $\alpha$ -cyano-4-hydroxycinnamic acid (CHCA), *p*-coumaric acid, chrysin, trialanine (Ala-Ala-Ala), caffeine and quercetin were purchased from Sigma (St. Louis, MO, USA). Cetyltrimethylammonium bromide (CTAB), hexyltrimethylammonium bromide (HTAB), dodecyltrimethylammonium bromide (DDTAB), tetrabutylammonium bromide (TBAB), decamethonium bromide (DMB), sodium dodecylsulfate (SDS) and Brij<sup>®</sup> 30 were obtained from Aldrich (Mississauga, ON, Canada). Deionized water,

methanol and acetone were all HPLC grade purchased from Fisher Scientific (Fair Lawn, New Jersey, USA). All chemicals were used without further purification.

### 2.2.2 Sample Preparation

CHCA stock solution was prepared fresh daily at a concentration of  $10 \text{ mg mL}^{-1}$  ( $52.9 \text{ mM}$ ) in a solution with a 1:4 volumetric ratio of water to methanol. All analytes were initially prepared as  $2.65 \text{ mM}$  solutions in acetone to insure dissolution and later diluted tenfold in the same solvent as CHCA solutions. Stock solutions of surfactants were also prepared at  $2.65 \text{ mM}$  in 80:20 methanol/water. When not in use, solutions were stored at  $4 \text{ }^{\circ}\text{C}$ . Fresh solutions of analytes and surfactants were prepared weekly.

Analytes ( $0.265 \text{ mM}$ ) were mixed with matrix at a 1:1 volume ratio ( $10 \text{ }\mu\text{L}$  of each) in a plastic centrifuge vial, and  $0.2 \text{ }\mu\text{L}$  aliquots of various concentrations of surfactant were added so that mole ratios of matrix : analyte : surfactant (M:A:S) of  $1000:5:S$  were achieved, where  $S$  ranged from 1 to  $1 \times 10^{-5}$ . All samples were vortex mixed for 30 seconds, then centrifuged at 3000 rpm for 30 seconds prior to spotting. For MALDI analysis,  $0.5 \text{ }\mu\text{L}$  spots were placed on a 96 x 2 well MALDI plate (Applied Biosystems, Framingham, MA, USA). The plate had a bonded hydrophobic surface with pre-punched holes having a diameter of 1.3 mm. This spotting surface is notably smaller than a regular MALDI plate (2 mm) and the hydrophobic perimeter helped produce a spot with more uniform thickness. It should be noted that samples containing surfactant required about 30 min to crystallize in a desiccator before being loaded into the MALDI-TOFMS.

Quercetin and chrysin (phenolics), trialanine (peptide), *p*-coumaric acid (phenolic acid), and caffeine (an alkaloid) were tested separately with each of the seven surfactants; five basic quaternary ammonium surfactants (HTAB, DDTAB, CTAB, TBAB and DMB), one anionic surfactant (SDS) and one neutral surfactant (Brij<sup>®</sup> 30) (Figure 2.1). Each surfactant was mixed into a fixed mole ratio matrix:analyte solution (1000:5) at varying surfactant mole ratios to examine the effect of both the chemical nature of the surfactant and its concentration on the resulting analyte signal. Parameters monitored were the analyte signal-to-noise ratio (S/N), resolution and ion intensities.

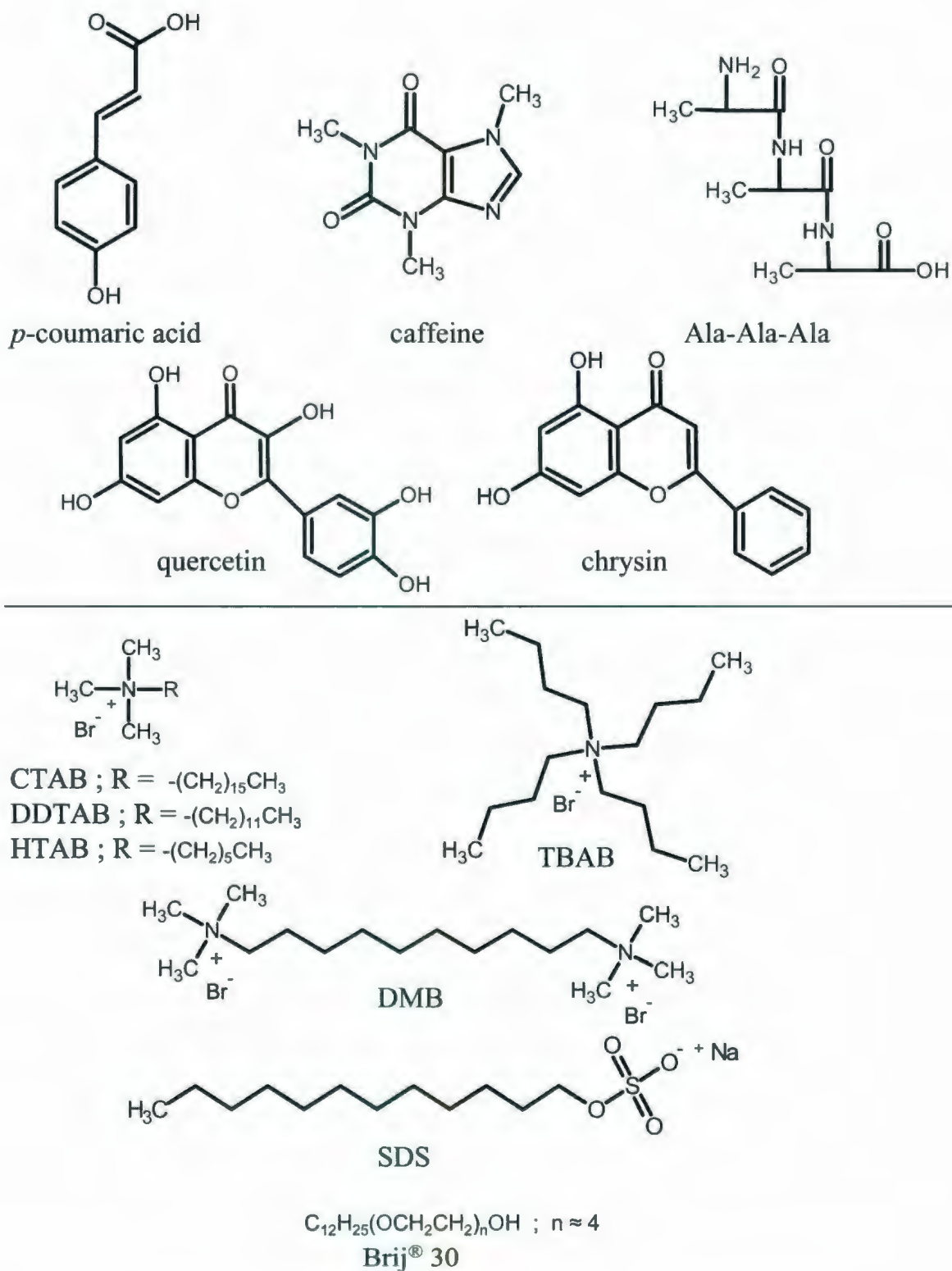


Figure 2.1. Molecular structure of analytes (top) and surfactants used (bottom).

### 2.2.3 Instrumentation

The MALDI-TOFMS was a Voyager DE<sup>TM</sup>-PRO purchased from Applied Biosystems (Framingham, MA, USA). The instrument was equipped with a video camera and the sample image was displayed on a monitor enabling the laser to be focused on a given spot and controlled manually. Positive ion reflectron mode was used. The instrument was equipped with a pulsed nitrogen laser (337 nm, 3 ns pulse duration, 3 Hz frequency) and a delayed extraction source. An accelerating voltage of 20 kV and a grid voltage setting of 71% were used. The laser fluence was set to 2400 arbitrary units and the extraction delay time of 145 ns (default parameter in software) was used. The acquisition mass range was 100-500 Da and all spectra were obtained by averaging 25 laser shots, unless otherwise stated. Spectra were analyzed using Version 4 of Data Explorer<sup>TM</sup> software. All resolution values were calculated at 50% of the maximum peak height.

## 2.3 RESULTS AND DISCUSSION

### 2.3.1 Influence of various surfactants

Figure 2.2(a) displays a MALDI-TOF mass spectrum of the CHCA matrix only. As can be seen, there are many ions that are typical of CHCA, such as a protonated molecular ion  $[M + H]^+$   $m/z$  190, a sodiated matrix adduct  $[M + Na]^+$   $m/z$  212, and a protonated matrix-dimer  $[2M + H]^+$   $m/z$  379. These and other matrix-related ions present in MALDI spectra are listed in Table 2.1 and agree with other reports [17,18]. These ions are all less than 500 Da and can complicate the analysis of small molecules.

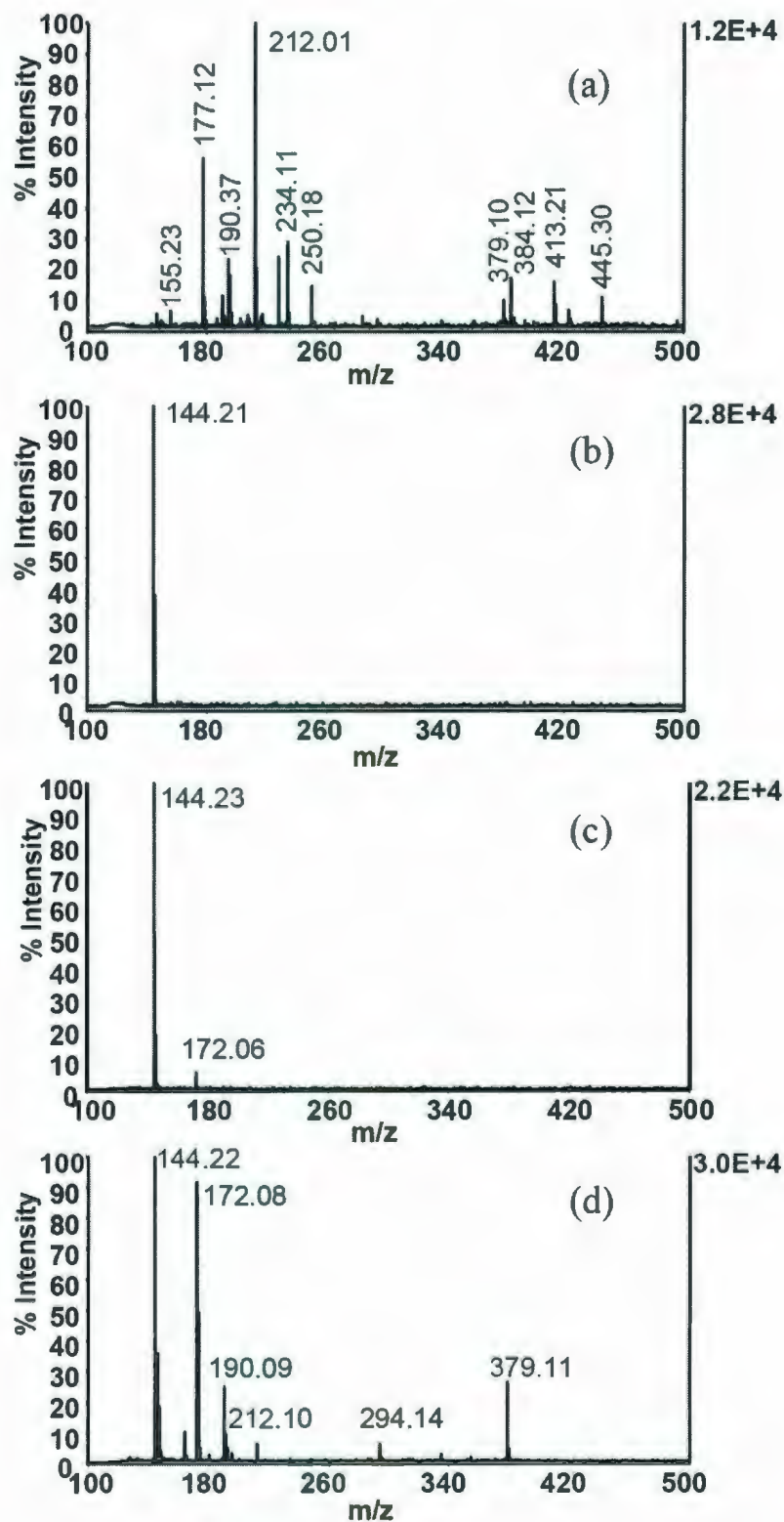


Figure 2.2. (a) MALDI mass spectra of CHCA matrix only. Resulting spectra of CHCA matrix /HTAB surfactant at mole ratio of (b) 1000:1, (c) 1000:0.01 and (d) 1000:0.0001.

Figure 2.2(b) shows the mass spectrum of CHCA with the addition of the cationic surfactant HTAB at a 1000:1 mole ratio of matrix/surfactant. The only ion observed is from the surfactant corresponding to  $[\text{HTAB} - \text{Br}]^+$   $m/z$  144. All matrix-related peaks are suppressed. Figure 2.2(c) shows the result of decreasing the mole ratio a hundred-fold to 1000: 0.01. The surfactant-related ion at  $m/z$  144 is still dominant, but one of the matrix fragment ions ( $m/z$  172) can be observed. When the ratio is finally lowered to 1000: 0.0001, as seen in Figure 2.2(d), matrix-ion suppression is lost and major CHCA ions listed in Table 2.1 are apparent.

Table 2.1. Common CHCA-fragment ions and adducts observed in mass spectra using a 337 nm  $\text{N}_2$  laser.

<i>m/z</i>	Ion form
122.08	$[\text{M} + \text{H} - \text{C}_3\text{H}_2\text{NO}]^+$
146.04	$[\text{M} - \text{CN} - \text{H}_2\text{O}]^+$
164.05	$[\text{M} + \text{H} - \text{CN}]^+$
172.04	$[\text{M} + \text{H} - \text{H}_2\text{O}]^+$
190.05	$[\text{M} + \text{H}]^+$
212.03	$[\text{M} + \text{Na}]^+$
234.02	$[\text{M} - \text{H} + 2\text{Na}]^+$
294.07	$[2\text{M} + \text{H} - \text{CO}_2 - \text{C}_2\text{H}_3\text{N}]^+$
335.10	$[2\text{M} + \text{H} - \text{CO}_2]^+$
379.09	$[2\text{M} + \text{H}]^+$

The ability of other surfactants to suppress the generation of CHCA-related ions while allowing the analyte ion signal to be observed, was of major interest; this phenomenon was tested individually for the analysis of five analyte molecules using each surfactant (at various concentrations) and the results are shown in Table 2.2. Figure 2.3(a) is representative of the results and illustrates a typical MALDI-TOF mass spectrum of *p*-coumaric acid (A) in the absence of surfactant. Two ions corresponding to the analyte are observed, a fragment ion  $[A + H - H_2O]^+$   $m/z$  147 and the protonated molecule  $[A + H]^+$   $m/z$  165. However, these analyte ions are accompanied by an abundance of matrix-ions, demonstrating that it would be quite difficult to identify or measure the ion signals of unknown low-mass compounds. Figure 2.3(b) shows the mass spectrum of the same analyte (A), but with the addition of CTAB (S) to the matrix (M) so that the M:A:S mole ratio is 1000:5:0.1. In this spectra, the analyte signals observed in Figure 2.3(a) are still present, but matrix-related ions have been successfully suppressed. The large signal at  $m/z$  284 is the surfactant-related ion  $[CTAB - Br]^+$ .

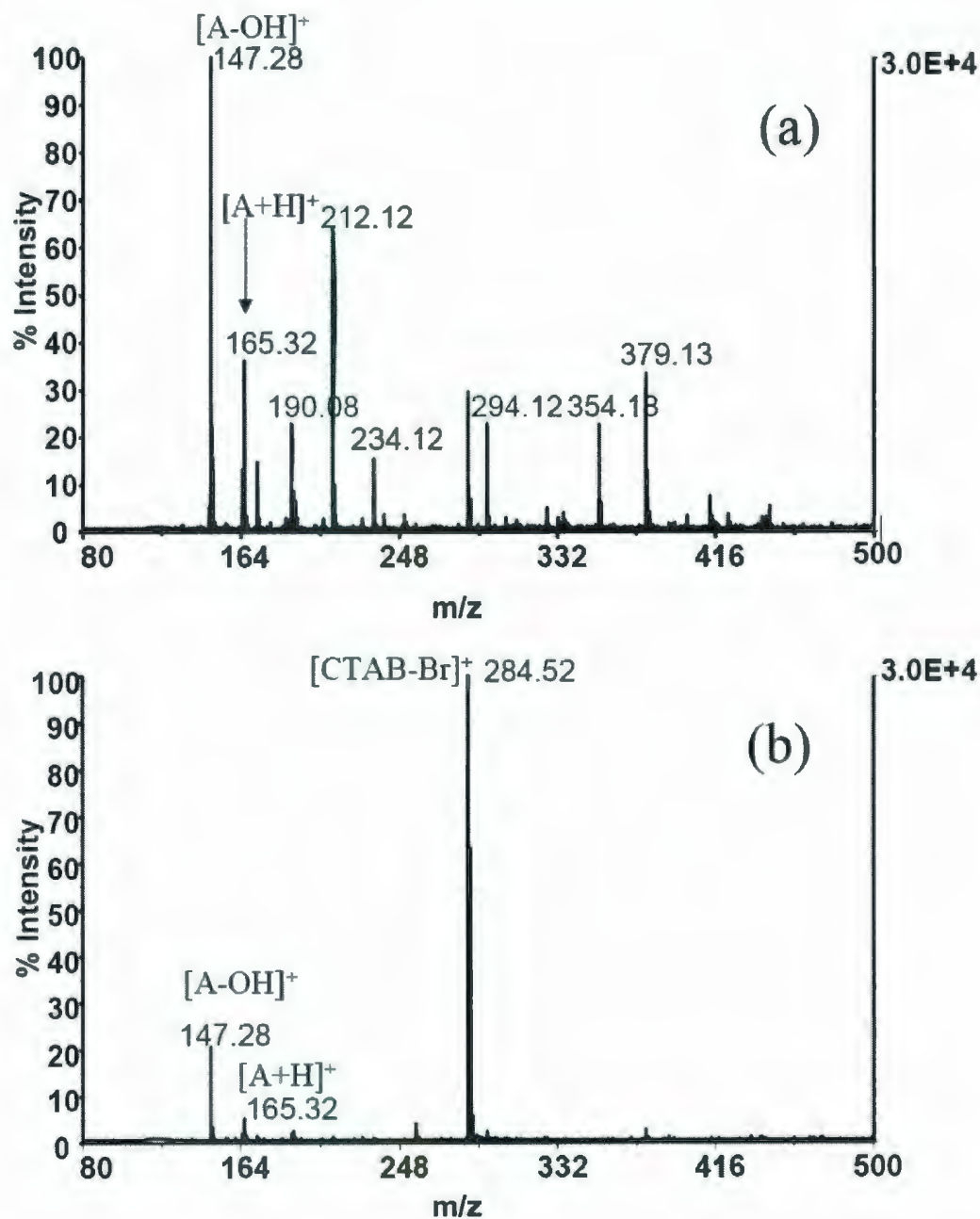


Figure 2.3. (a) MALDI mass spectra of CHCA/*p*-coumaric acid (A) at mole ratio of 1000:5, (b) mass spectra of CHCA/*p*-coumaric acid /CTAB at mole ratio of 1000:5:0.1.

It can be seen, however, that the *p*-coumaric acid signals are also partially suppressed (Figure 2.3(b)) resulting in a decrease in their net ion count. The average analyte ion intensity ( $n=5$ ) at  $m/z$  147 was  $10100 \pm 1400$  without surfactant, and decreased to  $3950 \pm 430$  when surfactant was added. Despite the decrease in signal intensity, the resolution of the signal was noted to increase. Without surfactant, the calculated resolution was  $2100 \pm 320$ . Resolution increased to  $2700 \pm 350$  when surfactant was used.

The matrix suppression effect from other surfactants at much lower surfactant concentration was also of interest. As an example, Figure 2.4 illustrates the mass spectra obtained when surfactant HTAB was used for the analysis of chrysin at a M:A:S mole ratio of 1000:5:0.001. This spectrum illustrates excellent matrix ion suppression while still observing a strong analyte signal even at very low surfactant concentration.

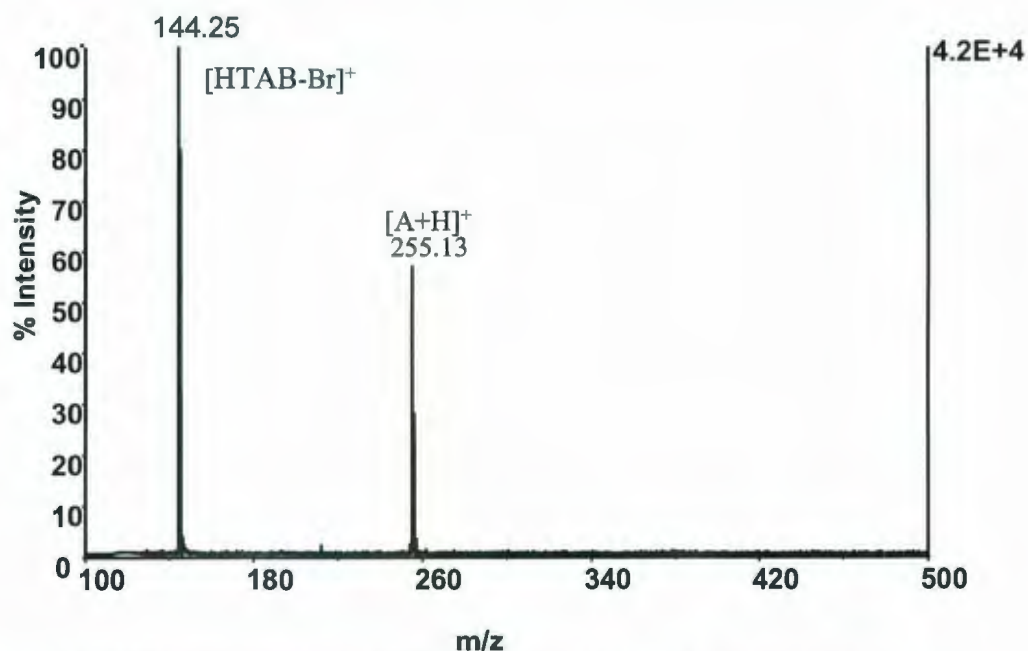


Figure 2.4. MALDI mass spectra of CHCA/chrysin(A)/HTAB at mole ratio of 1000:5:0.001.

However, from Table 2.2, only CTAB showed promise in matrix-suppression for a wide range of analytes while still providing good analyte ion signal. The shorter hydrocarbon chain monocationic surfactants, DDTAB and HTAB, showed usefulness at a low surfactant concentration, i.e., mole ratio of 1000:5: 0.001, but only for the analysis of phenolic analytes. In future studies, we would like to examine the effect of using a cationic quaternary ammonium surfactant with a longer hydrophobic tail than CTAB.

	M:S	Quercetin			Chrysin			<i>p</i> -coumaric acid			Ala-Ala-Ala			caffeine		
	Mole ratio	s	I	R	s	I	R	s	I	R	s	I	R	s	I	R
HTAB	1000 : 0.1	xx			xx			xx			xx			✓		
	1000 : 0.01	xx			✓			✓			✓			✓		
	1000 : 0.001	✓✓	8015	3010	✓✓	11033	3563	✓			✓✓	5311	3213	x		
	1000 : 0.0001	x			x			x			✓✓✓	11212	4543	✓		
DDTAB	1000 : 0.1	xx			✓✓	7591	3109	xx			xx			✓		
	1000 : 0.01	xx			✓			xx			xx			✓		
	1000 : 0.001	✓✓	13714	3242	x			x			✓✓✓	24948	5432	x		
	1000 : 0.0001	x			x			x			x			x		
CTAB	1000 : 0.1	✓✓✓	19554	4809	✓✓	12432	4562	✓✓	3949	2695	✓			✓		
	1000 : 0.01	✓✓✓	42373	6648	✓✓✓	34354	6436	✓✓	6253	2791	✓✓	5140	3432	✓✓✓	6494	4532
	1000 : 0.001	✓✓	58232	3618	✓✓	23242	4354	✓✓✓	9246	3322	x			✓		
	1000 : 0.0001	✓✓✓	17922	4151	✓			✓			x			✓		
TBAB	1000 : 0.1	xx			X			xx			xx			✓		
	1000 : 0.01	✓✓	11512	3435	✓			xx			x			✓		
	1000 : 0.001	✓✓✓	15766	5243	✓			xx			✓✓	21941	3456	x		
	1000 : 0.0001	x			✓			xx			✓✓✓	40153	4532	x		
DMB	1000 : 0.1	x			x			x			x			x		
	1000 : 0.01	✓			✓			x			x			✓✓	4747	4563
	1000 : 0.001	✓			x			✓			x			x		
	1000 : 0.0001	x			✓✓✓	36908	7635	x			x			x		
SDS	1000 : 0.1	x			x			x			✓✓✓	28044	4534	x		
	1000 : 0.01	x			x			x			✓✓✓	58011	6532	x		
	1000 : 0.001	x			✓✓✓	26709	7534	x			✓✓✓	9224	2335	x		
	1000 : 0.0001	✓			✓✓✓	9710	2532	x			✓✓✓	36734	4536	✓		
Brij <sup>®</sup> 30	1000 : 0.1	x			✓✓	2434	1532	x			x			✓✓✓	13898	2343
	1000 : 0.01	✓✓✓	16041	4323	✓✓✓	4802	3423	✓			✓✓	4134	3425	x		
	1000 : 0.001	✓			✓			x			✓✓✓	34621	6534	x		
	1000 : 0.0001	x			✓			x			✓			x		

Table 2.2. Analysis of analytes with each individual surfactant demonstrating the level of matrix ion suppression (Matrix :A mole ratio constant at 1000:5). Ions monitored were [quercetin + H]<sup>+</sup>, [chrysin + H]<sup>+</sup>, [*p*-coumaric acid - OH]<sup>+</sup>, [Ala-Ala-Ala + Na]<sup>+</sup> and caffeine + H]<sup>+</sup>. s = relative suppression indicator where x = no ion suppression, xx = both analyte and matrix signal suppressed, ✓ = fair matrix ion suppression, ✓✓ = good matrix ion suppression, ✓✓✓ = excellent matrix ion suppression. I = analyte ion intensity, R = analyte mass resolution. Analyte intensity and resolution values are reported for good or excellent matrix suppression only. Values are an average of triplicate analysis.

Aside from examining the hydrocarbon chain length of the quaternary ammonium surfactants, as was done in the series of HTAB, DDTAB, and CTAB, the other types of cationic surfactants, TBAB and DMB, were also examined. TBAB contains 4 butyl groups attached to the ammonium ion and DMB has two cationic ammonium functionalities, one on either side of a 10-carbon length chain. Only TBAB showed promising results, particularly for the analysis of the peptide trialanine (Table 2.2) and at low surfactant concentration. Figure 2.5 illustrates the result of mixing TBAB with CHCA for the analysis of trialanine (Ala-Ala-Ala). Matrix signal suppression was observed and the dominant ion at  $m/z$  242 corresponds to the surfactant ion  $[\text{TBAB} - \text{Br}]^+$ . The analyte signal shows up as a sodiated molecule  $m/z$  254 and, to a lesser extent, a doubly sodiated ion  $[\text{A} + 2\text{Na} - \text{H}]^+$   $m/z$  276. The presence of the sodiated ions for trialanine in all MALDI spectra is because steps were not undertaken to lower sodium levels in the reagents. As well, our method employed 80:20 MeOH/H<sub>2</sub>O as a solvent, rather than a mixture containing acetonitrile and 0.1 % TFA, normally used for the analysis of peptides. We maintained this solvent for simplicity, as it does not affect the pH of drying droplets and it is comparable to other relevant studies [24,25].

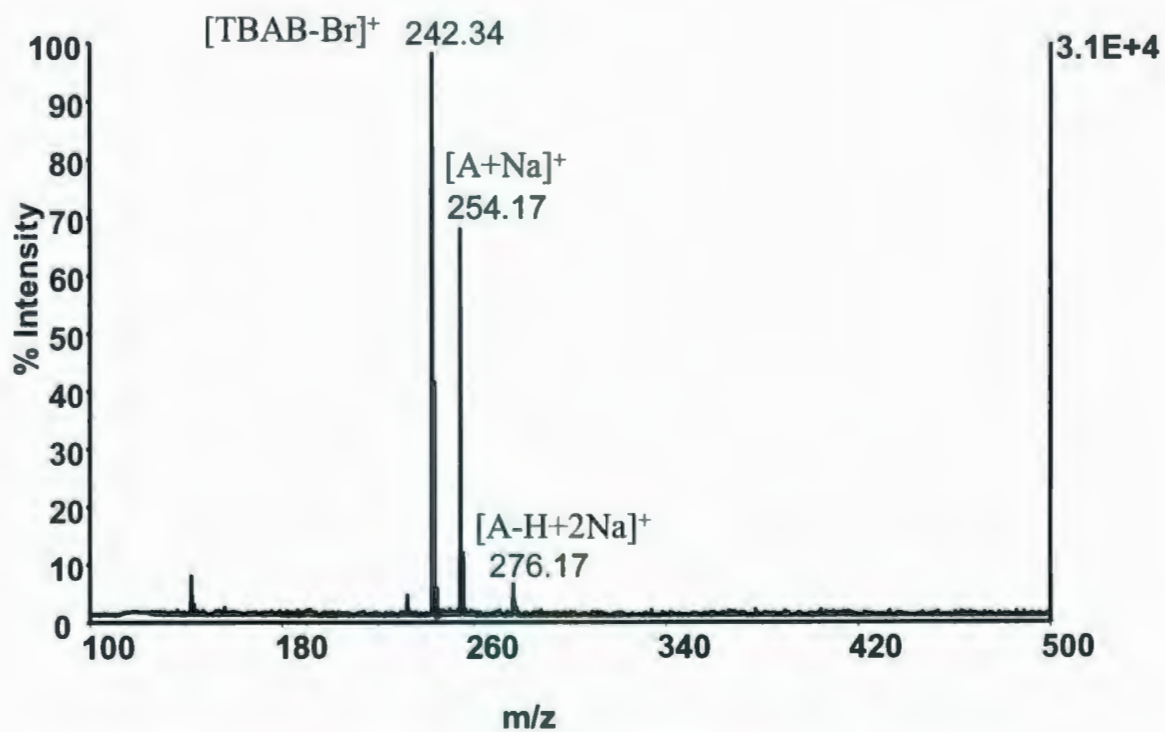


Figure 2.5. MALDI mass spectra of CHCA/trialanine(A)/TBAB at mole ratio of 1000:5:0.001.

Finally, the anionic surfactant, SDS, and the neutral surfactant, Brij<sup>®</sup> 30, were examined as potentially useful matrix ion suppressors. Both were able to suppress CHCA matrix ions. Except for the analysis of trialanine, their use often led to unacceptable suppression of the analyte signal. Unlike the cationic surfactants, neither of these yielded surfactant-related ions in either positive or negative ion mode. Figure 2.6(a) demonstrates the mass spectrum obtained when SDS is used in the analysis of trialanine at a M:A:S mole ratio of 1000:5:0.1. Both sodiated ( $m/z$  254) and doubly sodiated adducts ( $m/z$  276) are observed with minimal background signals from the matrix. Figure 2.6(b) is the result of a 1000-fold dilution of the peptide analyte, while keeping the matrix and surfactant ratio constant (i.e. 1000:0.005:0.1). The sodiated and potassiated analyte signals are clearly observed with a signal-to-noise ratio  $> 5$ . Although a preliminary result, it does show that the use of surfactant-mediated MALDI can be used for analysis of low levels of small peptides. Although large molecules routinely have SDS added to them to aid in solubilizing and in tryptic digests, they are usually removed before analysis. In these systems, they may be present in 5% v/v or more. It is possible, that if present in a much smaller amount (i.e. less surfactant than analyte) that SDS might aid in analysis as was demonstrated with trialanine. However, the study of large molecules was outside the scope of this thesis.

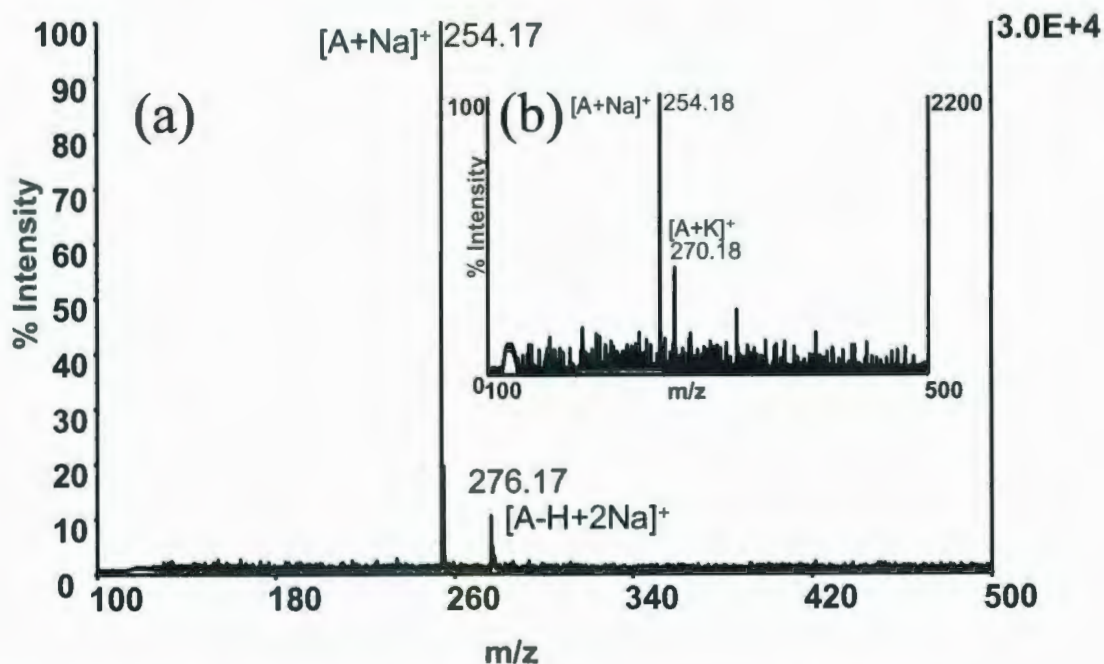


Figure 2.6. (a) MALDI mass spectra of CHCA/trialanine(A)/SDS at mole ratio of 1000:5:0.1, (b) MALDI mass spectra of CHCA/trialanine(A)/SDS when trialanine is diluted 1000-fold.

Despite the fact that the results shown in Table 2.2 are variable, some general trends in surfactant performance can be stated. For the analysis of phenolics, CTAB showed the best performance by far for surfactant-mediated MALDI-TOFMS with strong analyte signals at nearly all surfactant concentrations. CTAB was the only surfactant suitable for the analysis of the phenolic acid, *p*-coumaric acid. This last result is surprising as this analyte is chemically very similar to the matrix CHCA but without the cyano group. For small peptide analysis, SDS was superior, consistently showing excellent matrix-ion suppression with strong analyte signals over a range of surfactant

concentrations. This was surprising, as SDS is considered an ion suppressor and usually removed prior to mass spectrometric analysis of proteins. However, it is very effective in solubilizing these peptides and proteins. Finally, the neutral surfactant, Brij<sup>®</sup> 30, showed reasonable performance for the analysis of caffeine at relatively high surfactant concentration.

The resolution of analyte signals for the best case scenarios typically range from 3000-5000, considered acceptable using this instrument. Resolution measurements with and without surfactant showed that, in most cases, resolution increased by 25-75 % by using the most promising surfactant.

### **2.3.2 Effect of Concentration of Surfactant**

In a previous study by Guo *et al.* [24] and in the present one, the mole ratio of matrix to surfactant was found to be an important factor in matrix ion suppression while preserving the analyte signal. More detailed experiments were undertaken whereby the M:A mole ratio was maintained at 1000:5, while the amount of surfactant added was varied ( $1000:5:1 \rightarrow 1 \times 10^{-5}$ ) to yield a surfactant concentration-dependence profile. The signal intensity of the major analyte ion was carefully monitored. Each combination of surfactant to analyte was tested and replicated 5 times for each concentration. As an example, Figure 2.7 demonstrates the impact of changing the amount of Brij<sup>®</sup> 30 on the signal intensity of trialanine. When too much surfactant is added (M:S = 1000:1), the analyte signal is absent because both the CHCA and analyte ions are fully suppressed. As the amount of added surfactant decreases, the analyte ion intensity increases to a

maximum, then decreases at very low surfactant addition. Finally, as the amount of Brij<sup>®</sup> 30 becomes negligible (M:A:S = 1000:5:0.00001), the analyte signal increases again. This is because there is little or no suppression, and the resulting spectrum is comparable with matrix and analyte alone. Each point on the graph was averaged for 5 identical spots and %RSD values ranged from 7-22%. These RSD values are typical of MALDI experiments and comparable to those reported in the literature [26-28].

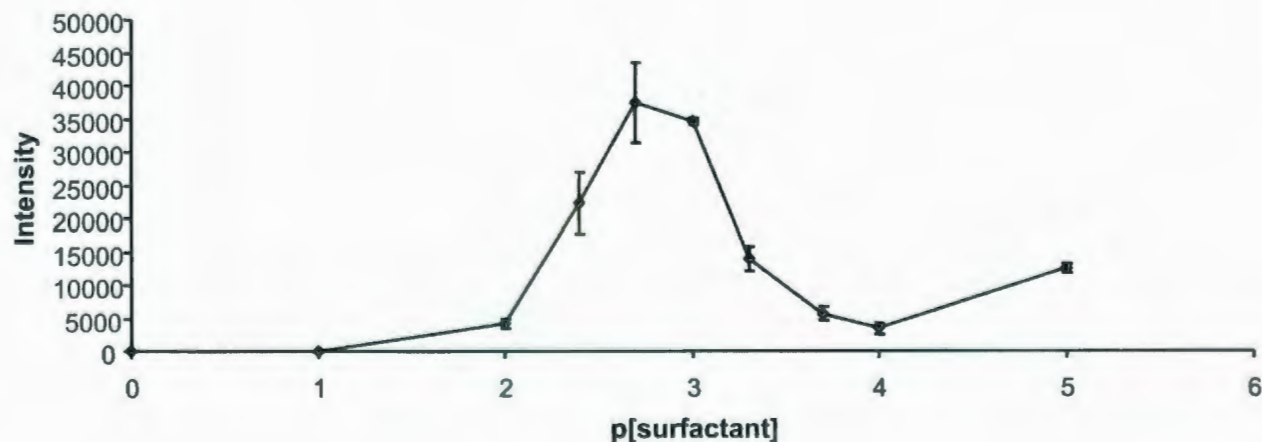


Figure 2.7. Molar concentration profile displaying the effect of Brij<sup>®</sup> concentration on [tralanine + Na]<sup>+</sup>, *m/z* 254 signal. The mole ratio of CHCA/tralanine held constant at 1000:5 (*n* = 5).

Generalizations regarding optimal surfactant loadings were difficult to make because they were both analyte and surfactant dependant. On the whole, M: S mole ratios of 1000:0.01 and 1000:001 provided the best results. If one has an unknown analyte, an initial M:A:S of 1000:5: 0.01 is a good starting point for analysis and CTAB should be used first.

### **2.3.3 Heterogeneity of surfactant-containing sample spots**

One desired feature of MALDI sample preparation is that a given spot should be homogeneous. However, we believe that spots containing added surfactant may lead to a heterogeneous sample. The use of a MALDI-TOFMS to examine sample spots containing heterogeneous layers has been investigated recently [29,30]. Hanton *et al.* demonstrated this by using electrospray deposition to create a two-layered sample of Poly(methyl methacrylate) (PMMA) and Polystyrene (PS) [29]. Controlling the number of laser shots used during analysis led to successful depth-profiling experiments where these polymers could be independently identified. Recently, the dried droplet spotting approach for poly(oxyethylene) and poly(oxypropylene) triblock copolymers was tested.<sup>30</sup> Changing the number of laser shots from 50 to 300 in this sample resulted in the emergence of a new ion distribution, particularly in the low-mass range. This was due to the presence of multiple layers within the deposit, with lighter products located near the core and heavier products spreading out on the surface of the drop.

The same approach to depth profiling was undertaken in this study. As a preliminary experiment, caffeine was chosen as a model analyte and CTAB as the

surfactant. Figure 2.8 represents the spectral results with increasing laser shots (5, 10 and 30 shots) on caffeine/CHCA matrix only. The intensity of analyte signal (A) and matrix ions (\*) remain relatively unchanged with increased laser shots suggesting these crystallized samples are fairly homogeneous.

Figure 2.9 shows the effect of increased laser shots on the MALDI spectra of a matrix/analyte/surfactant sample with a M:A:S mole ratio of 1000:5:1. With only 5 laser shots the spectrum shown in Figure 2.9(a) reveals that suppression of both analyte and matrix-related ions has occurred. The surfactant ion is the only one present in the spectrum. However, as the laser shots increase to 10 and then 30, a partially-suppressed analyte signal (A) is observed. In the meantime, the matrix-related ions remain totally suppressed. These results suggest that the surfactant concentration is too high and strong ion suppression is occurring, particularly near to the surface of the sample.

A further dilution of the surfactant concentration (M:A:S = 1000:5:0.1) reveals a somewhat different spectral pattern (Figure 2.10). When 5 laser shots are employed, both the surfactant and analyte ions are readily observed. When 10 laser shots are used, the analyte and surfactant ion are again observed along with two identifiable matrix-related ions. As the number of laser shots is increased to 30, matrix ions become more apparent and the surfactant signal decreases in intensity. Since the surfactant signal is strong after 5 and 10 laser shots but not at 30 shots suggests again that the surfactant it is a major component near the surface. That is, samples containing surfactant do not crystallize to a homogeneous spot, rather these spots are more heterogeneous with higher amounts of surfactant near the surface.

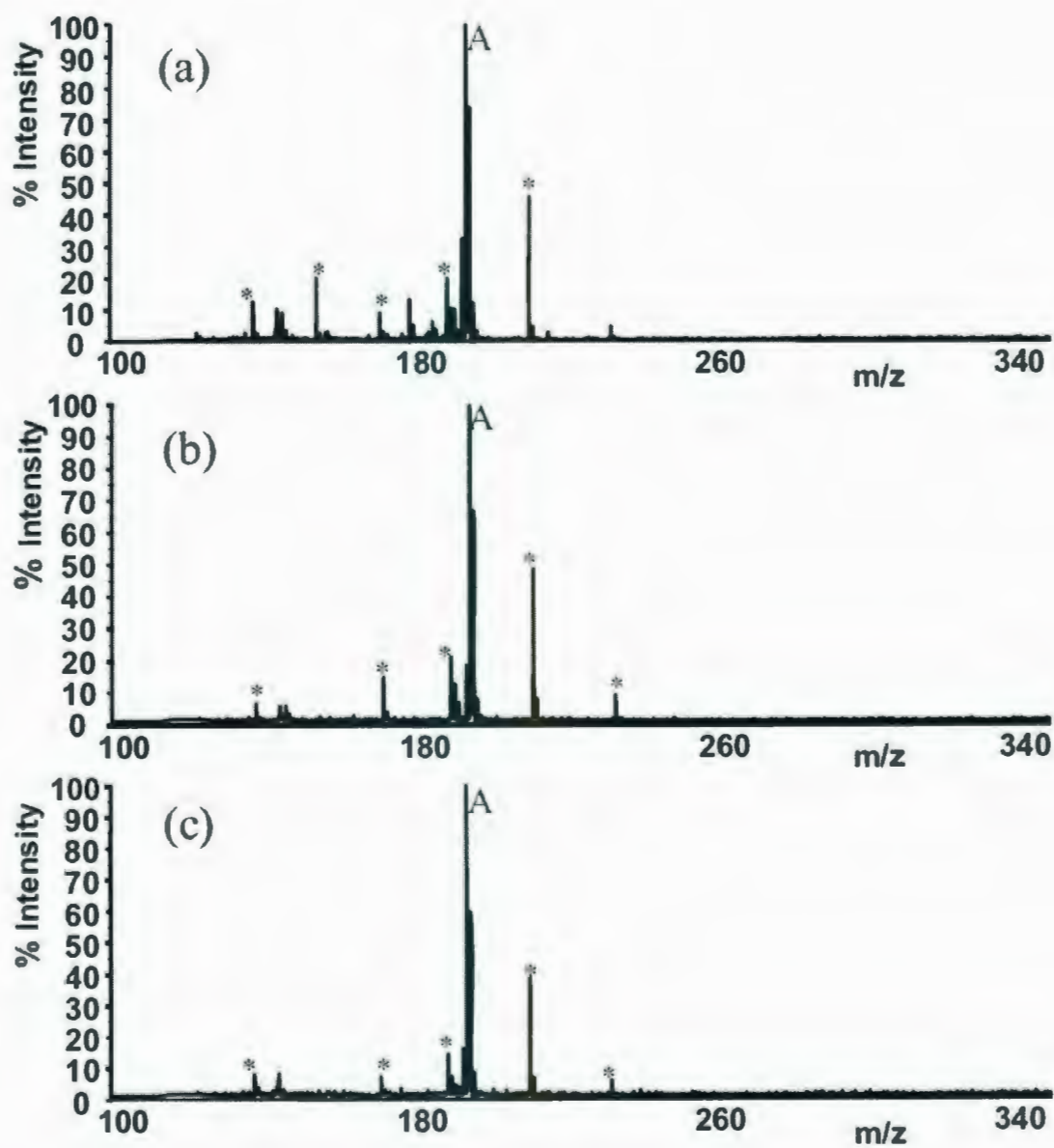


Figure 2.8. Monitoring the change in MALDI mass spectra of CHCA/caffeine (mole ratio 1000:5) as number of laser shots varied; (a) 5 shots, (b) 10 shots, (c) 30 shots. A= analyte; \* = matrix ions.

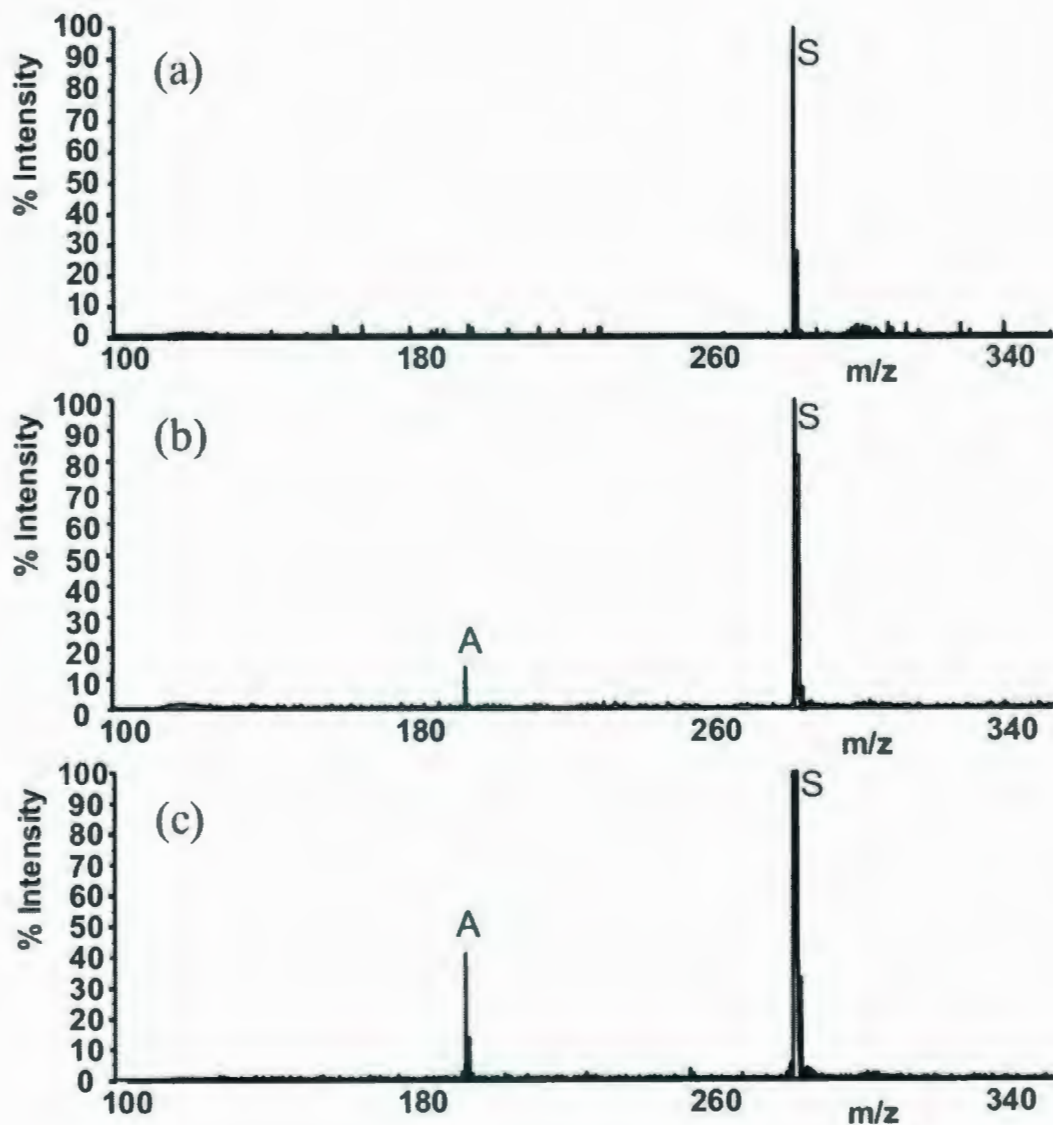


Figure 2.9. Monitoring the change in MALDI mass spectra of CHCA/caffeine/CTAB (mole ratio 1000:5:1) as number of laser shots varied; (a) 5 shots, (b) 10 shots, (c) 30 shots. A= analyte; S = surfactant.

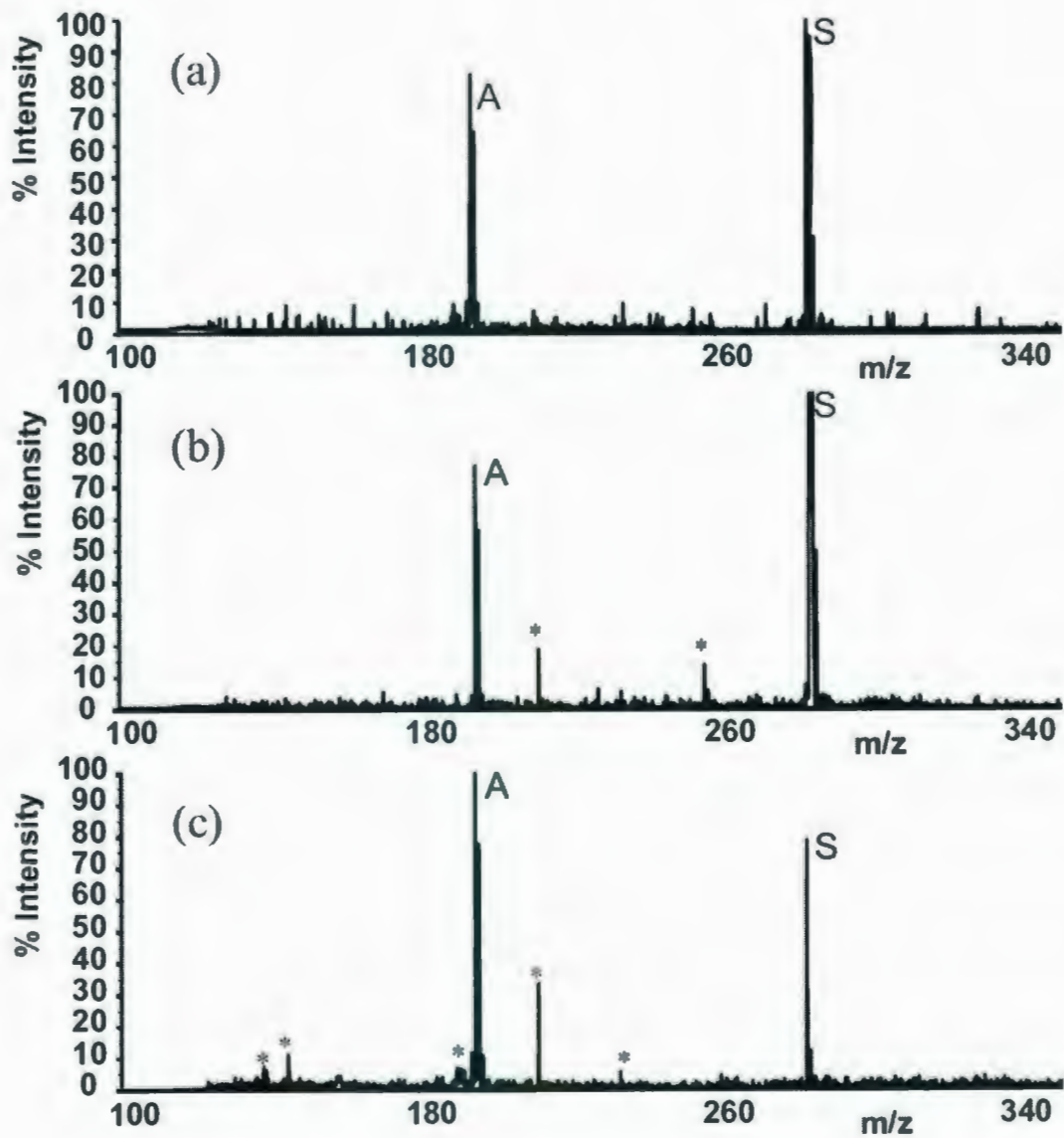


Figure 2.10. Monitoring the change in MALDI mass spectra of CHCA/caffeine/CTAB (mole ratio 1000:5:0.1) as number of laser shots varied; (a) 5 shots, (b) 10 shots, (c) 30 shots. A = analyte; S = surfactant; \* = matrix ions.

Aware that the MALDI spectra discussed above represent only a single analysis and that variations from spot to spot occurred, a more detailed experiment was undertaken whereby ion counts of selected ions borne from matrix, surfactant and analyte ionization were measured as the number of laser shots were increased from 5 to 50, in increments of 5. Signals at  $m/z$  195, 212, and 284 were monitored for the presence of caffeine  $[A+H]^+$ , matrix  $[CHCA+ Na]^+$  and surfactant  $[CTAB-Br]^+$ , respectively. Results of depth profiling of replicate spots containing matrix and analyte only is shown in Figure 2.11(a). The ion intensity profile of both analyte and matrix signals follow closely together indicating spot homogeneity. It should be noted that the results in Figure 2.11 are average ion counts from 10 replicate spots where relative standard deviations (RSD) range from 6-10%. The ion intensity recorded is the average ion count per laser shot. As can be seen in the graph, the intensity of the ion counts/shot began to decrease after approximately 30 laser shots, indicating that less sample remains after each subsequent laser shot and that the material is being depleted.

When CTAB was added so that M:A:S mole ratio was 1000:5:1, the  $[CTAB - Br]^+$  ion is the dominant ion in the mass spectra, as expected. At this M: S ratio, CHCA-related ions were totally suppressed. The caffeine signal is observable, but it is partially suppressed by the surfactant. As the number of laser shots is increased to 20, the surfactant signal decreases by half indicating a higher concentration of surfactant is nearer the surface of the drop.

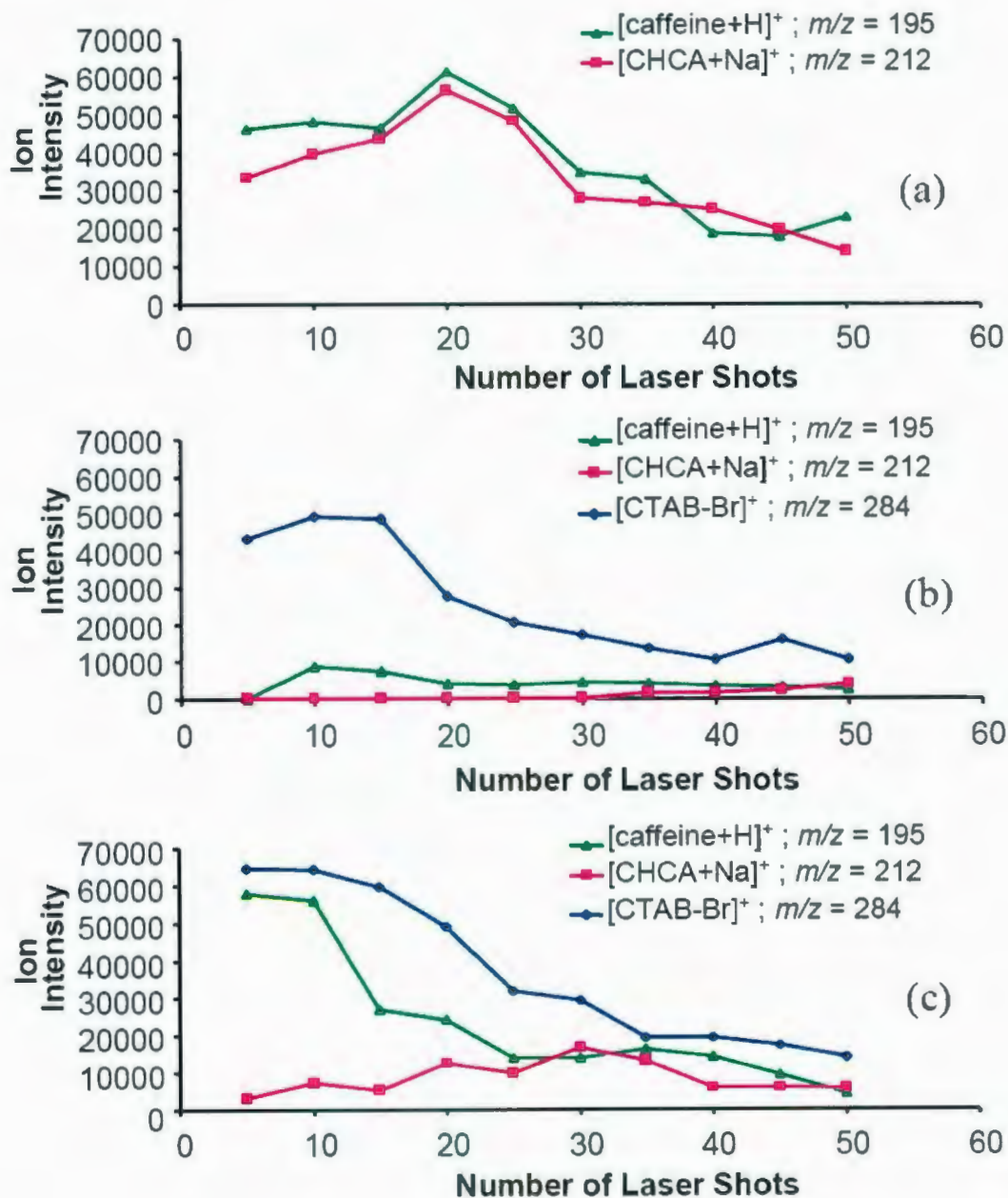


Figure 2.11. Monitoring the change in average ion intensity of selected ions as the number of laser shots is increased on individual spots ( $n=10$ ); (a) Ion profile of CHCA/caffeine, (b) of CHCA/ caffeine/CTAB where mole ratio is 1000:5:1, (c) of CHCA/caffeine/CTAB where mole ratio is 1000:5:0.1. %RSD values range from 6-10%.

Lowering the CTAB concentration so that M:A:S is now 1000:5:0.1 showed an even more intriguing result, particularly in the region of lower number of laser shots. Essentially, at the top of the droplet (ca. 5 laser shots) the caffeine signal is very intense and equal in intensity to that of the surfactant-related ion. In contrast, the matrix-related ion is of minor intensity. This indicates that surfactant and analyte concentration near the upper layer of the spots were ideal for surfactant-mediated MALDI. Interestingly, as soon as the number of laser shots was increased, the CTAB and caffeine signals suddenly dropped, suggesting a decrease in both their concentrations with depth. On the other hand, the matrix ion increased steadily, suggesting less and less surfactant is present to suppress the matrix.

From the above experiments, it is proposed that during the crystallization process, the surfactant tends to migrate towards the top of the droplet. Surfactants, in particular cationic surfactants, may be able to attract analyte molecules to the top of a droplet, particularly if a cationic surfactant forms ionic bonding or a complex to an electron-rich analyte. It is likely that at this point, the mole ratio of matrix:analyte is much lower than that expected by the initial mixing ratios. Thus, similar to the reported mechanism of the mole ratio dependant matrix suppression effect (MSE) [21], the matrix-matrix interactions are minimized and each analyte molecule is surrounded by just enough matrix to absorb the laser energy and ionize it. It is also possible that micelles may form in the top region of the spot so long as there is enough surfactant added initially and this may have an effect on matrix ion suppression.

Further depth profiling experiments on other types of surfactants and analytes, and the use of spectroscopic surface analysis methods (i.e. scanning electron microscopy), are required before the surfactant-mediated MALDI mechanism can be fully understood.

## **2.4 CONCLUSION**

Surfactant-enhanced MALDI is a useful technique for the analysis of various classes of small molecules. We have tested several cationic surfactants, all bromide salts, as well as SDS and a neutral surfactant, Brij<sup>®</sup> 30. Suppression of positive CHCA matrix-related peaks can be achieved, along with increased analyte resolution. The detection limit for the peptide trialanine was found to be in the 100 femtomole range. Trialanine may be a hydrophobic peptide as compared to other peptides, and so future studies might examine if this trend was similarly followed for the more general hydrophilic species. It seems that the surfactant is enriched near the surface of the spot along with the analyte and this enrichment lessens the production of interfering matrix-related ions. Surfactant-mediated MALDI will be further explored for use in identification of small biomolecules and analyte mixtures with the aid of MALDI MS-MS.

## 2.5 REFERENCES

1. Karas M, Bachmann D, Hillenkamp F. *Anal. Chem.* 1985; **57**: 2935.
2. Tanaka K, Waki H, Ido Y, Akita S, Yoshida Y, Yoshida T. *Rapid Commun. Mass Spectrom.* 1988; **2**: 151.
3. Karas M, Bahr U, Ingendoh A, Nordhoff E, Stahl B, Strupat K, Hillenkamp F. *Analytica Chimica Acta.* 1990; **241**:175.
4. Distler AM, Allison J. *Anal. Chem.* 2001; **73**: 5000.
5. Bahr U, Deppe A, Karas M, Hillenkamp F. *Anal. Chem.* 1992; **64**: 2866.
6. Weidner S, Kuhn G, Friedrich J. *Rapid Commun. Mass Spectrom.* 1998; **12**: 1373.
7. Michalak L, Fisher K, Alderdice D, Jardine D, Willett G. *Org. Mass Spectrom.* 1994; **29**: 512.
8. Cornett DS, Amster IJ, Duncan MA, Rao AM, Eklund PCJ . *J. Phys. Chem.* 1993; **97**: 5036.
9. Lai EPC, Owega S, Kulczycki R. *J. Mass Spectrom.* 1998; **33**: 554.
10. Zhang Q, Zou H, Gou Z, Zhang Q, Chen X, Ni J. *Rapid Commun. Mass Spectrom.* 2001; **15**: 217.
11. Schurenberg M, Dreisewerd K, Hillenkamp F. *Anal. Chem.* 1999; **71**: 221.
12. Kinumi T, Saisu T, Takayama M, Niwa H. *J. Mass Spectrom.* 2000; **35**: 417.
13. Ayorinde FO, Hambright P, Porter TN, Keith QL. *Rapid Commun. Mass Spectrom.* 1999; **13**: 2474.
14. Ayorinde FO, Garvin K, Saeed K. *Rapid Commun. Mass Spectrom.* 2000; **14**: 608.
15. Xu S, Li Y, Qiu J, Guo Z, Guo B. *Anal. Chem.* 2003; **75**: 6191.
16. Najam-ul-Haq M, Rainer M, Schwarzenauer T, Huch CW, Bonn GK. *Anal. Chimica Acta.* 2006; **561**: 32.
17. Hu L, Xu S, Pan C, Yuan C, Zou H, Jiang G. *Environ. Sci Technol.* 2005; **39**: 8442.

18. Pan C, Xu S, Hu L, Su X, Ou J, Zou H, Guo Z, Zhang Y, Guo B. *J. Am. Soc. Mass Spectrom.* 2005; **16**: 883.
19. Ren S, Zhang L, Chen Z, Guo Y. *J. Am. Soc. Mass Spectrom.* 2005; **16**: 333.
20. Chan TWD, Colburn AW, Derrick PJ. *Org. Mass Spectrom.* 1991; **26**: 342.
21. Knochenmuss R, Dubois F, Dale MJ, Zenobi R. *Rapid Commun. Mass Spectrom.* 1996; **10**: 871.
22. McCombie G, Knochenmuss R. *Anal. Chem.* 2004; **76**: 4990.
23. Knochenmuss R, Karbach V, Wiesli U, Breuker K, Zenobi R. *Rapid Commun. Mass Spectrom.* 1998; **12**: 529.
24. Guo Z, Zhang Q, Zou H, Guo B, Ni J. *Anal. Chem.* 2002; **74**: 1637.
25. Su AK, Liu JT, Lin CH. *Talanta.* 2005; **67**: 718.
26. Sleno L, Volmer DA. *Rapid Commun. Mass Spectrom.* 2006; **20**: 1517.
27. Dekker LJ, Dalebout JC, Siccama I, Jenster G, Smitt PAS, Luider TM. *Rapid Commun. Mass Spectrom.* 2005; **19**: 865.
28. Kang MJ, Pyun JC, Lee JC, Choi YJ, Park JH, Lee JG, Choi HJ. *Rapid Commun. Mass Spectrom.* 2005; **19**: 3166.
29. Hanton SD, Hyder IZ, Stets JR, Owens KG, Blair WR, Guttman CM, Giuseppetti AA. *J. Am. Soc. Mass Spectrom.* 2003; **15**: 168.
30. Terrier P, Buchmann W, Cheguillaume G, Desmazieres B, Tortajada J. *Anal. Chem.* 2005; **77**: 3292.

## Chapter 3

### **RAPID SCREENING OF ANTHOCYANINS IN BERRY SAMPLES BY SURFACTANT-MEDIATED MATRIX-ASSISTED LASER DESORPTION/IONIZATION TIME-OF-FLIGHT MASS SPECTROMETRY**

A version of this chapter has been published. Grant DC and Helleur RJ. Rapid screening of anthocyanins in berry samples by surfactant-mediated matrix-assisted laser desorption/ionization time-of-flight mass spectrometry. *Rapid Commun. Mass Spectrom.* 2008; 22: 156-164.

### 3.1 INTRODUCTION

Matrix-assisted laser desorption/ionization is an ionization technique which was proven useful in 1987 by two independent groups [1,2]. MALDI has been found to be an excellent ionization mechanism for the analysis of proteins, oligonucleotides, and synthetic polymers, especially when coupled to a time-of-flight (TOF) mass analyzer [1-7]. The theoretical unlimited mass range of the TOF makes possible the determination of masses not possible by GC-MS or even ESI. MALDI has become renowned for its sensitivity, high throughput capabilities, and its easily interpreted mass spectra, which consist predominantly of singly charged protonated species [8-10]. Recently, there has been a growing interest in the ability of MALDI to analyze a variety of small molecules. This has been quite difficult because of the small organic acids typically used as matrices for MALDI. These tend to fragment under most instrument conditions and the various decomposition reactions of the associated fragments tend to complicate mass spectra, making in particularly difficult to analyze compounds less than 1000 Da [11-13].

The surfactant cetyltrimethylammonium bromide (CTAB) was used as a CHCA matrix-ion suppressor by Guo *et al.*[14]. This additive was found to suppress the formation of CHCA matrix ions, while still allowing for adequate resolution of several analyte classes, including peptides and cyclodextrins. This method has been further explored in other studies [15-17]. Su *et al.* demonstrated that this technique can be used for screening of drug molecules in clandestine tablets. Recently, our group has shown that a larger variety of quaternary-ammonium surfactants can be used to induce matrix-ion suppression. This has led to successful analysis of phenolic acids and flavonoids

[17]. For these particular analytes, CTAB was found to be a viable surfactant choice and it was shown that the matrix/surfactant ratio can be lowered to 10000:1 or lower. It was demonstrated that these surfactant-containing samples yielded greater reproducibility than those without surfactant. As well, higher resolution values were obtained for multiple analytes, including a phenolic acid. Due to the specificity of this method of ion suppression, we have referred to this as “surfactant-mediated” matrix-assisted laser/desorption ionization.

Flavonoids are known to be a large class of biologically-active non-nutrients in plants, and these can be further divided into the following categories: flavonols, flavones, catechins, proanthocyanidins, anthocyanidins, and isoflavonoids [18]. In human health, flavonoids are known to be powerful antioxidants [19]. They also have anti-allergenic, anti-inflammatory and antiviral characteristics [19,20]. Several studies have shown that they decrease the risk of coronary heart disease, stroke, and stomach and lung cancer [21-23]. Both flavonol and anthocyanidin glycosides have been found in a multitude of fruit juices, wines, and berries which include blueberries, raspberries, partridgeberries, and strawberries [24-27]. These compounds are often responsible for the blue or reddish colour pigment of the berries. Several studies have focused on methods to extract these compounds, which have later been analyzed by LC-ESI-MS [26,27]. Typically, electrospray ionization (ESI) is used, but some studies have explored the use of MALDI-TOF-MS as an alternative [28,29]. Wang *et al.* demonstrated that 2,4,6-trihydroxyacetophenone (THAP) acts as a suitable matrix for anthocyanin-glycosides

[28]. Qualitative screening of fruit juices and berry samples was successful, and the linear response of anthocyanins indicated that quantitation was possible [28].

The current study carries forward the use of MALDI-TOF-MS with the focus on application of surfactant-mediated MALDI to aid in the rapid analysis of flavonoids from a variety of berry extracts. We investigated both CHCA and THAP as potential matrices for the flavonoids, with the assumption that the CTAB would cause suppression of the matrix ions, and in turn lead to mass spectra with minimal noise. We also illustrate separation of flavonoids via liquid chromatography with ESI mass spectrometry to aid in peak identification. We demonstrate this method as a complementary rapid-screening technique that can qualitatively identify flavonoids in just minutes, whereas LC methods require longer run times to adequately separate the flavonoids from berry extracts.

## **3.2 EXPERIMENTAL**

### **3.2.1 Chemicals**

The  $\alpha$ -cyano-4-hydroxycinnamic acid (CHCA), quercetin (302.24 g/mol) and rutin (610.52 g/mol), (quercetin 3-rutinoside) were purchased from Sigma (St. Louis, MO, USA). Cetyltrimethylammonium bromide (CTAB) was obtained from Aldrich (Mississauga, ON, Canada). Deionized water and methanol were HPLC grade and purchased from Fisher Scientific (Fair Lawn, New Jersey, USA). Cyanidin (287.25 g/mol), cyanidin 3-glucoside (cyanidin 3-O- $\beta$ -D-glucopyranoside) (449.39 g/mol), delphinidin (303.25 g/mol), malvidin (331.22 g/mol), and malvidin 3-galactoside (malvidin-3-O- $\beta$ -D-glucopyranoside) (493.44 g/mol) were all chloride salts and purchased from Fluka (Seelze, Germany). Petunidin chloride (aglycone molar mass of 317.27

g/mol) was purchased from Extrasynthese (Genay, France). All chemicals were used without further purification.

### **3.2.2 Sample Preparation**

CHCA stock solution was prepared fresh daily at a concentration of  $10 \text{ mg mL}^{-1}$  in a solution that had a 4:1 volumetric ratio methanol to water. THAP was prepared daily at  $20 \text{ mg mL}^{-1}$  in 50:50 methanol:water. We chose 4 analytes as standards due to their availability; quercetin, rutin (quercetin 3-rutinoside), petunidin, and cyanidin 3-glucoside. A four-component mixture was prepared from these that contained the following concentrations of each: 246, 125, 252 and  $24 \mu\text{mol L}^{-1}$ , respectively. Various dilutions were made of this standard to prepare calibration curves for HPLC and MALDI quantification. All standards were stored at  $-20^\circ\text{C}$ . For MALDI analysis, all samples were prepared by the dried-droplet preparation method in plastic centrifuge vials, which included being mixed with a matrix, vortexed for 30 seconds and centrifuged for 30 seconds. Then  $0.5 \mu\text{L}$  aliquots were spotted onto a 96 x 2 well MALDI plate with a hydrophobic coating (Applied Biosystems, Framington, MA, USA). Samples were left to crystallize in a desiccator before being loaded into the MALDI-MS instrument.

### **3.2.3 MALDI-TOF-MS Instrumentation**

The MALDI-TOFMS was a Voyager DE<sup>TM</sup>-PRO purchased from Applied Biosystems (Framingham, MA, USA). The instrument was equipped with a video camera and the sample image was displayed on a monitor, which enabled the laser to be focused on a given spot and controlled manually. Positive ion reflectron mode was used. The instrument was equipped with a pulsed nitrogen laser (337 nm, 3 ns pulse duration, 3 Hz

frequency) and a delayed extraction source. An accelerating voltage of 20 kV and a grid voltage setting of 69% were used. The guide wire was adjusted to 0.004%. The laser fluence was set to 2800 arbitrary units (unless otherwise stated) and an extraction delay time of 145 ns was used. The acquisition mass range was 100-1000 Da unless otherwise shown and all spectra were obtained by averaging 25 laser shots. Mass spectra were analyzed using Version 4 of Data Explorer™ software. All resolution values were calculated at 50% of the maximum peak height.

### 3.2.4 LC-UV-ESI-MS

An Agilent 1100 Series LC/MSD Trap SL (Palo Alto, CA, USA) was used. All chromatograms were processed using ChemStation for LC 3D software (Rev.A.10.02). The ESI-MS mass spectra were analyzed using Bruker© LC/MSD Trap Control 5.2. The parameters for the ion trap were as follows: nebulizer pressure, 60.0 psi; drying gas, 11.0 L/min; drying temperature, 350°C; target mass,  $m/z$  500; scan range,  $m/z$  150-900; capillary voltage, 3500 V. An Agilent diode array detector (G1315B) was used for quantitative experiments. UV wavelength detection for flavonols and anthocyanins was at 360 and 520 nm, respectively. A 25  $\mu$ L aliquot injected using the autosampler was separated on a Symmetry® C-18 RP column (150 x 3.9 mm i.d.- Waters, Mississauga, ON, Canada), protected by a Symmetry® C-18 guard column (W31921). A binary solvent system was employed, following the work of Wang *et al.* [29]. Solvent A was 5% aqueous formic acid (v/v) and solvent B was 100 % methanol (HPLC grade). The flow rate was maintained at 0.8 mL/min. The gradient elution profile was as follows: 0

min, 14% B; 1-10 min, 14-17% B; 10-35 min, 17-23% B; 35-60 min, 23-47% B; 60-80 min, 47-60% B; 80-85 min, 60-14% B.

### 3.2.5 Extraction Method

Three berry samples were chosen for analysis; a lowbush blueberry (*Vaccinium angustifolium*), a lingonberry (*Vaccinium vitis-idaea*), and a blackberry (*Rubus armeniacus*). Samples (30 g, frozen) were ground in a coffee grinder to a paste, and then 30 mL of 40:40:20:0.1 CH<sub>3</sub>CN/MeOH/H<sub>2</sub>O/formic acid was added. Samples were stirred for 10 minutes with a magnetic stirring bar before the solid residue was removed by suction filtration using Whatman No. 4 filter paper. The residue was rinsed with extra solvent to make the final volume of 50 mL. The extract was dried by rotary evaporation, and then re-dissolved in 50 mL of water. A 5 mL aliquot of the extract was loaded onto a C-18 Sep Pak cartridge (Supelclean<sup>TM</sup> ENVI<sup>TM</sup>-18 SPE Tubes, Supelco, Bellefonte, PA, USA) that had been pre-rinsed with 5 mL of water and 2 mL of methanol. Once loaded, the cartridge was rinsed with 5 mL of water to remove non-flavonoid components. The anthocyanins and flavonols were eluted with 10 mL of methanol containing 0.1% formic acid. Samples were stored at -20°C and later thawed 1 hour prior to analysis. For LC analysis the extracted samples were dried and re-dissolved in 86% (v/v) solvent A and 14% (v/v) solvent B.

### **3.3 RESULTS AND DISCUSSION**

#### **3.3.1 Identification and Quantification of Flavonoids by**

##### **LC-UV-ESI-MS**

To identify the flavonoids in berry extracts, LC-ESI-MS was employed. Table 3.1 lists the various anthocyanins and flavonols glycosides identified in the three chosen berry samples. A total of 28 compounds were identified, based on the chromatographic behaviour of the standards, the elution order as found in the literature [24-26] and from the resulting ESI mass spectra. ESI-MS was used to determine the major ions, and fragment ions also aided in peak identification. Some general chromatographic trends can be observed from this data. First, the general order of elution of anthocyanins under these conditions was delphinidin, cyanidin, petunidin, malvidin, peonidin; for the flavonols only quercetin and myricetin were identified, with quercetin generally eluting first. More specifically, the order of elution for a specific aglycone group was dependent on the attached glycosyl portion; the order being galactosyl < glucosyl < arabinosyl < rutinoside. Acetylated sugars were identified as well, with 3-acetylglucoside being the dominant species.

Table 3.1. Summary of chromatographic peaks and mass spectrometry information obtained by LC-ESI-MS of berry samples and quantification by UV detection.

\* Based on 30 g of berry and extract dissolved in 50 mL of water.

Peak #	Retention Time (min)	Structure	<i>m/z</i> values		Blueberry ( $\mu\text{g/mL}$ )*	Lingonberry ( $\mu\text{g/mL}$ )*	Blackberry ( $\mu\text{g/mL}$ )*
		<b><u>Anthocyanins</u></b>	<b><u>M<sup>+</sup></u></b>	<b><u>Major Fragment Ion</u></b>			
1	12.0	De 3-galactoside	465	303	46.4 ± 0.1		
2	14.5	De 3-glucoside	465	303	39.5 ± 0.2		
3	15.6	Cy 3-galactoside	449	287	36.1 ± 0.2	171.3 ± 0.3	
4	17.4	De 3-arabinoside	435	303	31.8 ± 0.2		
5	19.0	Cy 3-glucoside	449	287	28.6 ± 0.1	18.4 ± 0.5	222.2 ± 0.6
6	21.6	Cy 3-arabinoside	419	287	44.6 ± 0.3	29.1 ± 0.6	
7	24.0	Cy 3-rutinoside	595	449, 287			24.4 ± 0.6
8	25.5	Pt 3-galactoside	479	317	45.8 ± 0.2		
9	29.1	Pt 3-arabinoside	449	317	15.5 ± 0.1		
10	32.7	Mv 3-galactoside	493	331	42.5 ± 0.1		
11	37.3	Mv 3-glucoside	493	331	50.3 ± 0.1		
12	40.7	Pe 3-galactoside	463	301	24.9 ± 0.1		
13	43.3	Pe 3-glucoside	463	301	1.8 ± 0.1		
14	47.2	Cy 3-dioxalylglucoside	593	287			23.2 ± 0.6
15	47.3	De 3-acetylglucoside	507	303	13.8 ± 0.1		
16	50.5	Cy 3-acetylglucoside	491	287	13.5 ± 0.1		
17	51.4	Mv 3-acetylglucoside	535	331	16.0 ± 0.1		10.2 ± 0.6
18	52.5	Pt 3-acetylglucoside	521	317	9.0 ± 0.1		
19	54.7	Pe 3-acetylglucoside	505	301	3.1 ± 0.1		
20	55.4	Cy 3-malonylglucoside	535	387	29.6 ± 0.1		
		<b><u>Flavonols</u></b>	<b><u>[M-H]<sup>-</sup></u></b>	<b><u>Major Fragment Ion</u></b>			
21	44.7	Q 3-galactoside	463	301			9.5 ± 0.5
22	45.1	M 3-galactoside	479	319	171.3 ± 0.5		
23	45.6	Q 3-glucoside	463	301		64.5 ± 0.5	1.3 ± 0.4
24	46.1	M 3-glucoside	479	319	221.1 ± 0.6		
25	47.5	Q 3-rutinoside	609	301	83.4 ± 0.1		3.1 ± 0.1
26	52.1	Q 3-glucosylxyloside	595	433, 301		65.6 ± 0.5	
27	52.3	Q 3-acetylramnoside	489	301	41.4 ± 0.1	39.1 ± 0.5	12.2 ± 0.2
28	61.2	Q	301		< LOQ	< LOQ	

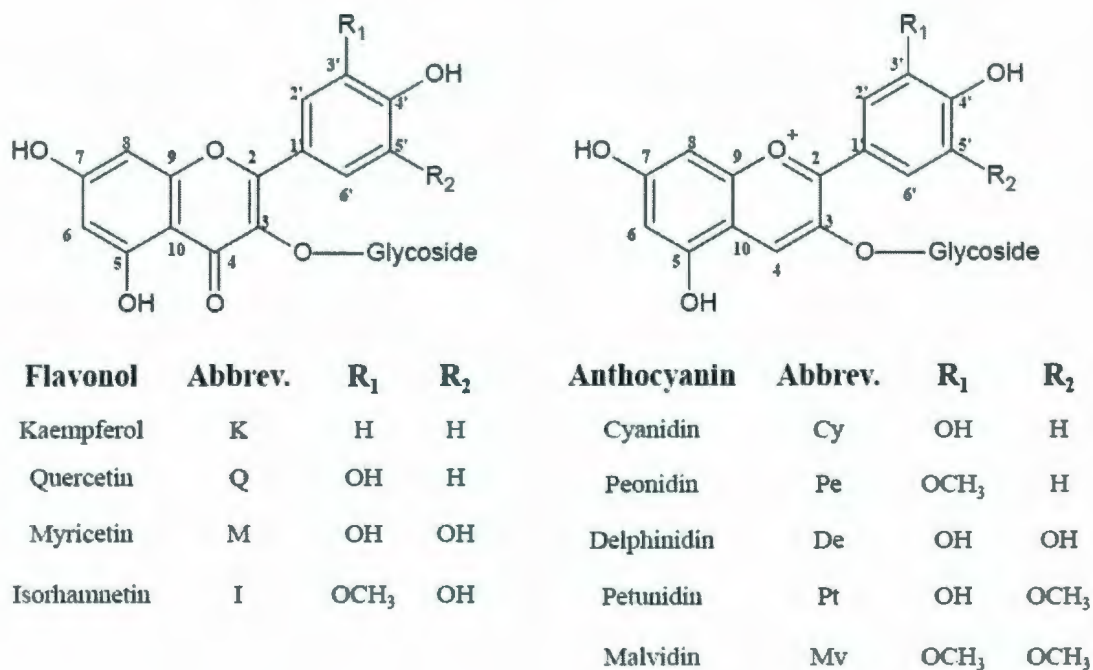


Figure 3.1 Structures of flavonols and anthocyanins.

The individual chromatograms for anthocyanins are shown in Figure 3.2, with specific detection set at 520 nm, which was also used to quantify the anthocyanins as listed in Table 3.1. Although flavonols were not measured by MALDI, Figure 2(d) shows their chromatogram at 360 nm from blackberry extract. The blueberry contained the largest variety of both anthocyanins and flavonols. In comparison, the lingonberry and blackberry contained mostly cyanidin-glycosides. The blackberry was the only species to contain cyanidin 3-dioxyalylglucoside.

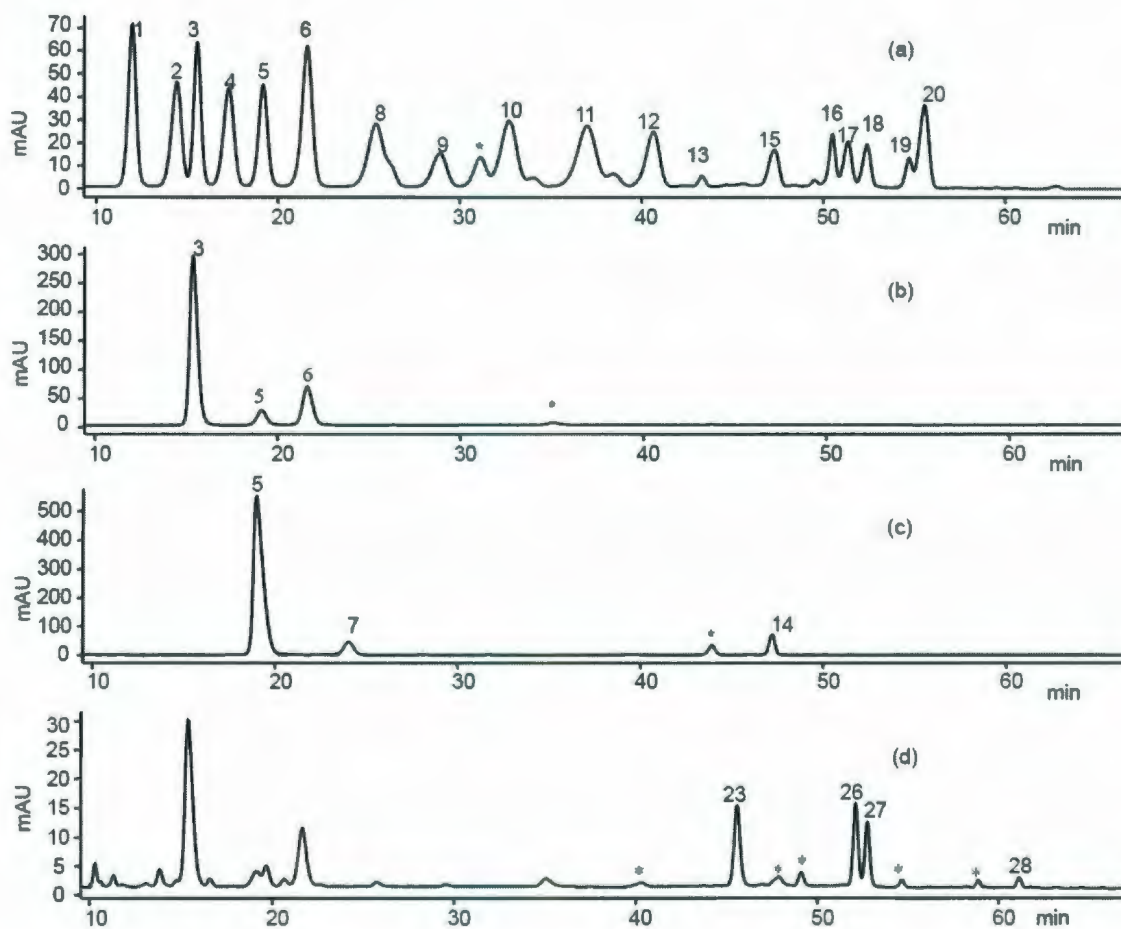


Figure 3.2. UV chromatographic profile of anthocyanins (520 nm) in extracts from (a) blueberry, (b) lingonberry, (c) blackberry, and (d) UV detection (360 nm) of blackberry flavonols.

The flavonoid concentrations (Table 3.1) were determined by calibration curves using peak area UV data from cyanidin 3-glucoside and quercetin 3-rutinoside standards. Thus, due to a lack of standards and the fact that it was previously demonstrated in the literature, it was assumed that all anthocyanins yielded a similar response to cyanidin, and all flavonols yielded a similar response to quercetin [28,29]. For anthocyanins, amounts were converted to cyanidin equivalents, and flavonols were determined using

rutin equivalents [24]. The blueberry extract had a fairly even distribution of anthocyanins, most ranging between 20 to 50  $\mu\text{g/mL}$  in the extract. The flavonols present included myricetin galactoside, myricetin glucoside and quercetin rutinoside at  $171.3 \pm 0.5$ ,  $221.1 \pm 0.6$  and  $83.4 \pm 0.1$   $\mu\text{g/mL}$ , respectively. The lingonberry may contain a much smaller variety of anthocyanin glycosides, but it contains a very large amount of cyanidin 3-galactoside ( $171.3 \pm 0.3$   $\mu\text{g/mL}$ ). The blackberry also had a smaller distribution of flavonoids, but a high abundance of cyanidin 3-glucoside. Our analysis is comparable to other studies, which have reported that cyanidin-glucoside accounted for 80% or more of the total anthocyanidin in blackberry species [30,31].

### 3.3.2 MALDI-MS versus Surfactant-Mediated MALDI-MS of Flavonoid Standards

Figure 3.3 shows the mass spectrum obtained when MALDI is tested as a method of flavonoid analysis for petunidin, cyanidin 3-glucoside, quercetin and rutin, with the use of either CHCA or THAP matrix. In each case, 10  $\mu\text{L}$  of matrix solution was mixed with 10  $\mu\text{L}$  of the standard stock solution. In the case of CHCA addition (Figure 3.3a), the masses observed correspond to the aglycones at  $m/z$  287 (cyanidin,  $[\text{M}^+]$ ) and 317 (petunidin,  $[\text{M}^+]$ ), with protonated molecules at  $m/z$  303 (quercetin,  $[\text{M}+\text{H}]^+$ ) and 611 (rutin,  $[\text{M}+\text{H}]^+$ ). The intact cyanidin 3-glucoside molecule  $[\text{M}]^+$  was identified at  $m/z$  449, but its intensity was fairly low. The detector was saturated when a laser power of 2800 (arbitrary units) was employed. Decreasing the power to 2400 was found to be sufficient for the CHCA matrix. As expected, many matrix-ion fragments due to CHCA are observed, including the protonated and sodiated molecules at  $m/z$  190 and 212. Note

that for all MALDI spectra, the ions with glycosides have been labeled such that glucoside = glu, galactoside = gal, arabinoside = arab, and rutinoside = rut.

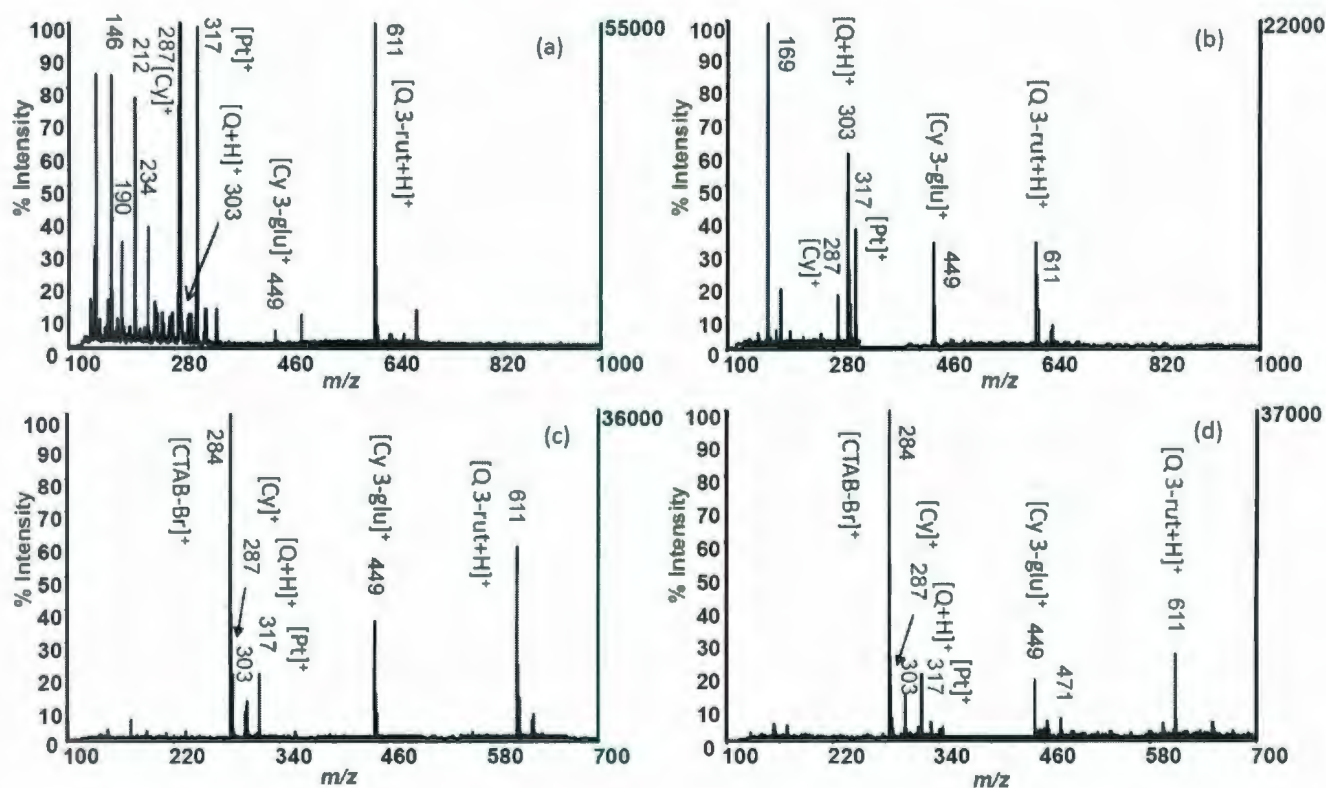


Figure 3.3. Positive ion mode MALDI-TOF-MS mass spectra of flavonoid standards obtained with the addition of (a) CHCA, (b) THAP, (c) CHCA/CTAB, and (d) THAP/CTAB.

When THAP was used as the matrix (Figure 3.3b), similar aglycone analyte ions were obtained; however, the  $[M]^+$  molecular ion of the intact glycoside was clearly observed. In addition, sodiated molecules were often observed at  $m/z$  471 ( $M-H+Na$ )<sup>+</sup> and 633  $[M+Na]^+$  for cyanidin 3-glucoside and rutin, respectively. The presence of sodiated molecules, in addition to the  $[M]^+$  or  $[M+H]^+$  ions, aided in identification when

considering samples with multiple analytes. The cyanidin and petunidin aglycones were observed as well, but with much lesser intensity than when CHCA was used. From our data, it is thought that CHCA is more energetic than THAP, making it a “hotter” matrix, and thus leading to more glycoside cleavage. However, this can possibly complicate the analysis, as the  $m/z$  values for certain flavonols  $[M+H]^+$  and aglycones  $[M]^+$  have the same value. For example, the protonated molecule of kaempferol and the aglycone of cyanidin 3-glucoside will yield a signal at  $m/z$  287. Therefore, THAP matrix has a distinct advantage in that it can more easily distinguish between the glycosides and aglycones. However, for the remainder of this work we will compare results with CHCA alongside those of THAP because of the common usage of CHCA.

Figure 3.3 also shows the spectrum resulting from the addition of a surfactant, cetyltrimethylammonium bromide (CTAB), to the mixture of standard with each matrix. As seen, the surfactant’s presence leads to ion suppression of matrix and to a lesser extent, analyte ions, as observed in our previous study [17]. In both mass spectra, the analyte ions are still readily observed. The surfactant seems to improve the analysis in terms of the standard deviation. For example, without the surfactant the resolution ( $n=5$ ) for cyanidin 3-glucoside, petunidin, quercetin and rutin were 3432 ( $\pm 19.0\%$ ), 3018 ( $\pm 18.6\%$ ), 3370 ( $\pm 17.1\%$ ) and 4352 ( $\pm 19.9\%$ ) when THAP matrix was used. In contrast, when the surfactant was used, the resolution was 3779 ( $\pm 5.9\%$ ), 3570 ( $\pm 6.0\%$ ), 4290 ( $\pm 5.3\%$ ) and 5485 ( $\pm 6.2\%$ ). This demonstrates that for each ion, the resolution was improved. The increase in resolution ranged from 10.1 to 27.3%. To the best of our knowledge, this is the first report of this surfactant being used to mediate matrix ions

from THAP. Since the surfactant does not contain conjugated moieties, it clearly does not allow for absorption in the wavelength of the N<sub>2</sub> laser (337 nm). Thus, the surfactant itself is not exhibiting matrix behaviour. Mixing the CTAB and standard mixture together without matrix resulted in a lack of any ionization from the mixture.

### **3.3.3 Analysis of Berry Extracts by MALDI-MS and Surfactant-Mediated MALDI-MS**

Useful MALDI mass spectra were obtained when berry extracts were analyzed by MALDI (10  $\mu$ L of the matrix with 10  $\mu$ L of original extract). A summary of these results is presented in Table 3.2. When CHCA matrix was used for the blueberry extract, we obtained a mass spectrum with ions due to only the aglycones of anthocyanins and flavonols. No flavonoid glycosides were observed. Using MALDI alone we can not confirm whether the ion at  $m/z$  287 is due to kaempferol or cyanidin, but considering other reports [25-29] regarding the composition of various blueberry species and our ESI-MS data, we believe that it is most likely due to cyanidin. For the lingonberry extract, ions for cyanidin, cyanidin 3-arabinoside and cyanidin 3-glucoside (or cyanidin 3-galactoside) were observed. Note that both cyanidin 3-glucoside and cyanidin 3-galactoside can yield an ion at  $m/z$  449, but unfortunately, MALDI cannot differentiate between isomers. As an example of our data, Figure 3.4(a) displays the analysis of the blackberry extract using the CHCA as a matrix, revealing only the presence of the cyanidin.

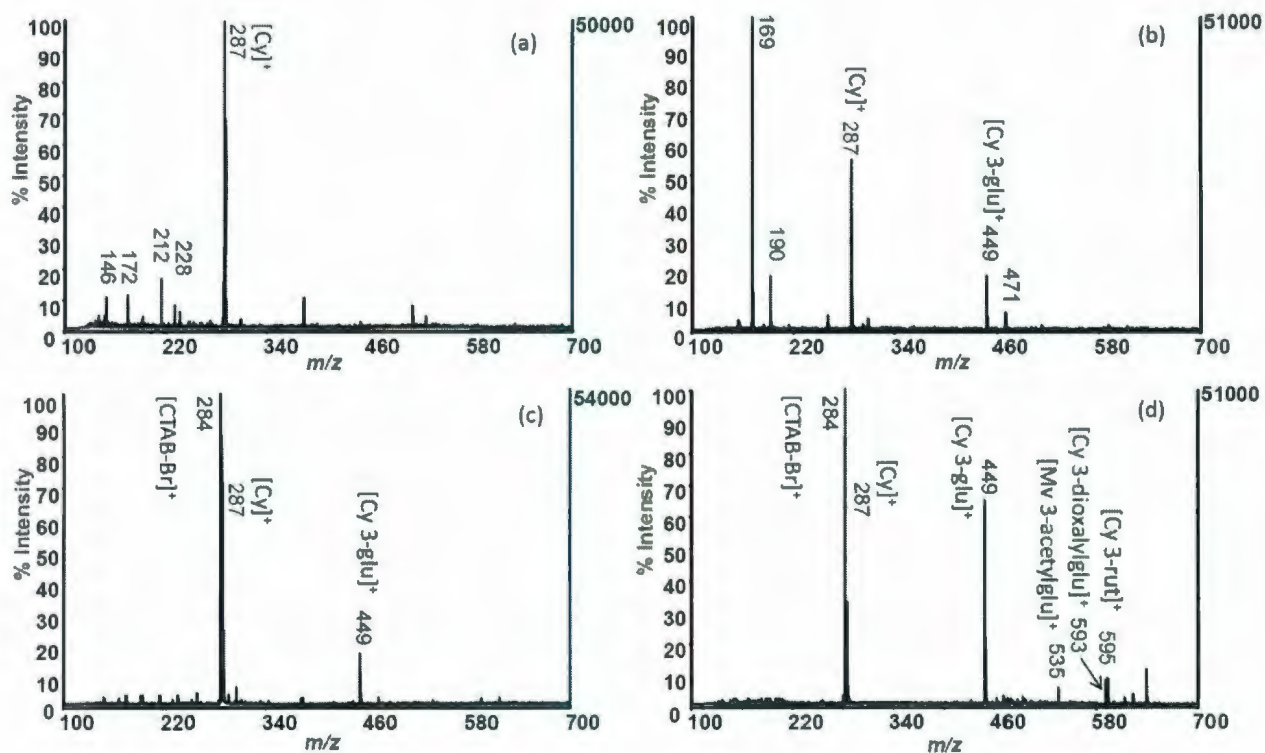


Figure 3.4. Positive ion mode MALDI-TOF-MS mass spectra of blackberry extract obtained with the addition of (a) CHCA, (b) THAP, (c) CHCA/CTAB, and (d) THAP/CTAB.

When THAP was used as a matrix for blueberries, all of the aglycone ions observed in the CHCA matrix spectra were present, but in addition, many intact glycosides observed by LC-ESI-MS were clearly visible, including cyanidin 3-arabinoside, cyanidin 3-glucoside, peonidin 3-glucoside, delphinidin 3-glucoside, petunidin 3-glucoside, malvidin 3-glucoside and malvidin 3-acetylglucoside. This demonstrated that THAP provided improved structural information for sugar-containing flavonoids. In the analysis of lingonberries, THAP again demonstrated improved resolution of glycosides, and that the aglycone of cyanidin observed with CHCA, could

be positively identified (Table 3.2). The blackberry analysis yielded results similar to those with the blueberries, with the glycoside ion being observed, as illustrated in Figure 3.4(b).

Table 3.2. Flavonoids detected in berries using MALDI-TOF-MS with CHCA or THAP matrix. (C = CHCA matrix, C/C = CHCA matrix + CTAB addition at a 10000:1 ratio, T = THAP matrix, T/C = THAP matrix + CTAB addition at a 10000:1 ratio.) \* denotes a minor ion; less than 2% relative intensity of largest ion intensity.

<i>m/z</i>	Compound	<u>Blueberry</u>				<u>Lingonberry</u>				<u>Blackberry</u>			
		C	C/C	T	T/C	C	C/C	T	T/C	C	C/C	T	T/C
287	cyanidin	✓	✓	✓		✓	✓	✓	✓	✓	✓	✓	✓
301	peonidin	✓	✓	✓									
303	delphinidin	✓	✓	✓									
317	petunidin	✓	✓	✓									
331	malvidin	✓	✓	✓	✓								
419	cyanidin 3-arabinoside			✓	*	*	*	✓	✓				
449	cyanidin 3-glucoside (galactoside)			✓	✓	*	✓	✓	✓	✓			✓
463	peonidin 3-glucoside (galactoside)			✓	✓								
465	delphinidin 3-glucoside (galactoside)			✓	*								
479	petunidin 3-glucoside			✓	✓								
493	malvidin 3-glucoside (galactoside)			✓	✓								
535	malvidin 3-acetylglucoside/ cyanidin 3-malonylglucoside			✓	✓								✓
593	cyanidin 3-dioxalylglucoside												✓
595	cyanidin 3-rutinoside					*							✓

The effect of CTAB addition to each sample was then monitored. CTAB was added to each sample so that the matrix : CTAB ratio was 10000 : 1. The results are shown in Table 3.2. For example, the blueberry extract demonstrated that the flavonoid ions were slightly suppressed, but they remained very well resolved in comparison with the matrix ions. All of the same ions were observed as when CHCA was used alone. The ion at  $m/z$  284 [CTAB-Br]<sup>+</sup> does make it difficult to observe the cyanidin aglycone ions, but careful observation, by enlarging the mass spectrum in the region of  $m/z$  280 to 290 using instrument data analysis software, did indeed reveal its presence. In the case of the lingonberry, all ions were still observed and well resolved, except for the quercetin 3-glucosylxyloside. However, in the blackberry analysis, Figure 3.4(c), the cyanidin aglycone ion was still observed, and in this case the glycoside ion was observed as well.

When CTAB was added to the THAP matrix at the same ratio, the blueberry analysis led to identification of the same glycoside ions, however, the aglycone ions were all suppressed except for malvidin. In the lingonberry analysis, the same ions were observed, showing a dominant ion at  $m/z$  449. The blackberry result, shown in Figure 3.4(d), demonstrated the appearance of glycoside ions that had not been detected in any other of these MALDI experiments (malvidin 3-acetylglucoside, cyanidin 3-dioxalylglucoside, quercetin 3-glucosylxyloside). Figure 3.5 illustrates the results of the surfactant addition to THAP in the analysis of lingonberry and blueberry extract.

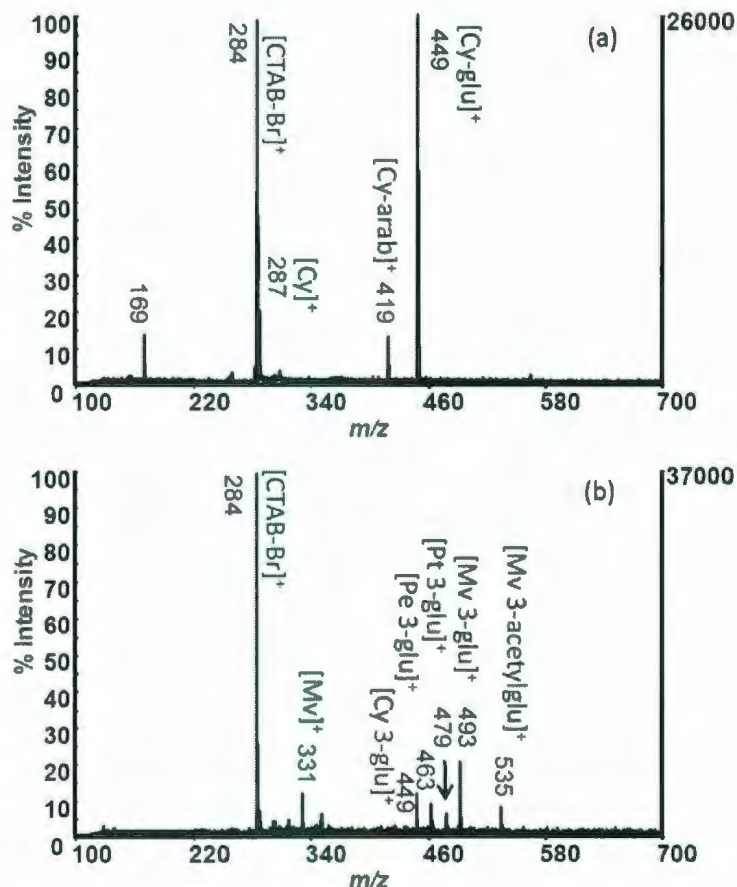


Figure 3.5. Positive ion mode MALDI-TOF-MS mass spectra obtained when THAP/CTAB was used for the analysis of (a) lingonberry extract, and (b) blueberry extract.

In comparison to the MALDI-TOF-MS analysis, LC-ESI-MS was able to identify a greater number of flavonoids in each sample. For example, delphinidin 3-acetylglucoside was present in the blueberry extract, but was not identified in the MALDI-MS spectra. One reason for this is that UV-VIS detection presents a method with almost no background interference, as opposed to the ubiquitous background noise of MALDI. Another problem with MALDI-TOF-MS of complex samples may stem from analyte-analyte ion suppression [32]. Essentially, species that are present in much larger quantity than others, or species that have a higher proton affinity than others, may

abstract protons more easily from a matrix. This can lead to an observed suppression of ions from the species with a lower concentration. MALDI will not always qualitatively identify as many species as LC-ESI-MS, but it can rapidly screen for major constituents and illustrate the main species from a sample.

In our MALDI-TOF-MS experiments, the anthocyanins were more easily detected than the flavonols. Thus, Table 3.2 contains information only on the former. Changing the solvent system to a more acidic medium, such as one containing some trifluoroacetic acid might improve this analysis, but we recognized that even then, many of the flavonols and anthocyanins would generate ions of the same  $m/z$  value. Thus, this is an inherent limitation of the method.

### **3.3.4 Quantification by Surfactant-Mediated MALDI-TOF-MS**

Although a very powerful qualitative analytical tool, MALDI-TOF-MS has not yet become as widely used for small molecule quantification. Wang *et al.* [28] demonstrated that under MALDI-TOF-MS analysis, anthocyanins ionize in a proportional manner. We designed an experiment to compare the results of quantification of the flavonoids in berry extracts by normal MALDI-TOF-MS and the surfactant-mediated approach. Mass spectral calibration was achieved using cyanidin 3-glucoside standard for both matrices with and without surfactant. Figure 3.6 shows the calibration curves for THAP matrix. Figure 3.6(a) shows the calibration curve by THAP only, yielding a correlation coefficient of 0.981 and the average RSD value of 32%, with a range from 24-46%. With the addition of CTAB surfactant in Figure 3.6(b), the

correlation coefficient increases to 0.996 and the average RSD was 18% (range of 13-21%).

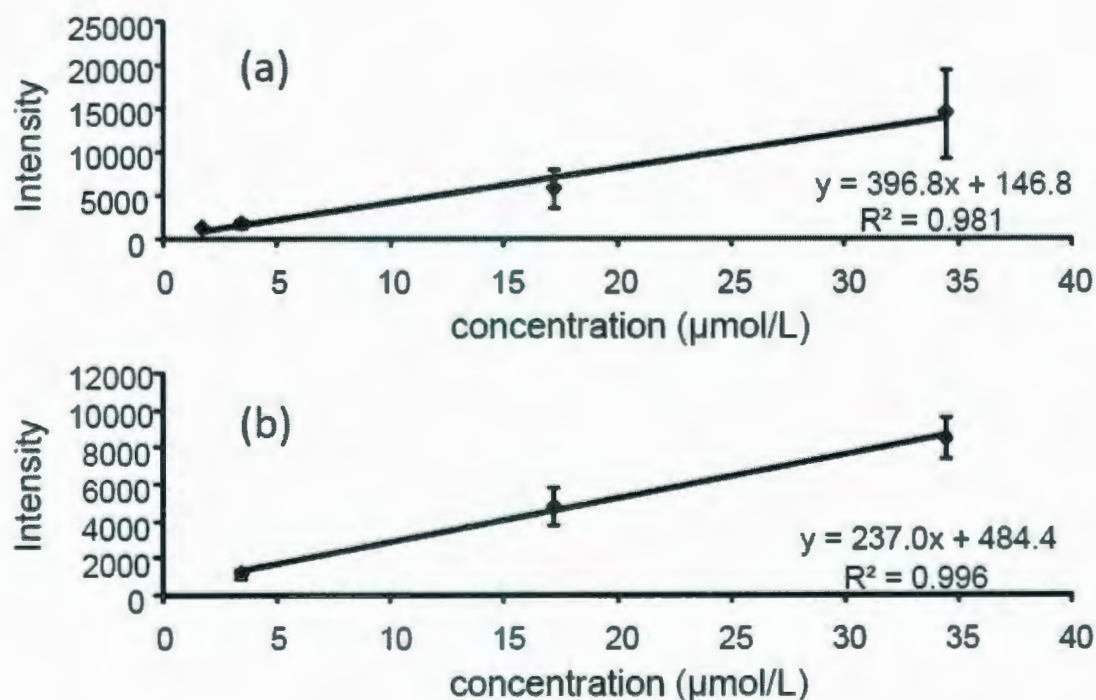


Figure 3.6. MALDI-TOF-MS calibration curves of cyanidin 3-glucoside standard by analysis with (a) THAP and (b) THAP/CTAB.

Each standard curve was prepared by analyzing 4 different concentration levels of a standard. However, in each case, the most dilute level (2 μmol/L) could not be detected by surfactant-mediated MALDI. As the ion-suppression also partially suppresses the analyte ions, they could not be distinguished from the background noise. We found that CHCA led to calibration curves with better correlation coefficients (data not shown), if

the aglycone ion was monitored, and lower standard deviations were observed. However, in this study we sought to quantify the intact glycosides, and thus, THAP was solely used.

Using the calibration curves from the THAP/CTAB work, quantification of anthocyanins in berry extracts was undertaken. Based on the LC quantitation results, the blueberry extract was found problematic since it was very complex and not all ions were observed. Analyte-analyte suppression would hinder quantification and as well, multiple species have the same *m/z* value, making it difficult to assign which component is giving a particular signal. MALDI-TOF-MS quantitation results are shown in Table 3.3.

Table 3.3. Results from quantitation by MALDI-TOF-MS analysis of anthocyanins in blackberry and lingonberry extract. Results shown are averaged (*n* = 5). %Disc. = Percentage of discrepancy from results obtained by LC-MS with UV detection. Note: THAP indicates that only THAP matrix was used; THAP/CTAB indicates THAP was used with added surfactant at a 10000:1 mole ratio. n/d = not detected.

Berry	Anthocyanin	<u>THAP</u>			<u>THAP/CTAB</u>		
		Amount ( $\mu\text{g/mL}$ )	%RSD	%Disc.	Amount ( $\mu\text{g/mL}$ )	%RSD	%Disc.
Blackberry	cyanidin 3-glucoside	189.2	38.5	14.8	209.9	8.3	5.5
	malvidin 3-acetylglucoside	n/d	-	-	13.4	16.7	11.3
	cyanidin 3-dioxalylglucoside	n/d	-	-	28.7	10.0	13.7
	cyanidin 3-rutinoside	n/d	-	-	29.0	14.0	18.9
Lingonberry	cyanidin 3-glucoside	213.4	47.3	12.5	191.3	6.1	1.8
	cyanidin 3-arabinoside	56.01	18.5	92.5	34.3	8.9	17.8

Using THAP matrix without surfactant, cyanidin 3-glucoside yielded a large discrepancy against the LC-ESI-MS results; 14.8% in blackberries and 12.5% in lingonberries. Both values have a RSD value greater than 30%. Cyanidin 3-arabinoside was also determined, but its percentage of discrepancy was over 90%. However, adding CTAB into the matrix greatly improved the discrepancy versus the LC results and the RSD. For the cyanidin 3-glucoside in both berries, the discrepancy decreased by about 10% in each berry to 5.5% and 1.8% and RSD dropped to less than 10%. As well, malvidin acetylglucoside, cyanidin 3-dioxalylglucoside and cyanidin 3-rutinoside could also be quantified with results differing from the LC-ESI-MS analysis for these by 11.3 to 18.9%, and RSD values ranging from 10.0 to 16.7%. These results show that quantitation is markedly improved using CTAB and reproducibility is excellent compared to traditional analyses, where experiments often have RSD of 30% or greater.

This work shows that surfactant-mediated MALDI-TOF-MS is a viable approach for fast screening of flavonoids in berries. Although LC-ESI-MS provides more qualitative and quantitative information, the long run times are a significant drawback compared to the speed of a MALDI-TOF-MS analysis. Thus, this is an example of MALDI as an excellent tool for rapid screening and providing a complementary analysis to the LC.

It is possible that off-line HPLC-MALDI would be useful to separate the various species of anthocyanins and flavonols. This would make possible the individual MALDI analysis of each species, and would remove the likelihood of analyte-analyte suppression.

### **3.4 CONCLUSION**

It has been shown that the addition of the surfactant CTAB to common matrices for analysis of flavonoids improves the MALDI-TOF-MS data by decreasing matrix-ion signals and providing more reproducible signals that can be used for quantitative purposes. CHCA led to more fragmentation of the glycosyl portion of the flavonoids than THAP. This method was successfully applied to an anthocyanin standard and extracts from multiple berry samples. Surfactant-mediated MALDI-TOF-MS can be a rapid screening technique for these flavonoids, reducing analysis time to just a few minutes as compared to LC methods using electrospray ionization mass spectrometry. Future work is being pursued to further the applications of screening small biomolecules using this method.

### 3.5 REFERENCES

1. Karas M, Bachmann D, Hillenkamp F. *Anal. Chem.* 1985; **57**: 2935.
2. Tanaka K, Waki H, Ido Y, Akita S, Yoshida Y, Yoshida T. *Rapid Commun. Mass Spectrom.* 1988; **2**: 151.
3. Karas M, Bahr U, Ingendoh A, Nordhoff E, Stahl B, Strupat K, Hillenkamp F. *Analytica Chimica Acta.* 1990; **241**:175.
4. Distler AM, Allison J. *Anal. Chem.* 2001; **73**: 5000.
5. Bahr U, Deppe A, Karas M, Hillenkamp F. *Anal. Chem.* 1992; **64**: 2866.
6. Weidner S, Kuhn G, Friedrich J. *Rapid Commun. Mass Spectrom.* 1998; **12**: 1373.
7. Schurenberg M, Dreisewerd K, and Hillenkamp F. *Anal. Chem.* 1999; **71**: 221.
8. Cohen SL, Chait BT. *Anal. Chem.* 1996; **68**: 31.
9. Dreisewerd K. *Chem. Rev.* 2003; **103**: 395.
10. Knochenmuss R. *Analyst.* 2006; **131**: 966.
11. Smirnov I, Zhu X, Taylor T, Huang Y, Ross P, Papayanopoulos I, Martin S, Pappin D. *Anal. Chem.* 2004; **76**: 2958.
12. Zhong G, Lin H. *Anal. Bioanal. Chem.* 2007; **387**: 1939.
13. Mugo S, Bottaro C. *Rapid Commun. Mass Spectrom.* 2007; **21**: 219.
14. Guo Z, Zhang Q, Zou H, Guo B, Ni J. *Anal. Chem.* 2002; **74**: 1637.
15. Su AK, Liu JT, Lin CH. *Talanta.* 2005; **67**: 718.
16. Su. AK, Liu JT, Lin CH. *Anal. Chimica Acta.* 2005; **546**: 193.
17. Grant DC, Helleur RJ. *Rapid Commun. Mass Spectrom.* 2007; **21**: 837.
18. Havsteen B. *Biochem. Pharmacology.* 1983; **32**: 1141.
19. Bravo L. *Nutr Rev.* 1998; **56**: 317.

20. Harborne JB. *The Flavonoids: Advances in Research Since 1986*. Chapman and Hall: London, 1994.
21. Hertog MG, Feskens EJ, Kromhout D. *Lancet*. 1997; **349**: 699.
22. Keli SO, Hertog MG, Feskens EJ, Kromhout D. *Arch Int Med*. 1996; **156**: 637.
23. Knekt P, Jarvinen R, Seppanen R, Hellovaara M, Teppo L, Pukkala E, Aromaa A. *Am J Epidemiol*. 1997; **146**: 223.
24. Cho MJ, Howard LR, Prior RL, Clark JR. *J. Sci. Food Agric*. 2004; **84**: 1771.
25. Hakkinen S, Auriola S. *Journal of Chromatography A*. 1998; **829**: 91.
26. Pati S, Losito I, Gambacorta G, La Notte E, Palmisano F, Zambonin PG. *J. Mass Spectrom*. 2006; **41**: 861.
27. Liang Q, Qian H, Yao W. *Eur. J. Mass Spectrom*. 2005; **11**: 93.
28. Wang J, Sporns P. *J. Agric. Food Chem*. 1999; **47**: 2009.
29. Wang J, Kalt W, Sporns P. *J. Agric. Food Chem*. 2000; **48**: 3330.
30. Rossi A, Serraino I, Dugo P, Di Paola R, Mondello L, Genovese T, Morabito D, Dugo G, Sautebin L, Caputi AP, Cuzzocrea A. *Free Radical Research*. 2003; **37**: 891.
31. Torre LC, Barritt BH. *J. Food Science*. 1977; **42**: 488.
32. Knochenmuss R, Stortelder A, Breuker K, Zenobi R. *J. Mass Spectrom*. 2000; **35**: 1237.

## Chapter 3 Addendum

The data presented in this addendum supplements the manuscript publication of Chapter 3. This data will be beneficial to researchers and students wanting to repeat or continue this work.

LC-MS results for the anthocyanin and flavonoid standards were obtained. The mass spectra that were used to interpret the individual species are shown in Figure 3.7. As an example, the spectrum of delphinidin 3-galactoside was interpreted exhibiting what is believed to be its intact oxonium ion at  $m/z$  465 and another ion at  $m/z$  303 due to the loss of the sugar moiety and is believed to be the aglycone ion. Under the conditions used, the major ions, in all cases, were due to the intact glycosated molecule. Figure 3.8 shows the LC-ESI-MS results that were used to identify all the flavonoid species. The intact molecular ion which was the dominant ion, and the aglycone were also observed in the resulting mass spectra.

Figure 3.9 shows the detection of flavonols by LC-UV analysis in each of the three berry samples. In the submitted manuscript, only one of these was illustrated, along with the analysis of anthocyanins. The identity of the labeled peak is recorded in Table 3.1

To illustrate the spotting of different matrices used, Figure 3.10 shows the crystals formed for the standard mixture with (a) CHCA matrix and (b) THAP matrix. These were acquired using a scanning electron microscope (SEM) at 220x-300x magnification.

Finally, Figure 3.11 highlights the calibration curves obtained by LC-UV analysis of standards used to quantify the (a) anthocyanins and (b) flavonols.

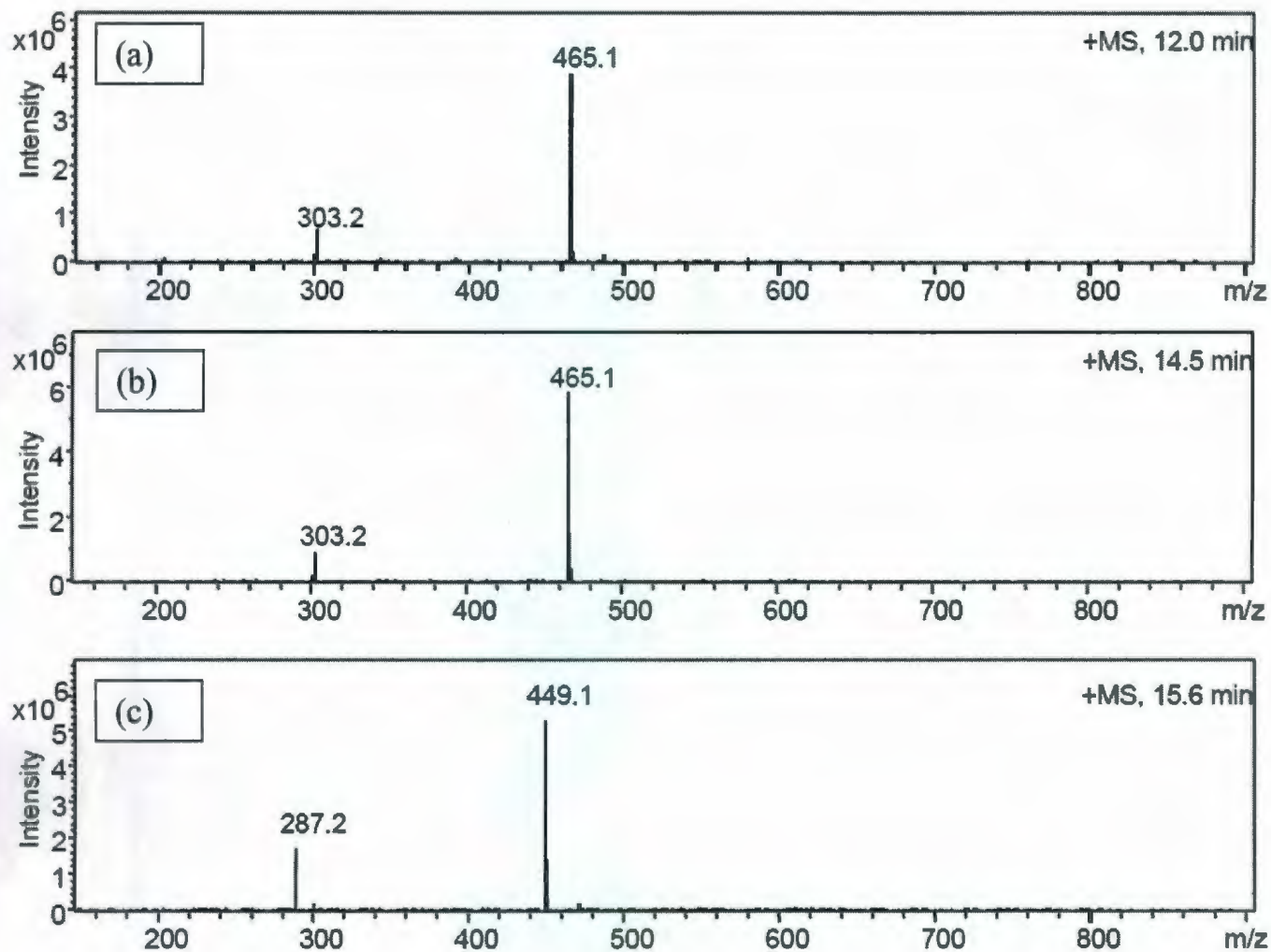


Figure 3.7. Electrospray ionization mass spectra of anthocyanins (a) delphinidin 3-galactoside, (b) delphinidin 3-glucoside and (c) cyanidin 3-galactoside.

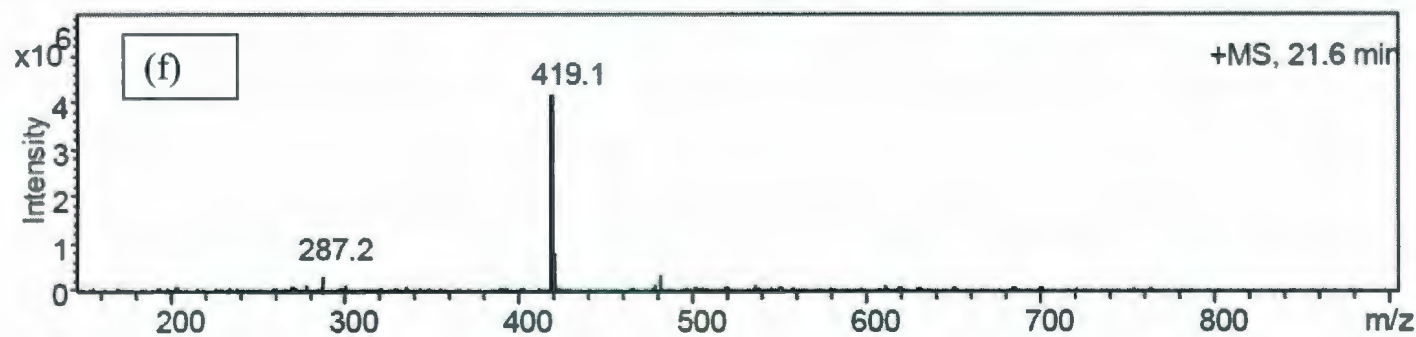
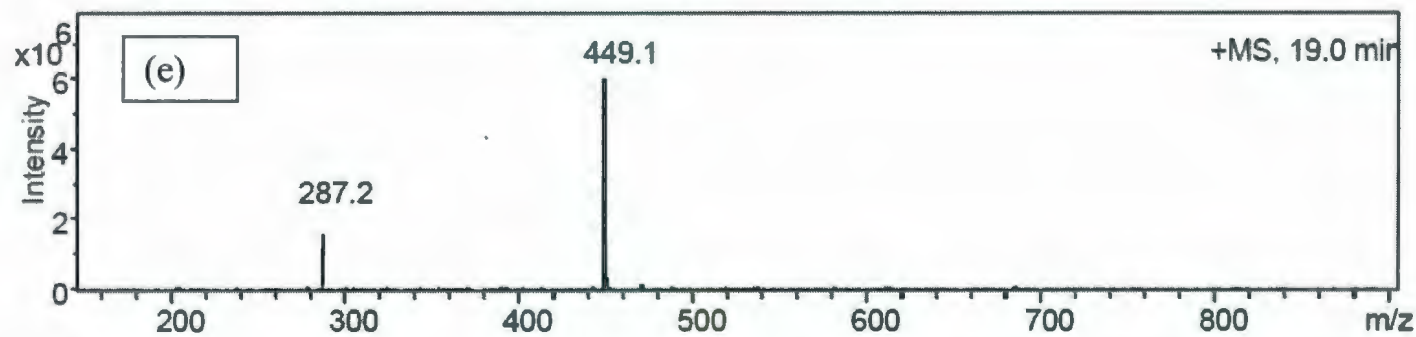
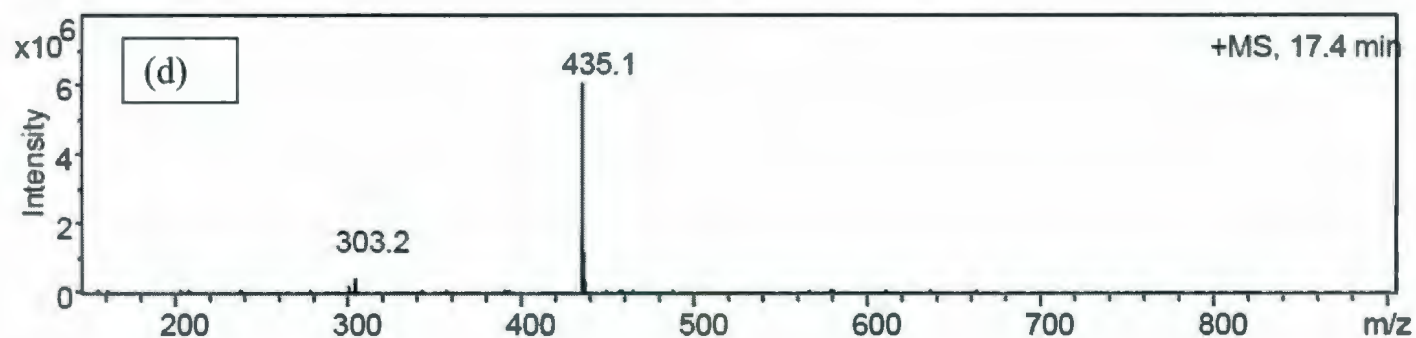


Figure 3.7 (continued). Electrospray ionization mass spectra of anthocyanins (d) delphinidin 3-arabinoside, (e) cyanidin 3-glucoside and (f) cyanidin 3-arabinoside.

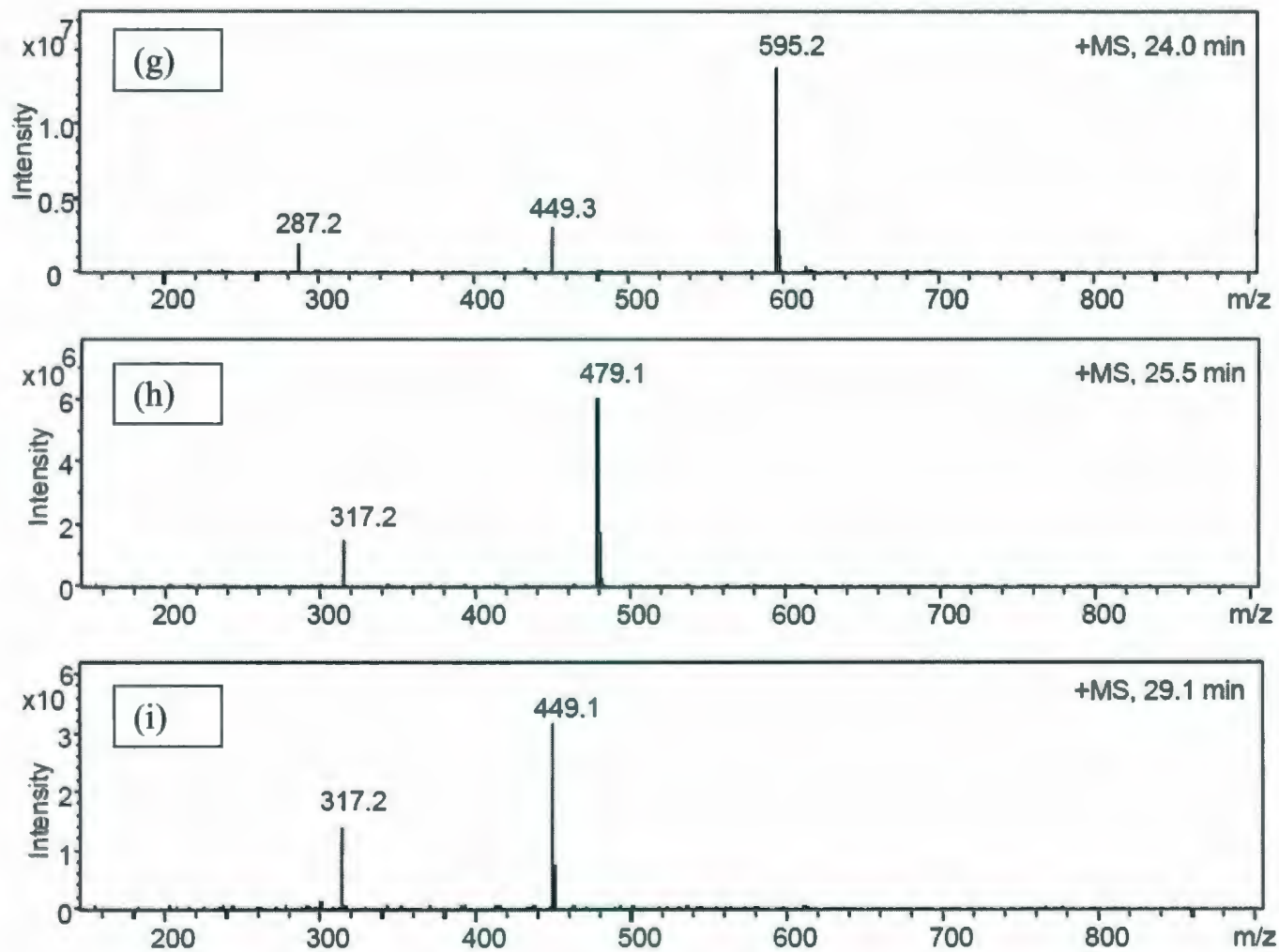


Figure 3.7 (continued). Electrospray ionization mass spectra of anthocyanins (g) cyanidin 3-rutinoside, (h) petunidin 3-galactoside and (i) petunidin 3-arabinoside.

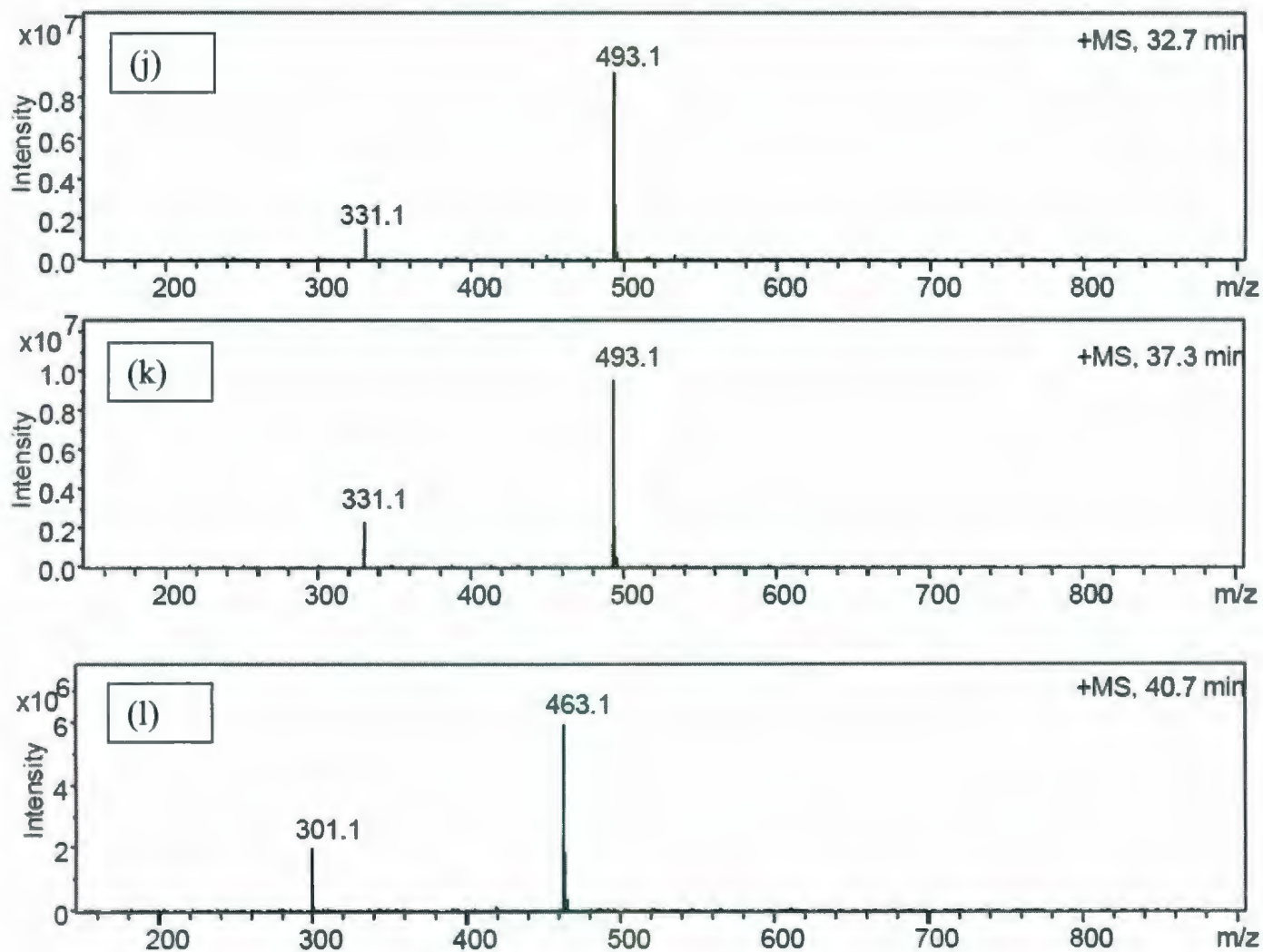


Figure 3.7 (continued). Electro spray ionization mass spectra of anthocyanins (j) malvidin 3-galactoside, (k)malvidin 3-glucoside and (l) peonidin 3-galactoside.

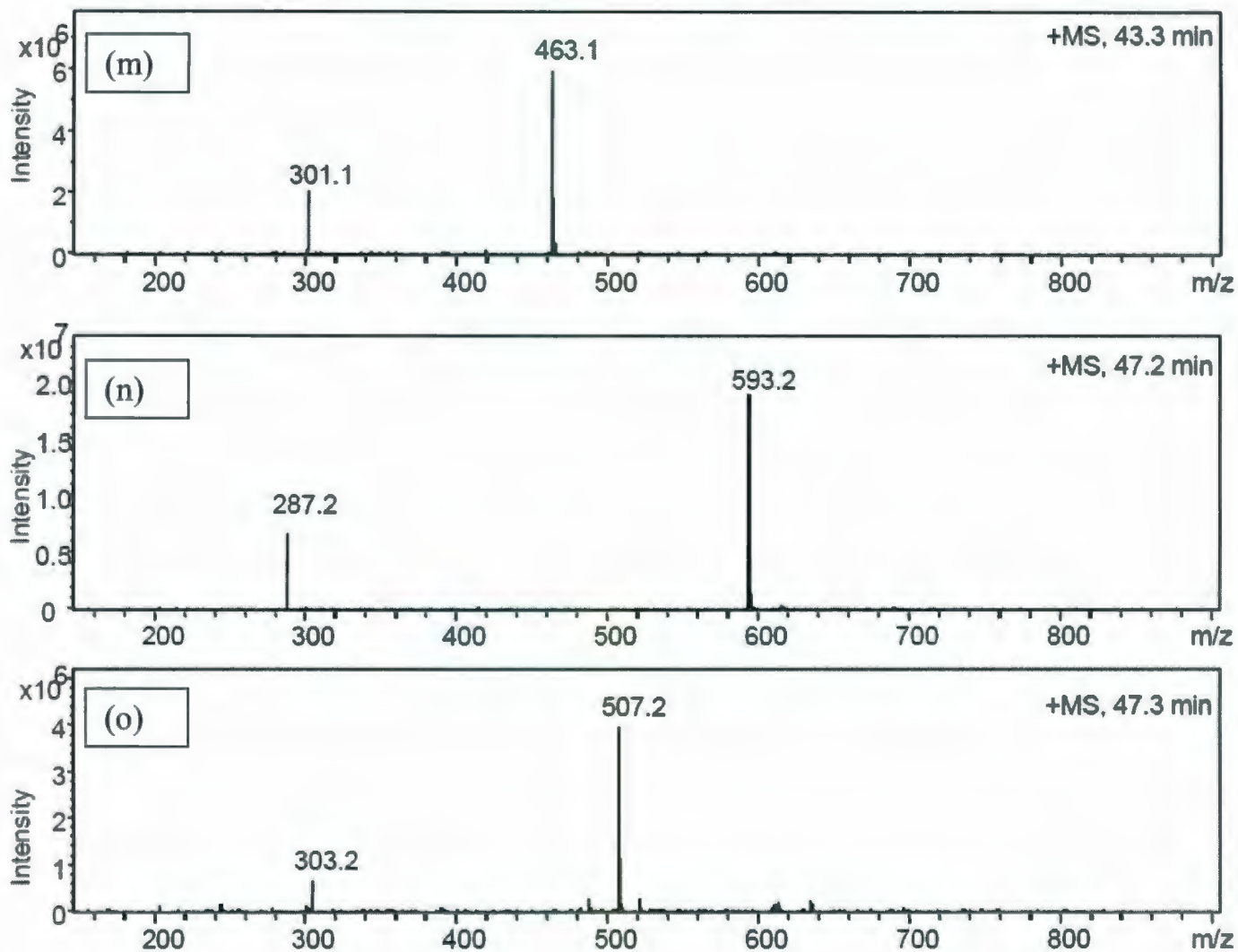


Figure 3.7 (continued). Electrospray ionization mass spectra of anthocyanins (m) peonidin 3-glucoside, (n) cyanidin 3-dioxalylglucoside and (o) delphinidin 3-acetylglucoside.

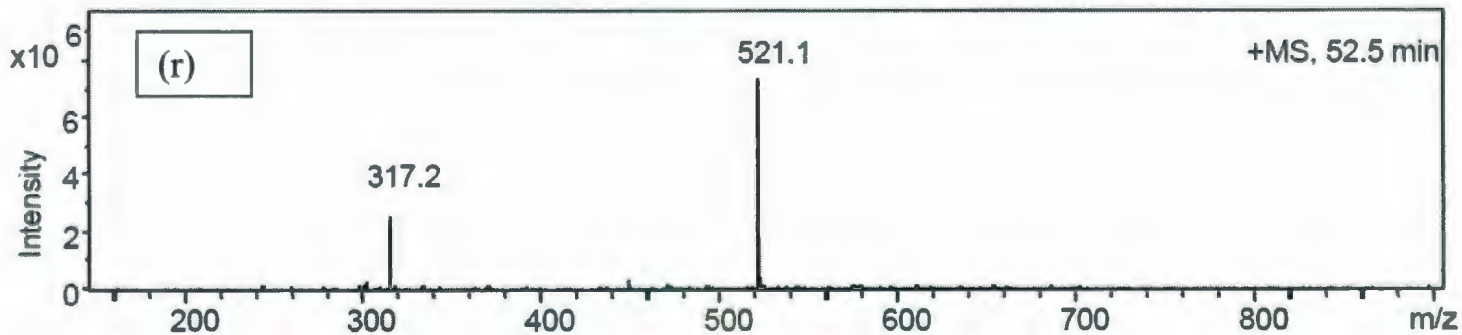
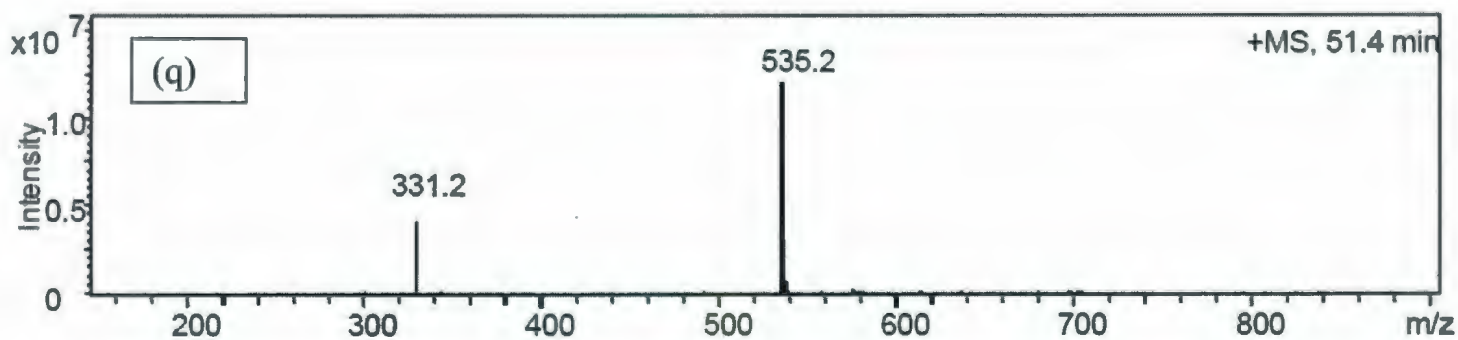
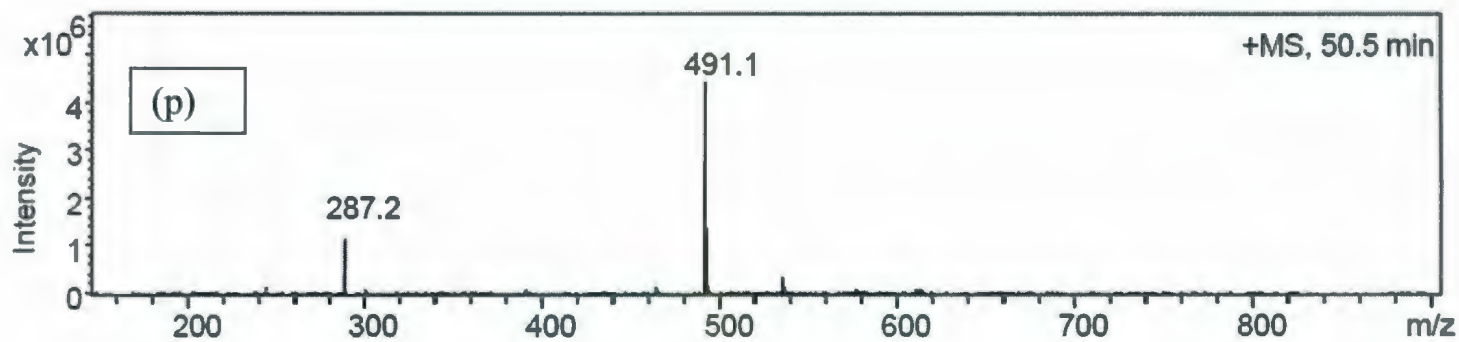


Figure 3.7 (continued). Electrospray ionization mass spectra of anthocyanins (p) cyanidin 3-acetylglucoside, (q) malvidin 3-acetylglucoside and (r) petunidin 3-acetylglucoside.

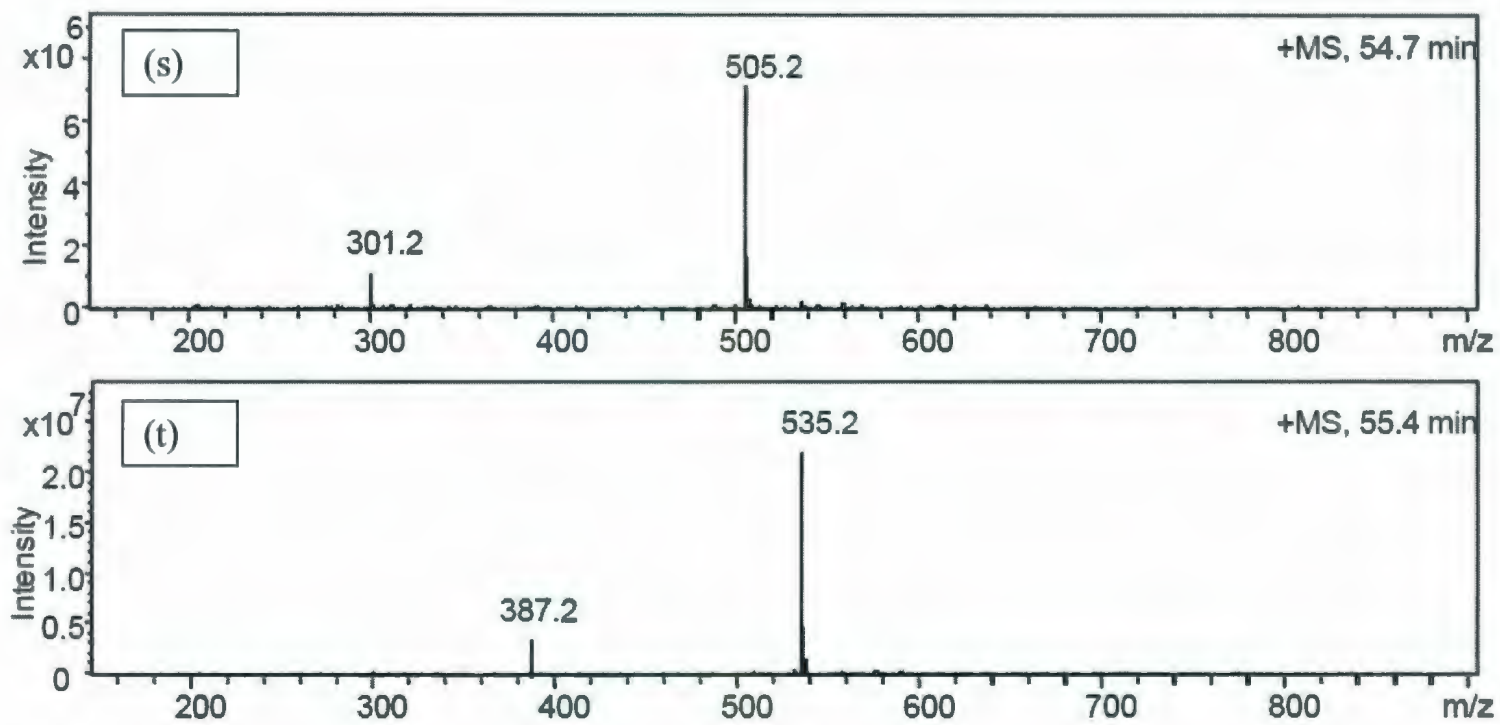


Figure 3.7 (continued). Electrospray ionization mass spectra of anthocyanins (s) peonidin 3-acetylglucoside and (t) cyanidin 3-malonylglucoside.

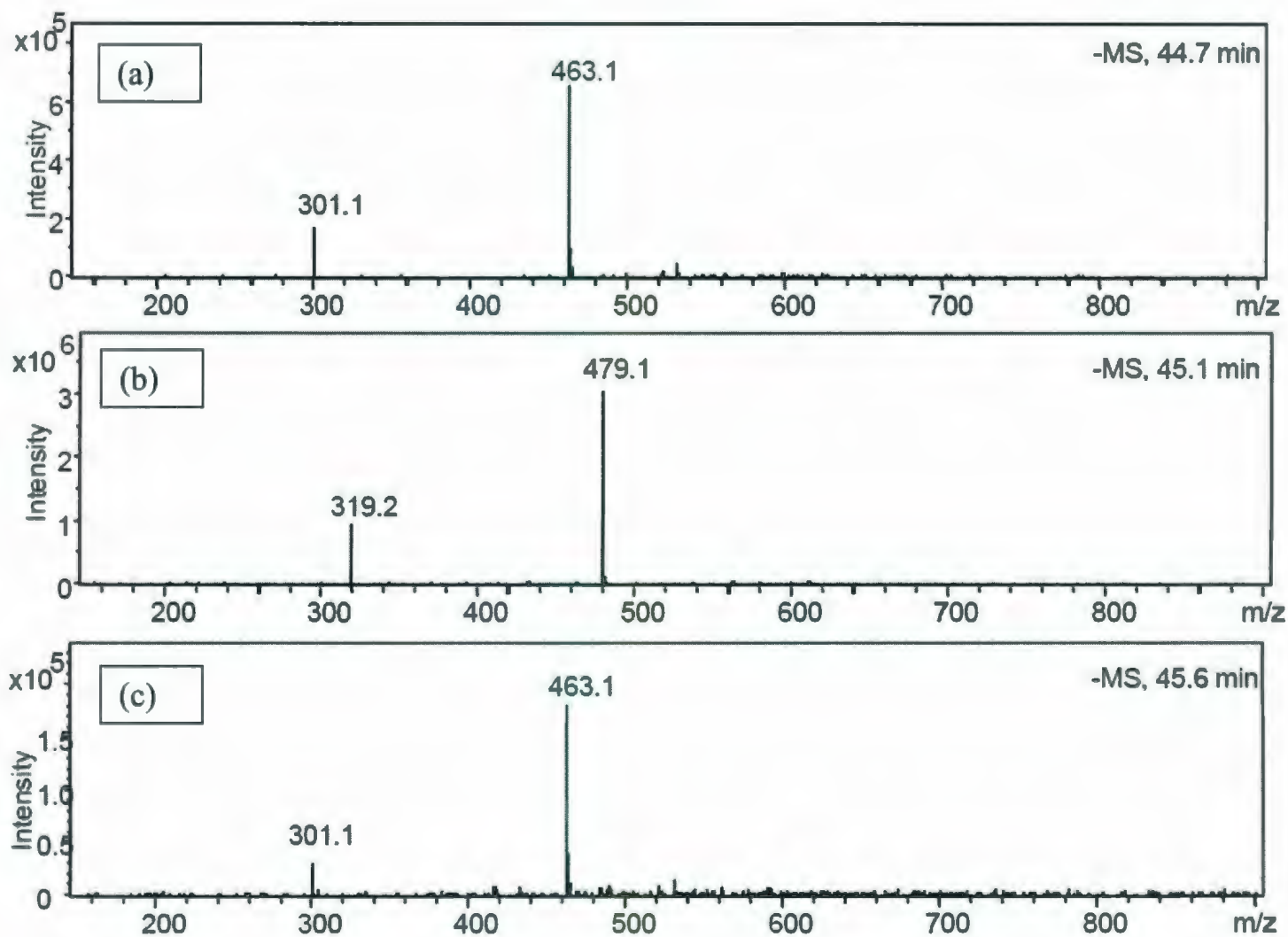


Figure 3.8. Electrospray ionization mass spectra of flavonols (a) quercetin 3-galactoside, (b) myricetin 3-galactoside and (c) quercetin 3-glucoside.

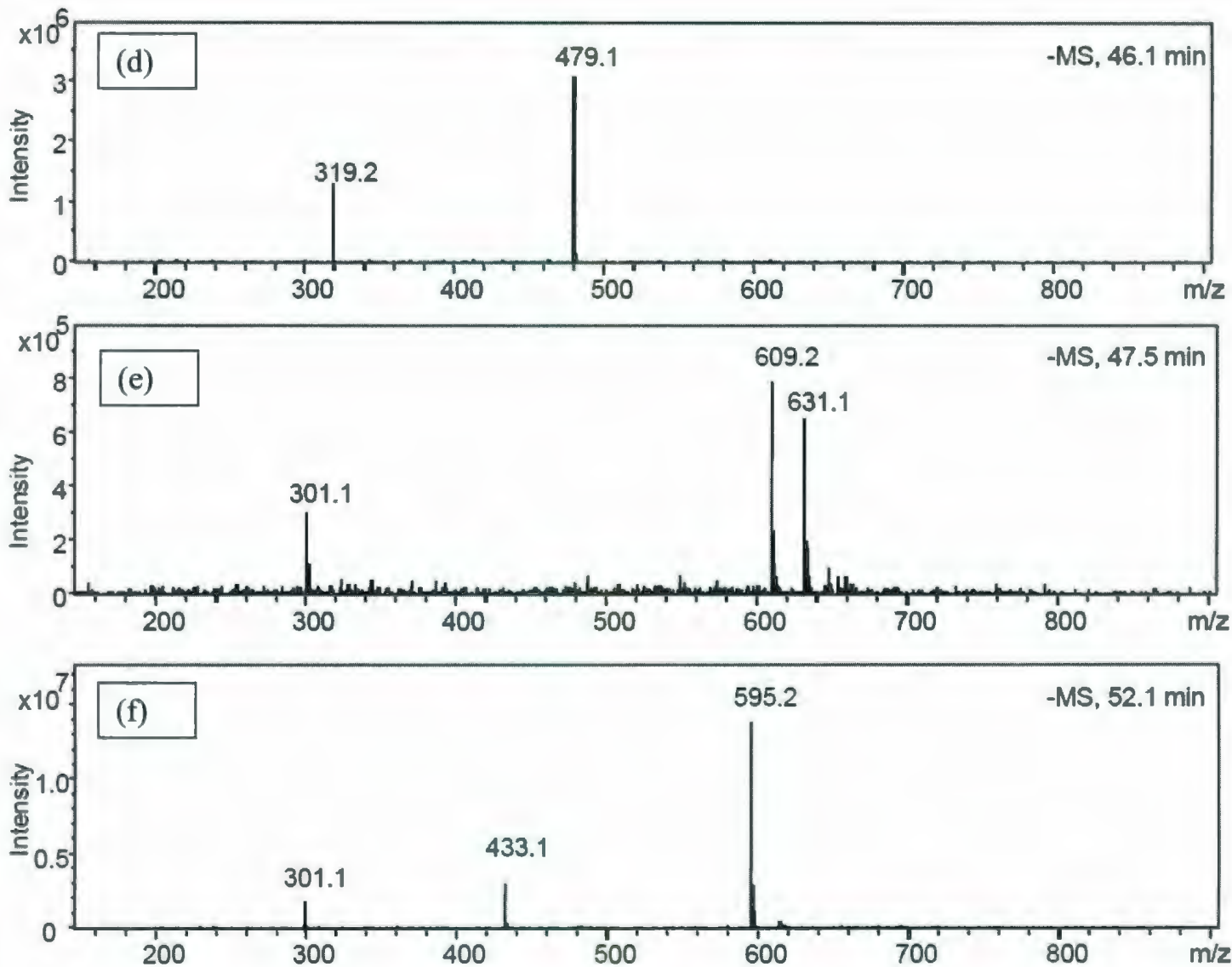


Figure 3.8 (continued). Electrospray ionization mass spectra of flavonols (d) myricetin 3-glucoside, (e) quercetin 3-rutinoside and (f) quercetin 3-glucosylxyloside.

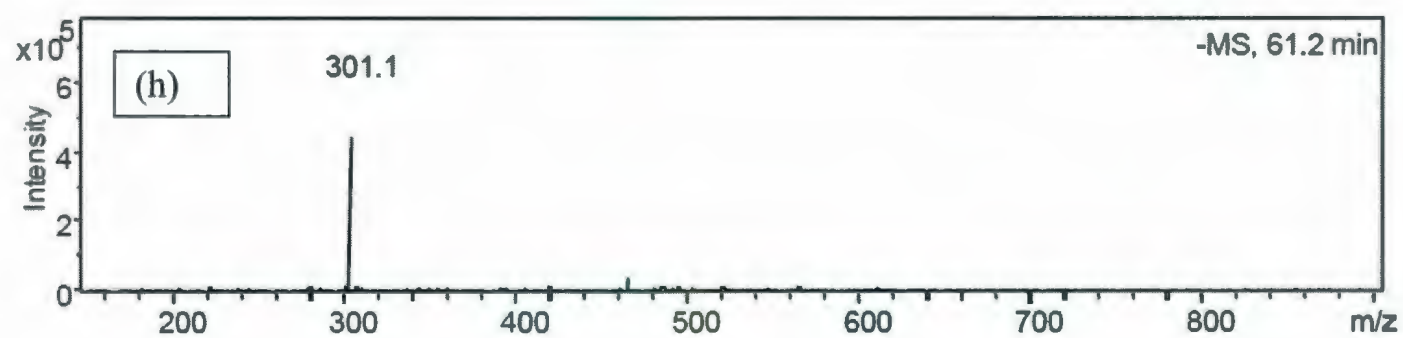
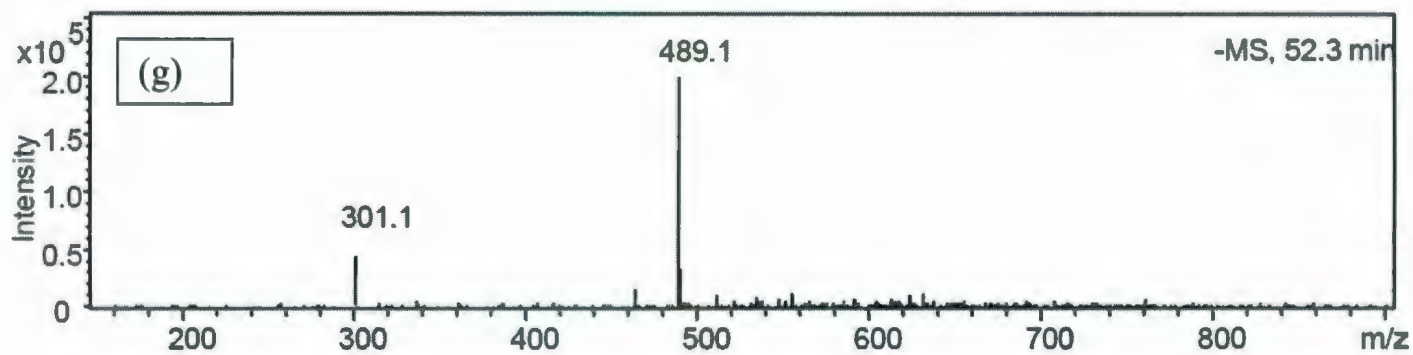


Figure 3.8 (continued). Electrospray ionization mass spectra of flavonols (g) quercetin 3-acetylglucoside and (h) quercetin aglycone.

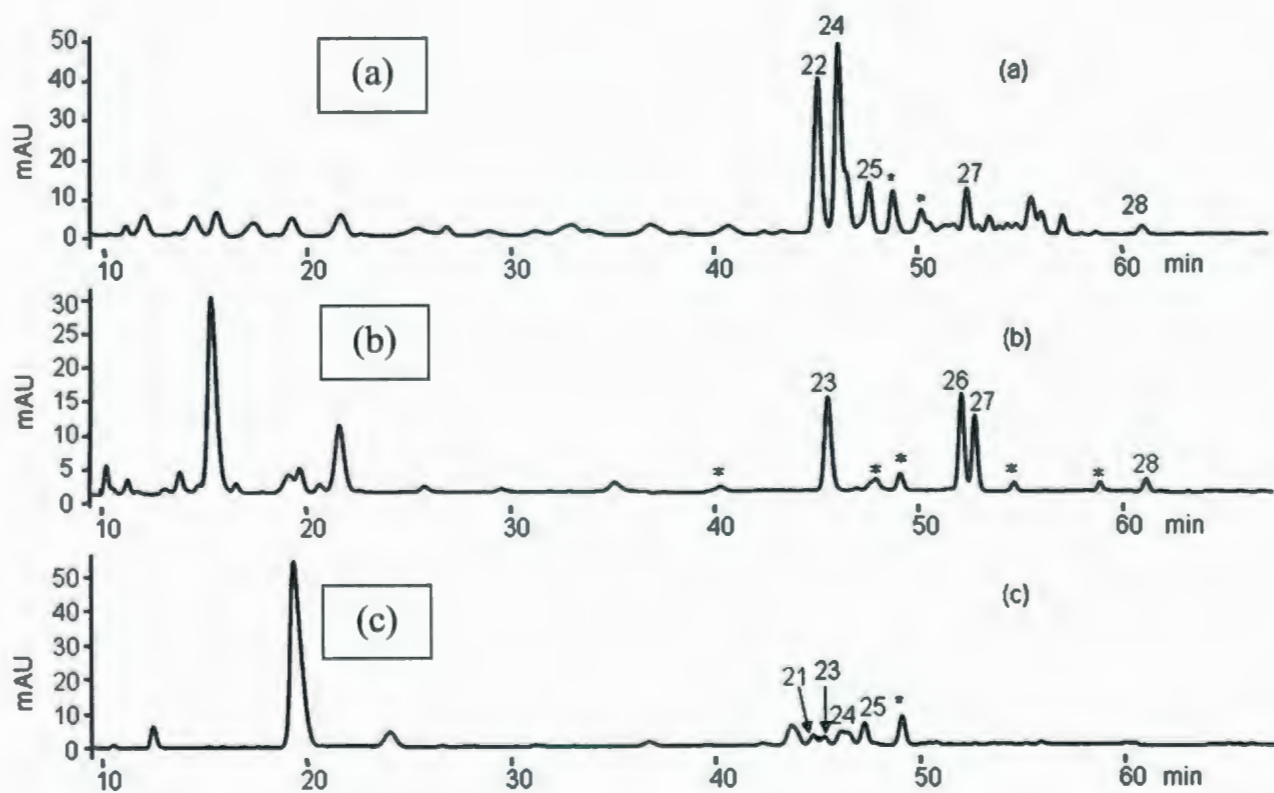


Figure 3.9. LC results: UV detection (360 nm) of (a) blueberry extract, (b) lingonberry extract and (c) blackberry extract. For the identity of peak labels, refer to Table 3.1.



Figure 3.10. Scanning electron microscope images of (a) standard with CHCA matrix and (b) standard with THAP matrix.

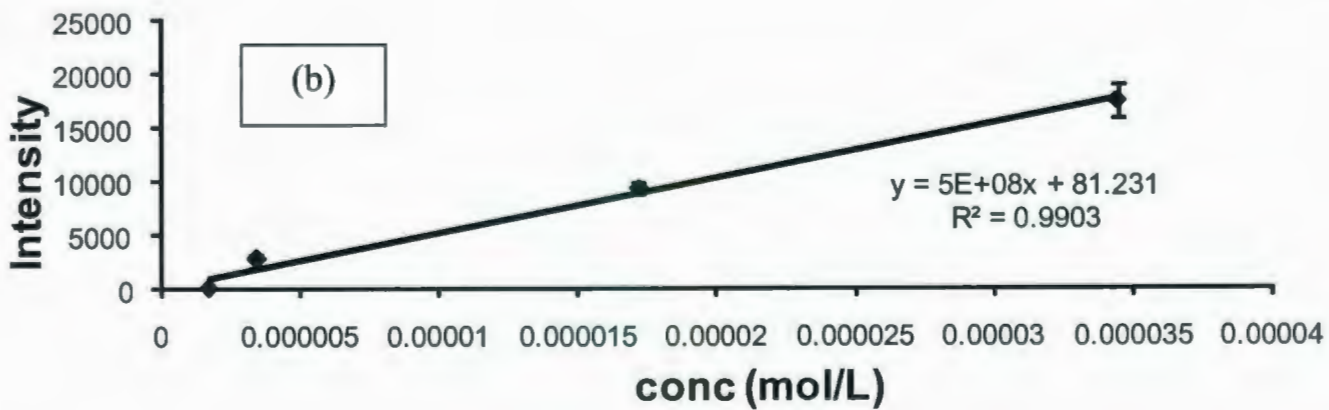
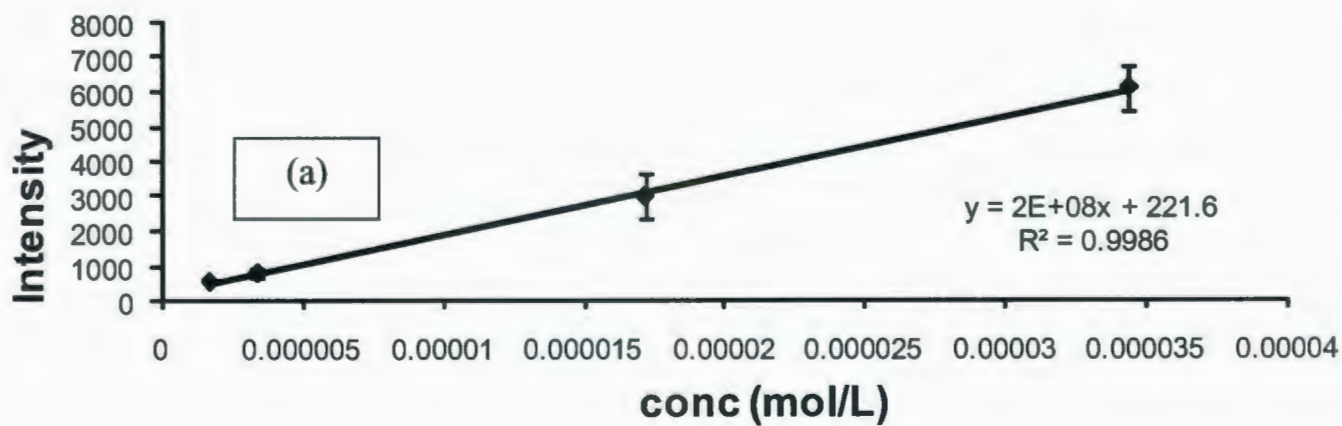


Figure 3.11. Calibration curves produced by LC analysis for (a) anthocyanins and (b) flavonols.

## Chapter 4

### **SIMULTANEOUS ANALYSIS OF VITAMINS AND CAFFEINE IN ENERGY DRINKS BY SURFACTANT-MEDIATED MATRIX-ASSISTED LASER DESORPTION/IONIZATION**

A version of this chapter has been published. Grant DC and Helleur RJ. Simultaneous analysis of vitamins and caffeine in energy drinks by surfactant-mediated matrix-assisted laser desorption/ionization. *Anal. Bio. Chem.* 2008; **391**:2811-2818.

## 4.1 INTRODUCTION

“Energy drinks” are beverages that contain water-soluble vitamins, carbohydrates, caffeine and taurine. In 2004, the industry sold over 2.4 million liters, and this amount is expected to increase [1]. Traditional methods for screening of the major constituents are primarily undertaken by LC-MS with UV detection for quantification. Recently, HPLC-ESI-MS methods have been developed for the detection of taurine and multiple vitamins [2,3]. Quantification was carried out using internal standards and the mass spectrometric detection which required polarity switching continuously from positive-ion to negative-ion mode.

More specifically for single analytes, caffeine is generally analyzed by HPLC-UV [4-7] or HPLC-MS [8-9]. The B-group vitamins can be analyzed by HPLC methods with UV-visible, fluorescence, or MS detection [10-16]. However, energy drinks are complex mixtures with other additives and with a large amount of sugars. For quality-control purposes, a rapid-screening method for simultaneous analysis of these vitamins and caffeine would be useful. Recently, a planar chromatography-ESI MS method was developed for their identification [1]. The vitamins monitored included riboflavin (Vitamin B<sub>2</sub>), nicotinamide (Vitamin B<sub>3</sub>), pyridoxine (Vitamin B<sub>6</sub>), and caffeine. UV detection was used for nicotinamide and caffeine, and fluorescence for riboflavin and pyridoxine. However, it would be beneficial if a procedure existed that would identify all of these species simultaneously using one detection technique.

Matrix-assisted laser desorption/ionization is a method used largely for analysis of proteins, nucleic acids and polymers. Some of the benefits of matrix-assisted laser desorption/ionization time-of-flight mass spectrometry (MALDI-TOF-MS) include high

sensitivity, high throughput, and easily interpreted mass spectra, because mainly molecular ions and cationized species (i.e. adduct ions) are observed [17-19]. The analysis of small molecules has been limited by the use of small organic matrix molecules, which often decompose to produce many associated matrix-related ions in the low-mass region. Nevertheless, attempts have been made to analyze these vitamins by MALDI. The B-group vitamins have been detected using MALDI-TOF-MS using high-molecular weight porphyrin matrices [20]. However, these matrices are not commercially available. It would be beneficial if a method was developed that used one of the more conventional MALDI matrices.

Cetyltrimethylammonium bromide (CTAB) has been used as a matrix-ion suppressor for CHCA ( $\alpha$ -cyano-4-hydroxycinnamic acid) matrix ions for the analysis of small molecules [21-25]. When added to a matrix/analyte sample in a low molar ratio, the matrix-related ions are suppressed, while many analytes still display adequate mass spectral resolution. Some analytes tested include peptides, cyclodextrins, small drug molecules, phenolic acids, and anthocyanins. Our group has demonstrated that these surfactant-containing MALDI spots dry more homogeneously than those without surfactant, and that this leads to better reproducibility and quantification for phenolic acids and anthocyanins [24,25]. In addition, other quaternary ammonium bromide surfactants have been tested, as well as anionic and neutral species. Because of the specificity of this mode of ion suppression, our group has referred to this as surfactant-mediated MALDI. The analysis of caffeine has previously been demonstrated, and CTAB was found to be the preferred surfactant [24].

The current study focuses on the application of surfactant-mediated MALDI for analysis of B group vitamins and caffeine in high-sugar-containing energy drinks. This method was developed as a rapid-screening technique where a number of different energy drinks were successfully analyzed. An important optimization condition was the choice of matrix, i.e. one which can work well with high sugar content. In order to show that quantification can be achieved with high-throughput capability, the results from MALDI-TOF-MS were compared with those from HPLC.

## **4.2 EXPERIMENTAL**

### **4.2.1 Chemicals**

Nicotinamide (122.13 amu)(99.5%) and riboflavin (376.38 amu)(98.0%) were purchased from Fluka (Seelze, Germany). Pyridoxine (169.18 amu)(98.0%), caffeine (194.19 amu)(99.0%), cetyltrimethylammonium bromide (CTAB)(364.46 amu),  $\alpha$ -cyano-4-hydroxycinnamic acid (CHCA)(189.17 amu), sinapinic acid (224.21 amu), 2,5-dihydroxybenzoic acid (DHB)(154.12 amu), dithranol (226.23 amu) and 2',4',6'-trihydroxyacetophenone (THAP)(168.16 amu) were obtained from Sigma (St. Louis, MO, USA). HPLC grade water, formic acid, and acetonitrile were from Fisher Scientific (Fair Lawn, New Jersey, USA). Structures of analytes and surfactant used are shown in Figure 4.1.

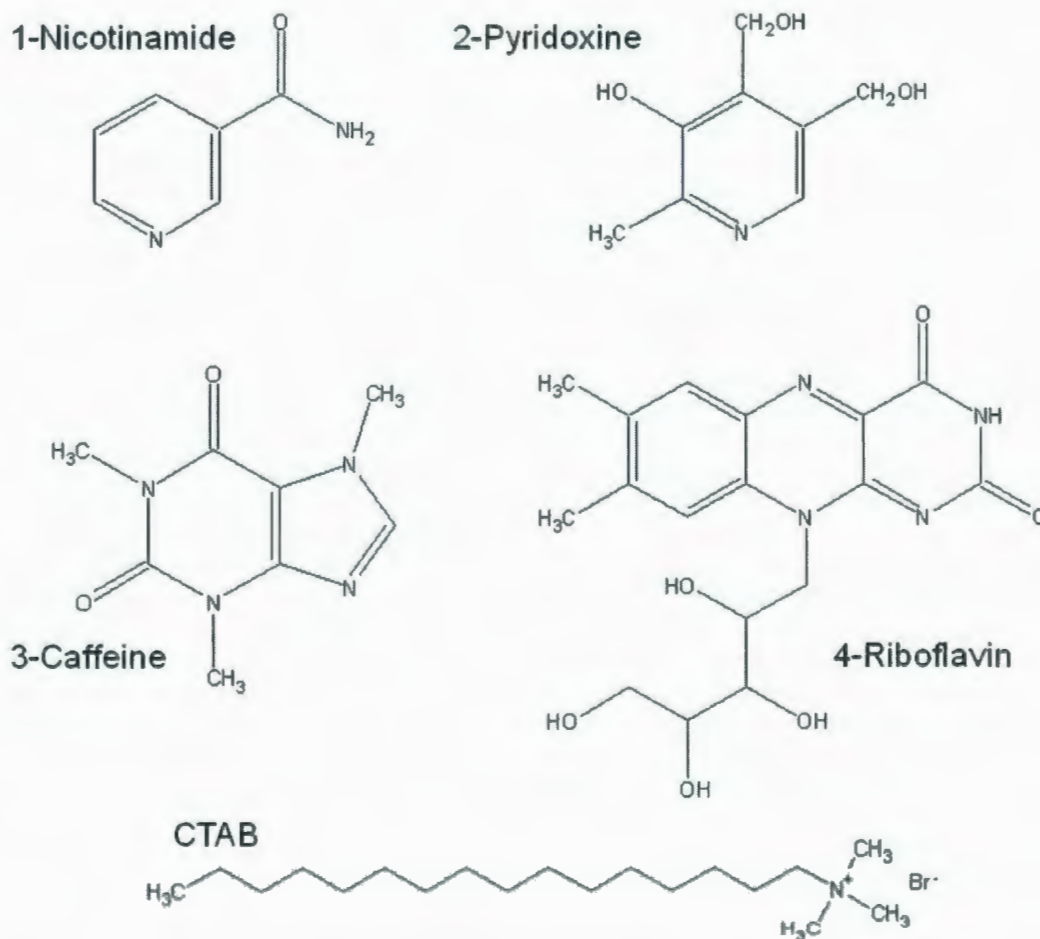


Figure 4.1. Structures of the analytes and surfactants used.

#### 4.2.2 Standard Preparation

Standards were made up by dissolving each individual analyte in separate 100.00 mL volumetric flasks: nicotinamide, 25.3 mg; pyridoxine, 21.8 mg; caffeine, 21.2 mg; and riboflavin, 2.1 mg. Then 5.00 mL of each solution were added together to form the initial standard solution. This solution was composed of  $0.518 \text{ mmol L}^{-1}$  nicotinamide,  $0.322 \text{ mmol L}^{-1}$  pyridoxine,  $0.273 \text{ mmol L}^{-1}$  caffeine and  $0.014 \text{ mmol L}^{-1}$  riboflavin. The initial solution was diluted 2x, 10x, and 20x for analysis of standard curves. Solutions

were stored at 4° C and wrapped in tin-foil to protect them from light. Samples were stored for no more than 14 days. For MALDI analysis, to mimic as close as possible the signal of sugar-containing energy drinks, the initial 100 mL individual standards had 6 g of fructose and 6 g of sucrose dissolved in each.

### **4.2.3 Energy Drink Samples**

Four commercially available energy drinks were purchased from a local convenience store. The drink codes were RB, FT, RS and SB. They represent a variety of energy drinks which have unique concentrations of vitamins, caffeine, and an array of sugars. Each of these samples was sonicated for 20 minutes to remove dissolved gases, then diluted ten-fold before MALDI (and LC) analysis.

### **4.2.4 MALDI Preparation**

All matrices were dissolved at 10 mg mL<sup>-1</sup> in 50:50 H<sub>2</sub>O/acetonitrile containing 1% TFA. Each was vortex mixed for 30 seconds and then centrifuged for 30 seconds before any aliquots were taken.

For MALDI-TOF-MS analysis, 10 µL of matrix was mixed with 10 µL of sample. For samples that had surfactant added, 0.5 µL of CTAB (1 mg mL<sup>-1</sup> in 80:20 MeOH/H<sub>2</sub>O) was added. All samples were vortex mixed in plastic centrifuge tubes for 30 s and centrifuged for 30 s at 3000 rpm prior to spotting. Samples were spotted as 0.5 µL aliquots on a 96 x 2 well MALDI plate (Applied Biosystems, Framingham, MA, USA). Samples were allowed to crystallize and thoroughly dry in a desiccator.

#### 4.2.5 MALDI-TOF-MS Analyses

The MALDI-TOF-MS instrument was a Voyager DE<sup>TM</sup>-PRO purchased from Applied Biosystems (Framingham, MA, USA). The instrument was equipped with a video camera and the sample image was displayed on a monitor. These enabled manual control to position and focus the laser on a given spot. Positive ion reflectron mode was used unless otherwise stated. The instrument was equipped with a pulsed nitrogen laser (337 nm, 3 ns pulse duration, 3 Hz frequency) and a delayed extraction source. An accelerating voltage of 20 kV and a grid voltage setting of 69% were used. The guide wire was adjusted to 0.004%. The laser fluence was set to 2800 arbitrary units (unless otherwise stated) and an extraction delay time of 145 ns was used. A mass acquisition range of 100-1000 Da was used unless otherwise shown and all spectra are the result of 25 averaged laser shots. Mass spectra were analyzed using Version 4 of Data Explorer<sup>TM</sup> software.

#### 4.2.6 LC Analyses

An Agilent 1100 Series LC/MSD Trap SL was used. All chromatograms were processed using ChemStation for LC 3D software (Rev.A.10.02). The mass spectra were analyzed using LC/MSD Trap Control 5.2. The ion trap conditions were: nebulizer pressure, 60.0 psi; drying gas, 11.0 L min<sup>-1</sup>; drying temperature, 350°C; target mass, *m/z* 250; target, 30000; max acquisition time, 200 ms; speed, 13000 *m/z/s*; scan range, *m/z* 100-500; capillary voltage, 3500 V. For quantitative analysis, a diode array detector from Agilent (G1315B) was used. A 100.0  $\mu$ L aliquot was injected using the autosampler and separation was achieved on a Symmetry<sup>®</sup> C-18 RP column (150 x 3.9 mm i.d.- Waters, Canada), protected by a Symmetry<sup>®</sup> C-18 guard column (W31921). A binary mobile

phase was employed; solvent A was 5% aqueous formic acid (v/v) and solvent B was 100% acetonitrile. A flow rate of 0.8 mL min<sup>-1</sup> was maintained. The gradient elution profile was: 0 to 4 min, 0% B; 11 min, 12 % B; 15 min, 15 % B; 22 min, 25 % B; 30 min, 30 % B; 35 min, 100 % B. A five minute post-run was utilized to allow the column to recondition itself before subsequent runs.

## 4.3 RESULTS AND DISCUSSION

### 4.3.1 Identification and Quantification by LC-MS

Figure 4.2 illustrates the results of LC with UV detection for the standard mixture. Figures 4.2(a) and 4.2(b) show detection at 261 and 290 nm, respectively, while Figure 4.2(c) illustrates the corresponding positive mode electrospray ionization total-ion chromatogram (ESI-TIC).

Individual positive-ion ESI mass spectra of the standards were acquired. Nicotinamide yielded a protonated molecular ion at  $m/z$  123 and a sodiated adduct at  $m/z$  145 (data not shown). Pyridoxine yielded a protonated molecular ion at  $m/z$  170 and the  $[M+H-H_2O]^+$  ion at  $m/z$  152. Similarly, caffeine yielded a protonated molecular ion ( $m/z$  195) and a sodiated adduct at  $m/z$  217, while riboflavin produced only a protonated molecular ion at  $m/z$  377. The LC-MS was used to verify the identity of the various analytes in energy drinks.

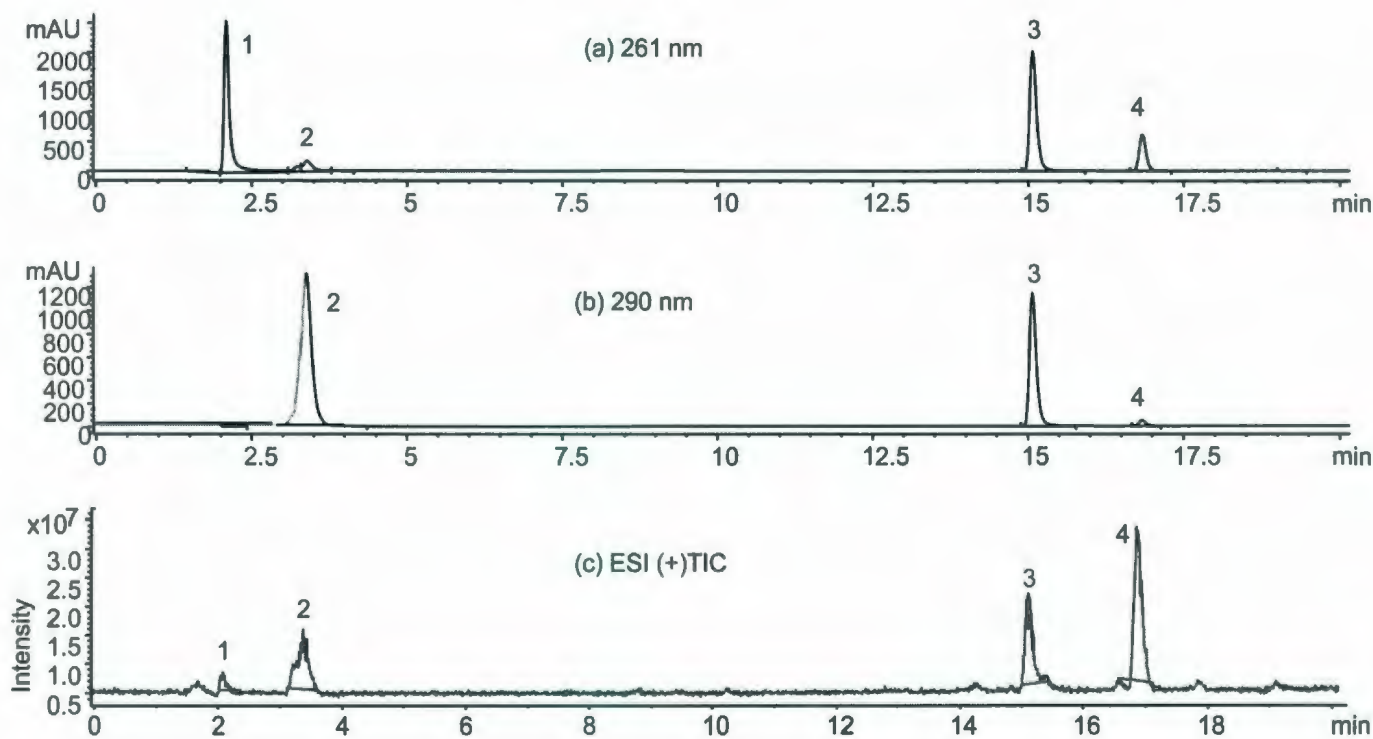


Figure 4.2 LC chromatograms obtained from a standard mixture with UV detection at (a) 261 nm and (b) 290 nm, and (c) ESI (+) TIC. 1 = nicotinamide; 2 = pyridoxine; 3 = caffeine; 4 = riboflavin.

Calibration curves of the energy drink standards (not shown) were constructed from the peak area data as determined by LC with UV detection. Each analyte calibration curve had a correlation coefficient of at least 0.99, constructed from the four concentration standards described in the experimental section. Finally, the four energy drinks were analyzed for vitamin and caffeine content. The concentrations are reported in Table 4.1. Taurine (125 g/mol) was excluded from the analyses due to the fact that our instrument often yielded a noisy signal in the mass region of 120-130 Da due to limitations in its electronics.

Table 4.1. Analyte concentrations determined by LC-UV and surfactant-mediated MALDI-TOF-MS in four energy drinks (sample codes BF, FT, RS and SB; n=10 replicates). The percentage of discrepancy (%disc) illustrates the difference in quantification between the two methods.

Drink Code	Nicotinamide			Pyridoxine			Caffeine			Riboflavin		
	LC-UV mg/100 mL	MALDI mg/100 mL	%disc	LC-UV mg/100 mL	MALDI mg/100 mL	%disc	LC-UV mg/100 mL	MALDI mg/100 mL	%disc	LC-UV mg/100 mL	MALDI mg/100 mL	%disc
<b>BF</b>	6.93	6.56	13.66	0.99	1.00	1.01	30.60	30.68	0.26	0.69	0.73	5.80
<b>FT</b>	6.95	6.14	11.65	0.77	1.03	33.77	25.50	28.76	12.78	0.62	0.76	20.97
<b>RS</b>	4.61	4.81	4.34	0.67	0.67	0.11	27.30	35.59	30.33	1.48	1.61	8.78
<b>SB</b>	2.89	3.17	9.82	0.84	0.92	9.67	30.39	32.75	7.76	1.99	1.97	1.02

### 4.3.2 Identification by Surfactant-Mediated MALDI-TOF-MS

One important condition in MALDI experimentation is selection of the matrix for the type of sample to be analyzed. All four analytes must be clearly observed in the presence of matrix-related ion and sugar-related ion signals. Figure 4.3 shows the positive-ion mode spectra from three of the most promising compounds tested (CHCA, sinapinic acid and 2,5-dihydroxybenzoic acid) as a matrix for the standards. Figures 4.3(a) to 4.3(c) illustrate analysis in the absence of surfactant, and Figures 4.3(d) to 4.3(f) illustrate the analysis when CTAB was added to each matrix. In Figure 4.3(a), the CHCA matrix produces many matrix and sugar-fragment ions which make it hard to resolve the protonated analyte molecules. With care, each analyte can be observed as a molecular ion  $[M+H]^+$ , with  $m/z$  values of 123 (nicotinamide), 170 (pyridoxine), 195 (caffeine) and 377 (riboflavin). When sinapinic acid was used a matrix (Figure 4.3(b)), nicotinamide could not be observed and the signal for riboflavin was weak. The matrix produced fewer matrix ions than CHCA. In Figure 4.3(c), DHB successfully identified nicotinamide, pyridoxine and caffeine, but riboflavin was not observed. Of the remaining matrices (spectra not shown) dithranol only identified pyridoxine, while THAP matrix produced an unacceptable number of sugar-related ions in its spectra.

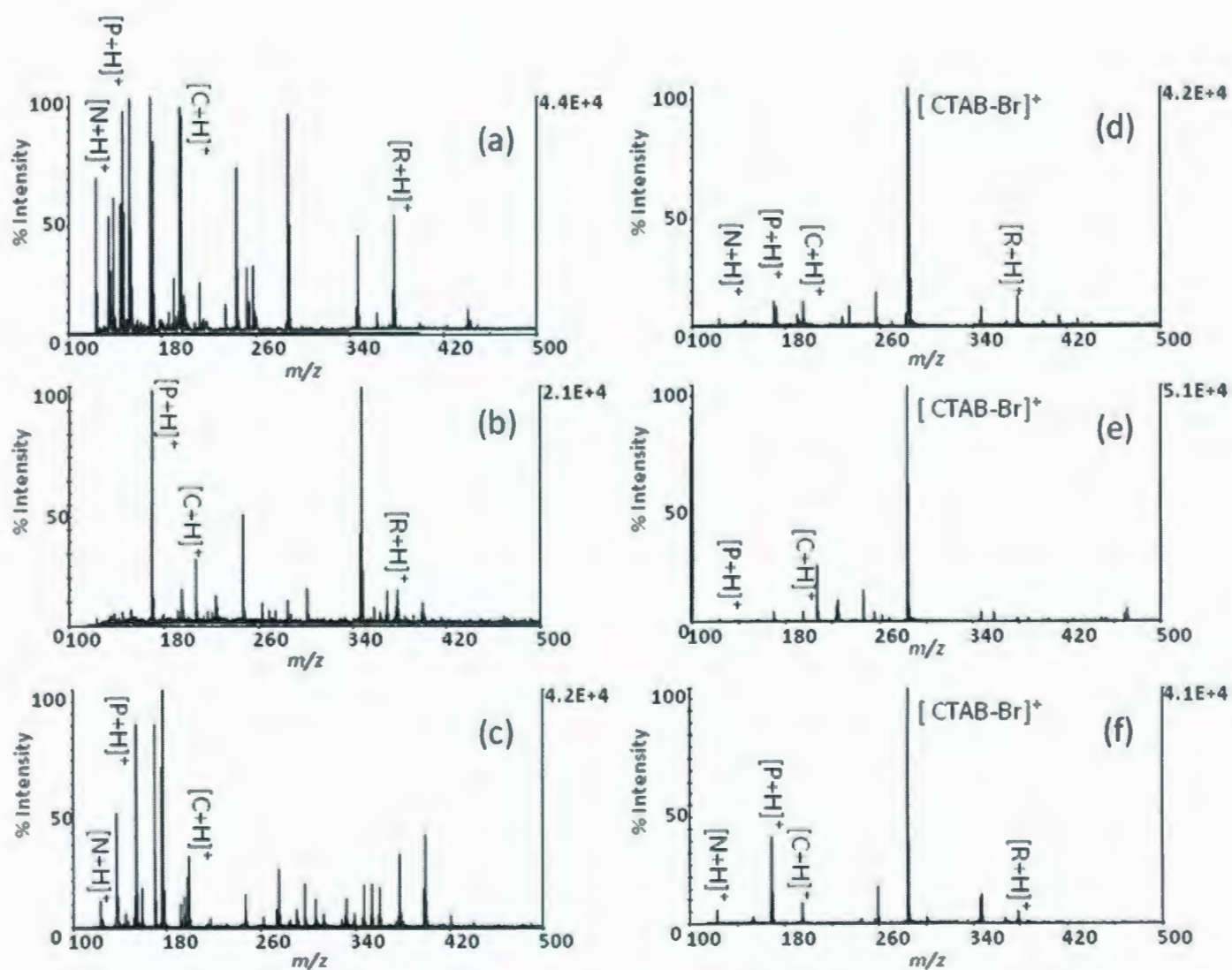


Figure 4.3 Selection of a suitable matrix. MALDI-TOF-MS mass spectra obtained from four-component energy drink standard mixture when analyzed using (a) CHCA, (b) sinapinic acid, (c) DHB, (d) CHCA/CTAB, (e) sinapinic acid/CTAB, and (f) DHB/CTAB. Assigned labels are N (nicotinamide), P (pyridoxine), C (caffeine) and CTAB (cetyltrimethylammonium bromide).

When CTAB was added to CHCA matrix for analysis of the standards (Figure 4.3(d)), most matrix-fragment ions were suppressed while the four standards were clearly identified. Suppression of matrix ions was, perhaps, most noticeable with this matrix. With sinapinic acid matrix, CTAB suppression led to the loss of the riboflavin signal. The DHB matrix led to the identification of all analytes (Figure 4.3(f)), but the riboflavin signal was either weak or obscured by the sugar-related ions. The dithranol matrix was the worst of all (results not shown). The only analyte identified was nicotinamide as the sodiated  $[N+Na]^+$  and potassiated adducts  $[N+K]^+$ .

Due to the previous use of CHCA by our group and in other studies [21-25], and the fact that CHCA crystallized more homogeneously than the other matrix/surfactant combinations when spots were studied under scanning electron microscopy (SEM; data not shown), we chose CHCA as our preferred matrix. In a previous study the homogeneity of MALDI spots was found to be a critical factor for successful quantification of small molecules analytes by MALDI [24].

Figure 4.4 shows the resulting MALDI-TOF-MS mass spectra of the energy drink samples when tested with CHCA matrix and CTAB surfactant. In each of the energy drinks, all four of our target analytes were clearly identified, while ion suppression of the matrix-related ions was observed. Analyte ion suppression always occurs to some extent; however, the target molecular ions were still well resolved from background noise. Some ions in the spectra were identified as protonated sugar molecules and sodiated adducts. These are marked with a \* in the mass spectra.

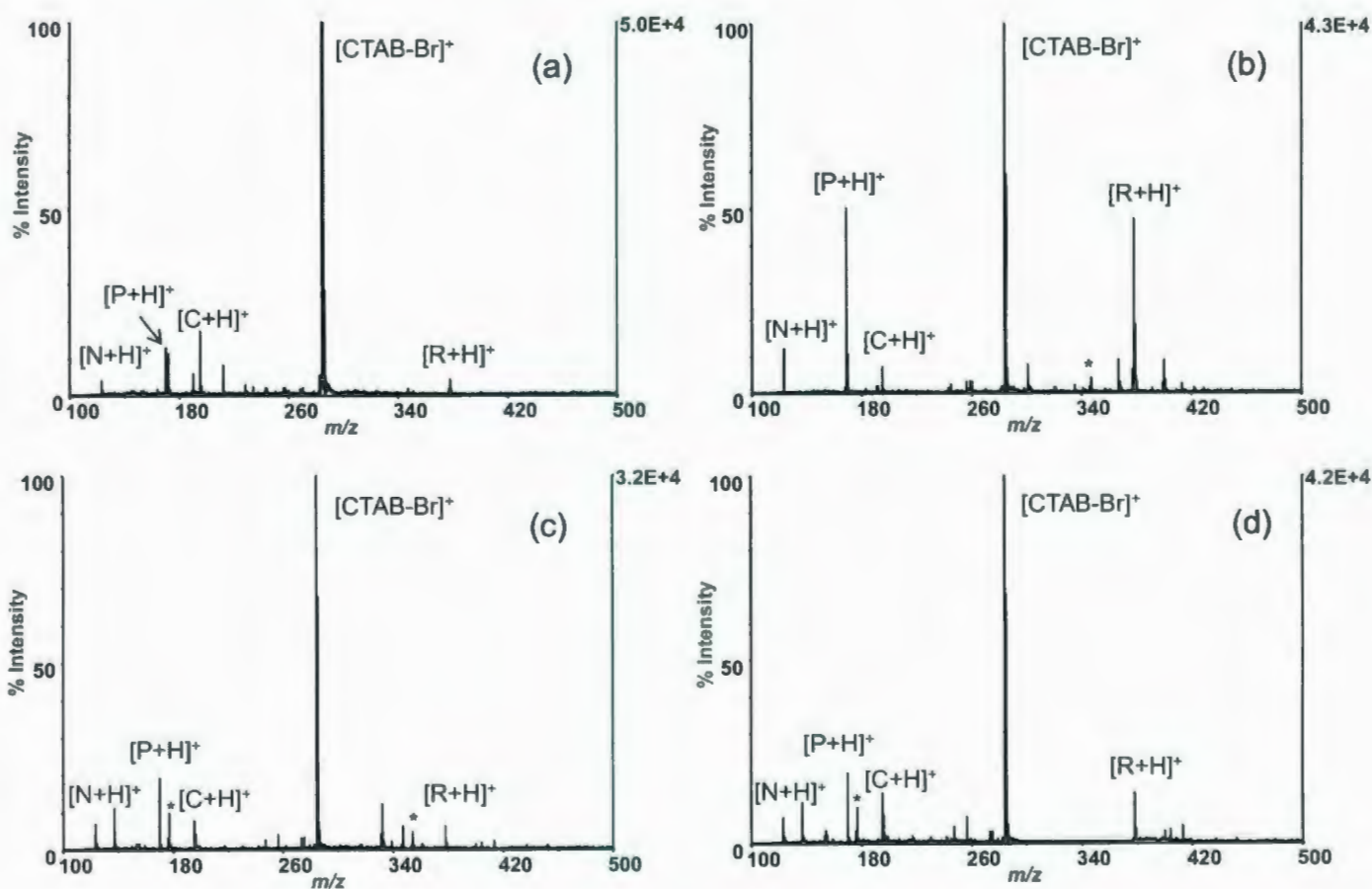


Figure 4.4 MALDI-TOF-MS mass spectra obtained by use of CHCA/CTAB in analysis of energy drinks with code names (a) BF, (b) FT, (c) RS, and (d) SB. Labels are identified in Figure 4.3.

### 4.3.3 Quantification by MALDI

Calibration curves of the standards were constructed by analyzing the data from MALDI-TOF-MS and surfactant-mediated MALDI-TOF-MS (Figure 4.5) for comparative purposes. Figure 4.5(a) illustrates the results of using CHCA matrix only. The correlation coefficients ( $R^2$ ) are 0.946 (nicotinamide), 0.939 (pyridoxine), 0.954 (caffeine) and 0.944 (riboflavin). Although these are reasonably linear, there is a large amount of error, as demonstrated by the error bars. These are averaged values over ten replicate measurements. This is typical in attempting quantitation by MALDI and is likely the result of poor homogeneity among sample spots, which leads to decreased reproducibility.

Figure 4.5(b) illustrates the calibration curves obtained as a result of using CHCA with added CTAB surfactant. The correlation coefficients increased to 0.989, 0.991, 0.983 and 0.987, a substantial improvement in linear correlation in comparison with samples that did not contain surfactant. Also, the error bars decreased in magnitude. The linearity of these curves compares well to those achieved by LC with UV detection (data not shown). For this analysis, each of the standard compounds were spotted together on one individual target. This was completed in an effort of trying to remain consistent with the composition of energy drinks

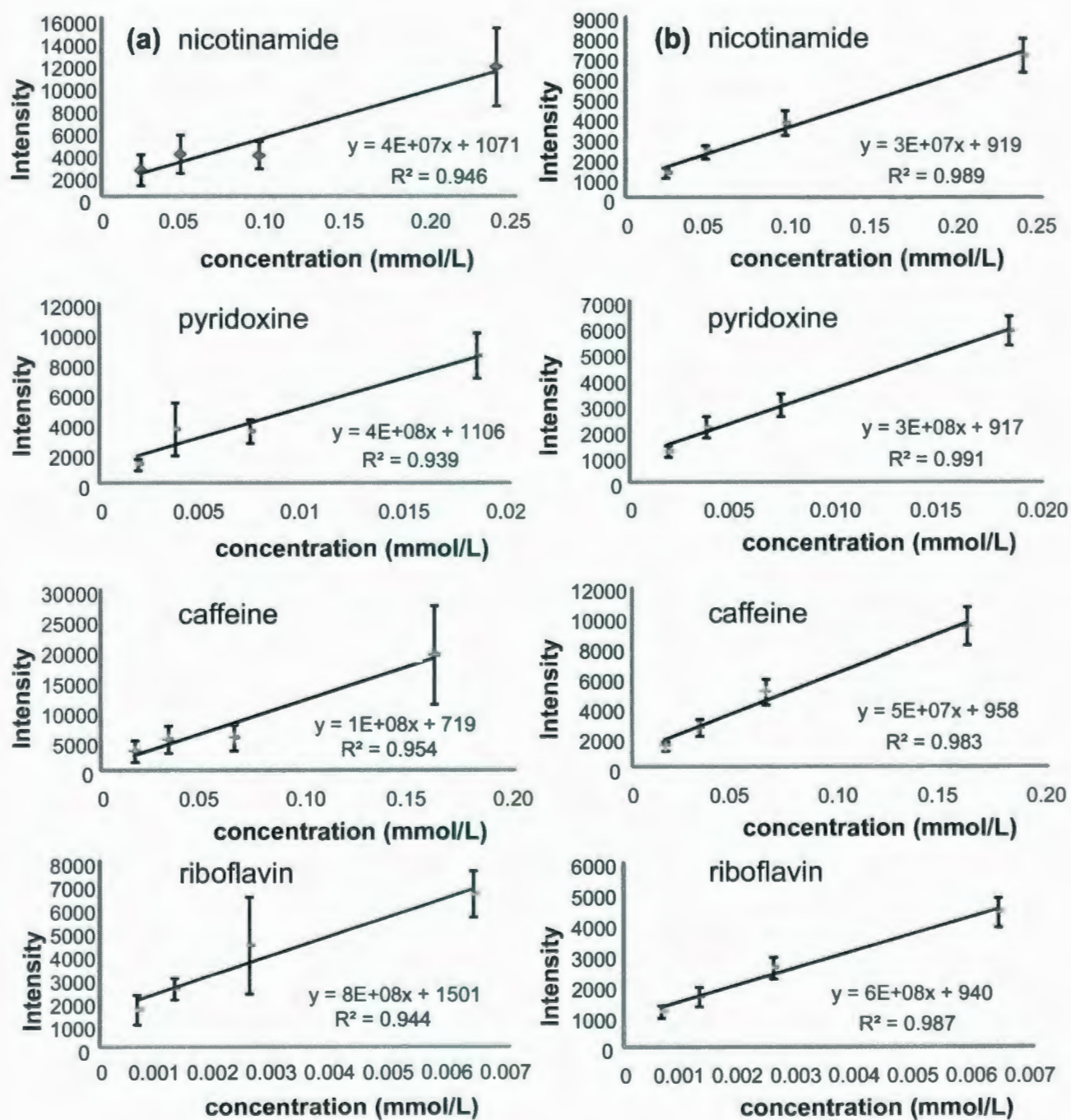


Figure 4.5 MALDI-TOF-MS calibration curves for standards using (a) CHCA and (b) CHCA with CTAB surfactant, in the analysis of nicotinamide, pyridoxine, caffeine, and riboflavin.

Table 4.1 lists the concentration of analytes found in the drinks as determined by the surfactant-mediated MALDI-TOF-MS method. These values are in good agreement with those obtained by LC-UV. This can be seen by noting that the calculated data, which lists the percentage of discrepancy between an LC and MALDI analysis. As well, a +/- indicates whether the surfactant-mediated method quantified a larger or smaller amount of the target analyte than LC. Clearly, the technique is not consistently in error under- or over-estimating the concentrations of analytes.

As a measure of reproducibility, Table 4.2 lists the percentage relative standard deviation (RSD) in the quantitation results produced by the surfactant-mediated method (n = 10). These values are all less than 20%, which is very good compared with other MALDI studies, where RSD values of greater than 50% and up to 200% have frequently been reported.

Table 4.2. Relative standard deviation (RSD) values among analyte concentrations in energy drinks as determined by surfactant-mediated MALDI-TOF-MS. Note: n = 10.

<b>Drink Codes</b>	<b>Nicotinamide</b>	<b>Pyridoxine</b>	<b>Caffeine</b>	<b>Riboflavin</b>
<b>BF</b>	14.6	15.8	17.0	17.3
<b>FT</b>	15.2	14.9	14.2	9.7
<b>RS</b>	18.1	11.8	12.5	13.8
<b>SB</b>	10.1	9.1	13.5	14.8

#### **4.4 CONCLUSION**

As a novel MALDI approach to small molecule analysis, surfactant-mediated matrix-assisted laser desorption/ionization time-of-flight mass spectrometry (MALDI-TOF-MS) was successfully used for identification and quantification of caffeine and the B-group vitamins riboflavin, nicotinamide and pyridoxine in energy drink samples. The MALDI matrix that was the most suitable for high-sugar content drinks was CHCA. With the addition of CTAB as a matrix-ion suppressor, the majority of matrix-related and sugar-related ions were not observed and sample spots crystallized more homogeneously with the analytes. Satisfactory calibration of analyte standards by MALDI-TOF-MS was achieved and results yielded calibration curves with correlation coefficients ranging from 0.983 (caffeine) to 0.991 (pyridoxine). Quantitative results for analytes in energy drinks obtained by the established MALDI technique were comparable with those obtained by LC-UV. This chapter thus describes a rapid-throughput screening MALDI technique for quality-control purposes, with reduced analysis time in comparison with chromatographic methods.

## 4.5 REFERENCES

1. Aranda M, Morlock G. *J. Chromatography A*. 2006; **1131**; 253.
2. Chen Z, Chen B, Yao S. *Anal. Chimica Acta*. 2006; **569**, 169.
3. Luo X, Chen B, Ding L, Tang F, Yao S. *Anal Chimica Acta*. 2006; **562**, 185.
4. Pena A, Lino C, Silveira M. *Food Addit. Contam.* 2005; **22**, 91.
5. Aresta A, Palmisano F, Zambonin C. *Food Chem*. 2005; **93**, 177.
6. Thomas J, Yen JH, Schantz MM, Porter B, Sharpless KE. *J. Agric. Food Chem*. 2004; **52**, 3259.
7. Bispo M, Veloso M, Pinheiro H, De Oliveira R, Reis J, De Andrade J. *J. Chromatogr. Sci*. 2002; **40**, 45.
8. Marchei E, Pellegrini M, Pacifici R., Palmi I, Pichini S. *J. Pharm. Biomed. Anal.* 2005; **37**, 499.
9. Zhu XL, Chen B, Ma M, Luo XB, Zhang F, Yao S, Wan Z, Yang D, Hang H. *J. Pharm. Biomed. Anal.* 2004; **34**, 695.
10. Chen YT, Ling Y. *J Mass Spectrom*. 2002; **37**, 716.
11. Midttun O, Hustad S, Solheim E, Schneede J, Ueland P. *Clin. Chem*. 2005; **51**, 1206.
12. Gatti R, Gioia M. *Anal. Chim. Acta*. 2005; **538**, 135.
13. Ekinci R, Kadakal C. *Acta Chromatogr*. 2005; **15**, 289.
14. Markopoulou C, Kagkadis K, Koundourellis J. *J. Pharm. Biomed. Anal.* 2002; **30**, 1403.
15. Heudi O, Kilinc T, Fontannaz P. *J. Chromatogr. A*. 2005; **1070**, 49.
16. Chatzimichalakis P, Samanidou V, Verpoorte R, Papadoyannis I. *J. Sep. Sci.* 2004; **27**, 1181.
17. Cohen SL, Chait BT. *Anal. Chem*. 1996; **68**: 31.
18. Dreisewerd K. *Chem. Rev*. 2003; **103**: 395.
19. Knochenmuss R. *Analyst*. 2006; **131**: 966

20. Cehn Y, Ling Y. *J. Mass Spec.* 2002; **37**, 716.
21. Guo Z, Zhang Q, Zou H, Guo B, Ni J. *Anal. Chem.* 2002; **74**: 1637.
22. Su AK, Liu JT, Lin CH. *Talanta.* 2005; **67**: 718.
23. Su AK, Liu JT, Lin CH. *Anal. Chimica Acta.* 2005; **546**: 193.
24. Grant DC, Helleur RJ. *Rapid Commun. Mass Spectrom.* 2007; **21**: 837.
25. Grant DC, Helleur RJ. *Rapid Commun. Mass Spectrom.* 2008; **22**: 156.

## Chapter 4 Addendum

The data presented in this addendum supplements the manuscript publication of Chapter 4. This data will be beneficial to researchers and students wanting to repeat or continue this work.

Figure 4.6 showcases the ESI-MS results that were used to interpret the standards for the energy drinks; nicotinamide, pyridoxine, caffeine and riboflavin. These were useful in combination with the LC-UV detection to ensure that peak identities were made properly, and they also illustrate the various analyte ions that are formed. For example, nicotinamide and caffeine were both observed as mainly molecular ions along with a minor sodiated adducts.

The HPLC calibration curves based on the standards for the 4 analytes of interest are shown in Figure 4.7. As expected, they yielded excellent correlations with  $R^2$  values of 0.99 or higher.

Figures 4.8 to 4.17 show the SEM imaging results of each of the 5 matrices with CTAB being used when mixed with a sugar-containing synthetic standard, and then with a non-sugar containing standard. The images have been included to illustrate the formation of sample spots. Each example is shown at a low (ca. 20x) and high magnification (ca. 100x). As can be clearly seen, the added sugar does alter the spot formation and results in an abundance of solid material on the plate.

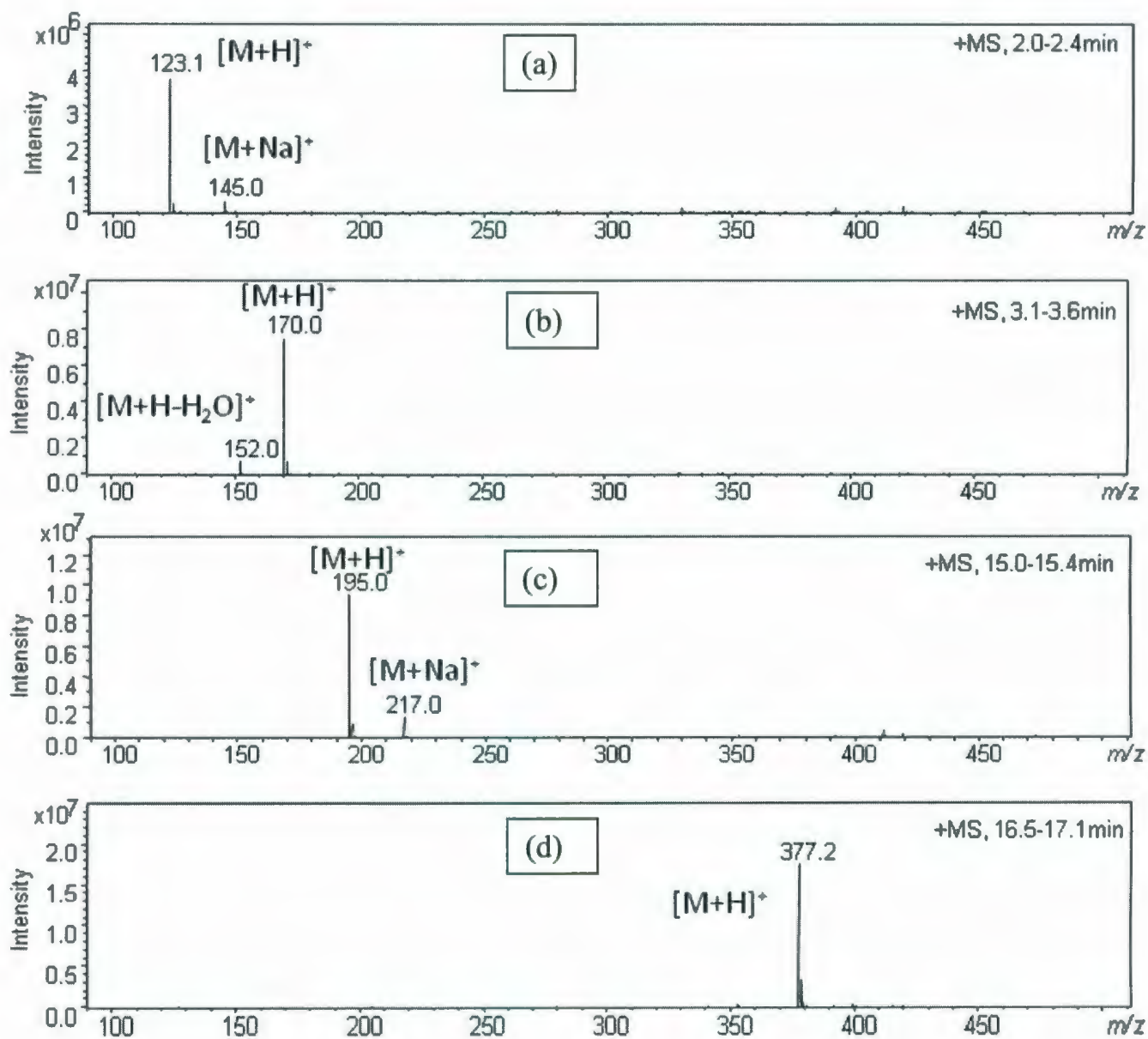


Figure 4.6. LC-ESI-MS mass spectra of standards of (a) nicotinamide, (b) pyridoxine, (c) caffeine, and (d) riboflavin.

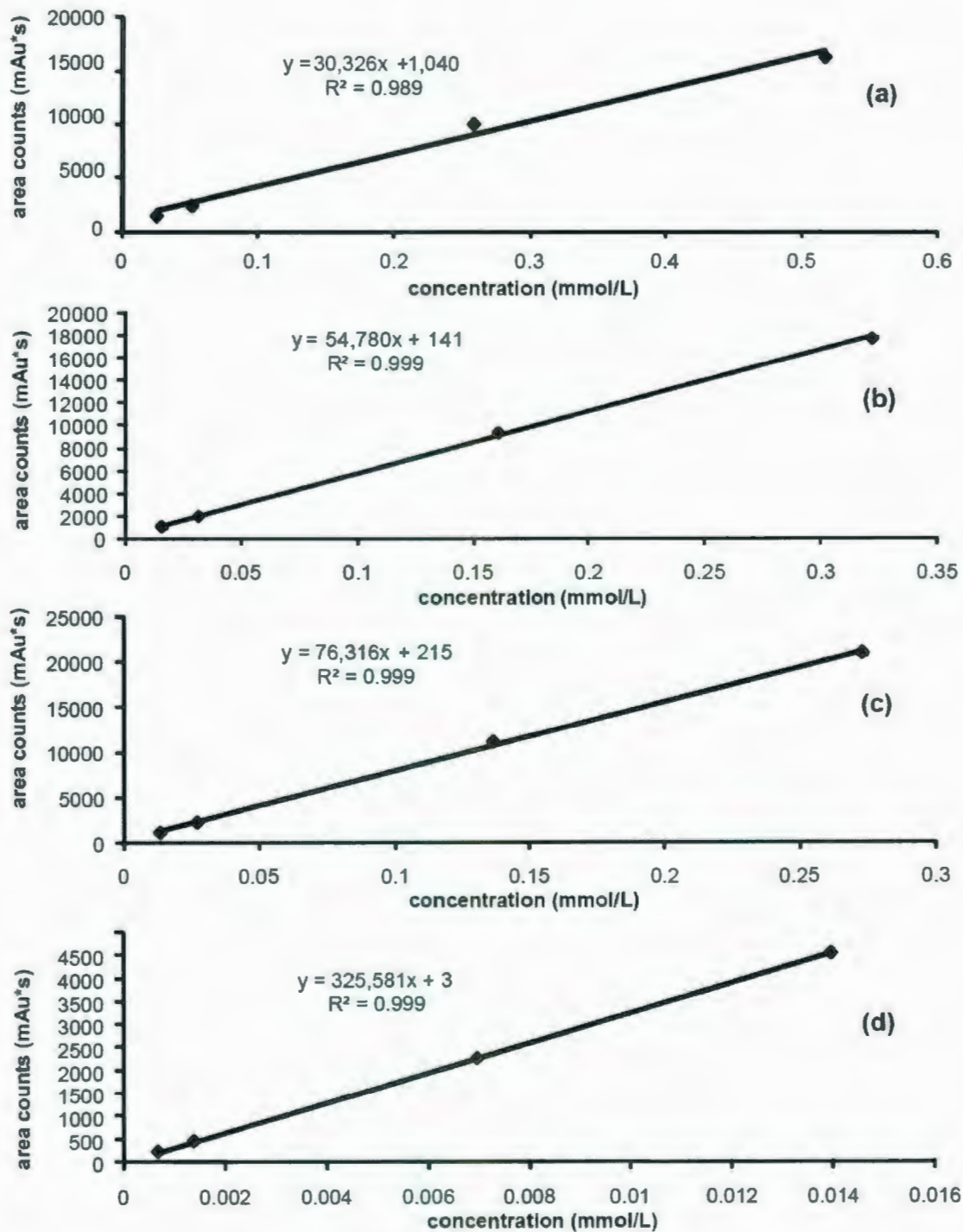


Figure 4.7. HPLC calibration curves of standards of standards of (a) nicotinamide, (b) pyridoxine, (c) caffeine, and (d) riboflavin.

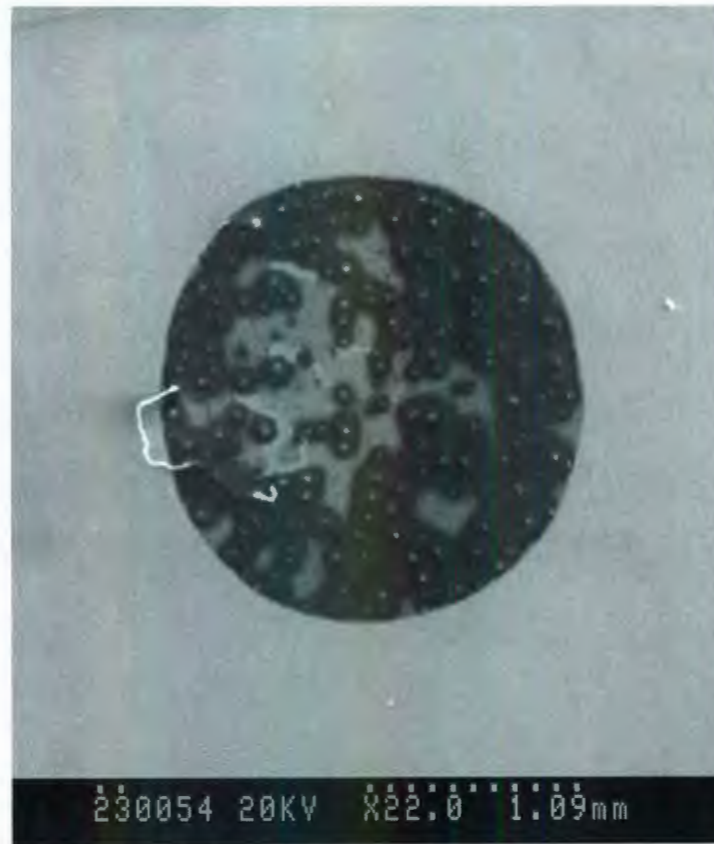


Figure 4.8. SEM image of sugar drink/CHCA/CTAB.



Figure 4.9. SEM image of sugar drink/sinapinic acid/CTAB.

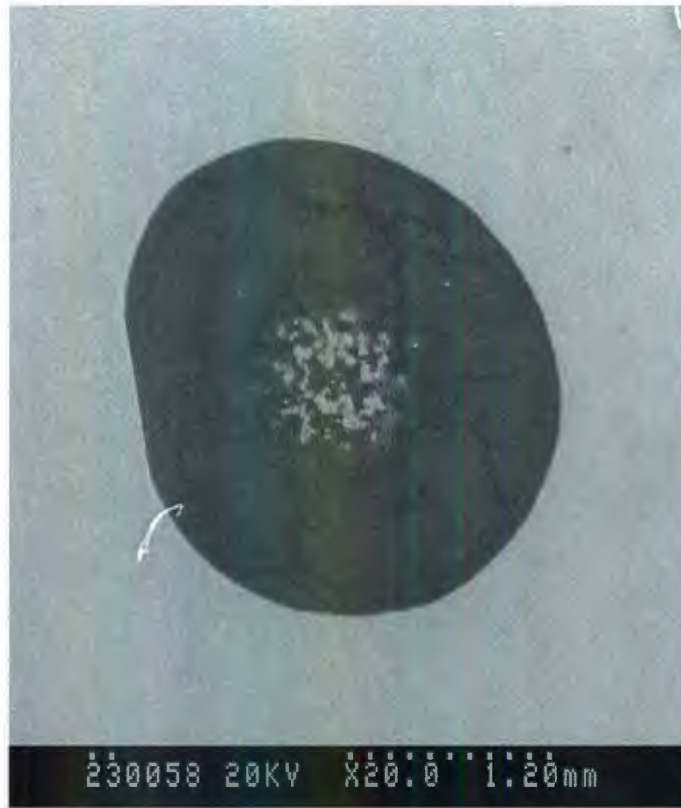


Figure 4.10. SEM image of sugar drink/dithranol/CTAB.

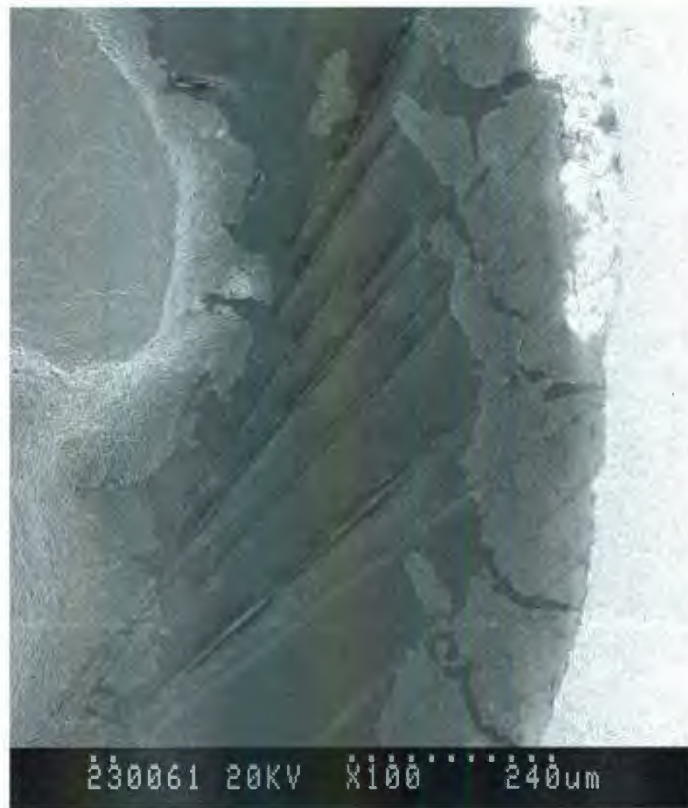


Figure 4.11. SEM image of sugar drink/DHB/CTAB.

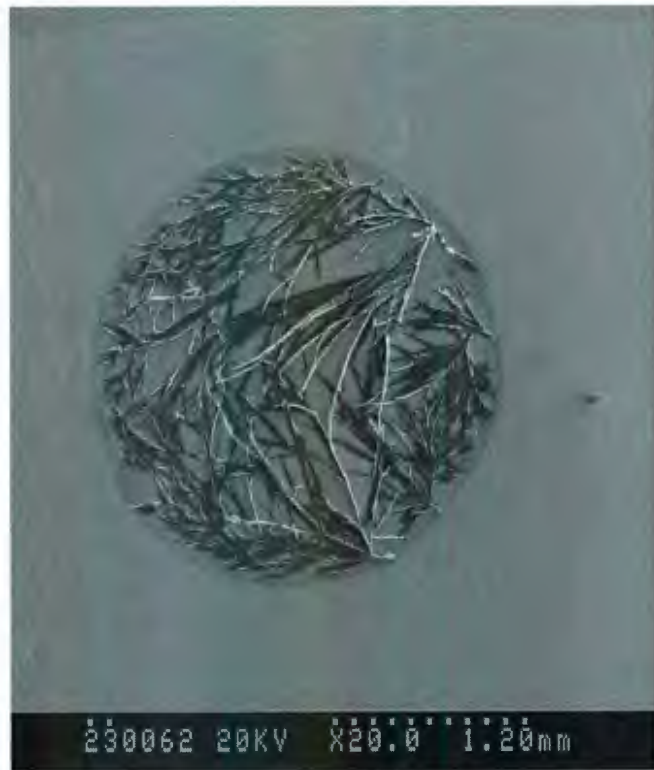


Figure 4.12. SEM image of sugar drink/THAP/CTAB.

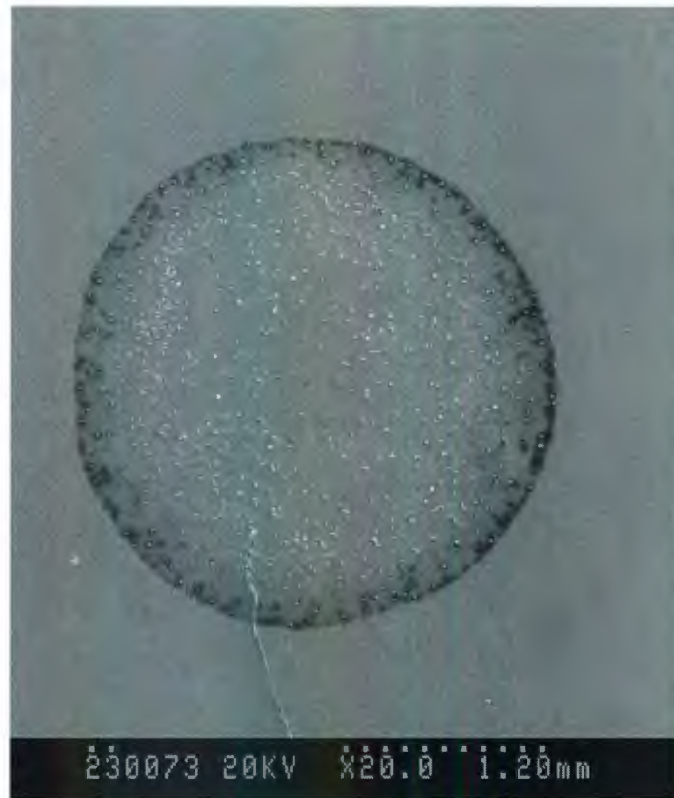


Figure 4.13. SEM image of non-sugar drink/CHCA/CTAB.



Figure 4.14. SEM image of non-sugar drink/sinapinic acid/CTAB.



Figure 4.15. SEM image of non-sugar drink/dithranol/CTAB.



Figure 4.16. SEM image of non-sugar drink/DHB/CTAB.



Figure 4.17. SEM image of non-sugar drink/THAP/CTAB.

## **Chapter 5**

### **CONCLUSIONS AND FUTURE RESEARCH**

## CONCLUSIONS AND FUTURE RESEARCH

This thesis began as a project aimed at identifying methods that could be used to improve the analysis of small molecules by matrix-assisted laser desorption/ionization (MALDI). After careful consideration of the literature, it was decided to focus on analyte molecules less than 1000 Da, and where possible, even less than 500 Da. Guo *et al.* demonstrated that alkyl ammonium bromide salts could be used to suppress matrix ions for the analysis of cyclodextrins and various drug molecules with amino functional groups [1]. Thus, the theme for this thesis was fully developed whereby the ultimate goal was to induce suppression of matrix ions, particularly matrix-specific suppression so that target (and unknown) analytes were still well resolved in the mass spectra. The methodology of surfactant-mediated MALDI was researched and published as a manuscript [2] represented by Chapter 2 of this thesis. This work detailed experimental parameters such as mixing ratios, instrument conditions and how surfactant selection played a role in the effect of ion suppression. It was demonstrated that sample spots were not homogenous from top to bottom and depth profiling experiments suggested that surfactants were primarily concentrated at the top of the droplet.

Research moved on to pursuing applications of surfactant-mediated MALDI that could be beneficial to the scientific community and industrial research. Chapter 3 describes the use of the method to analyze anthocyanins and other flavonoid classes in wild and commercial berry samples. A manuscript was published on this research [3]. The optimized methods developed in Chapter 2 were used and results of surfactant-mediated MALDI compared favourably with those of traditional liquid-chromatography mass-spectrometry (LC-MS). The advantage of MALDI is its speed, being that it took

mere seconds in the analytical step to identify and quantify species. This can potentially eliminate the much longer separation times required for LC-MS analysis.

In Chapter 4, surfactant-mediated MALDI was used to analyze caffeine and the B-group vitamins that are present in “energy drinks”. These included riboflavin, nicotinamide and pyridoxine. These standard analytes could be readily identified in the presence of matrix and high sugar content, which were suppressed down to background levels in the mass spectra. Store-bought samples were then analyzed and again, the MALDI analytical results were seen to be comparable to those of LC-MS. The ability of surfactant-mediated MALDI technique to analyze high-sugar containing drinks was noted. The results were successfully published in *Analytical and Bioanalytical Chemistry* [4].

There are several possible routes in which future work can be carried out on surfactant-mediated MALDI.

First, there are many other possible applications and other classes of analytes that could be analyzed by surfactant-mediated MALDI. For example, the chemical profiling of nutraceuticals, plant-based medicines, is a good candidate. Hypericin (4,5,7,4',5',7'-hexahydroxy-2,2'-dimethylnaphthodianthrone), shown in Figure 5.1, is one of the principal active agents in the medicine, St. John's Wort [5,6]. It has been the subject of much research due to its ability to treat viruses that include cytomegalovirus, human papillomavirus, hepatitis B, herpes and human immunodeficiency virus (HIV), as well as its traditional use in treating patients with mild depression [5-8].

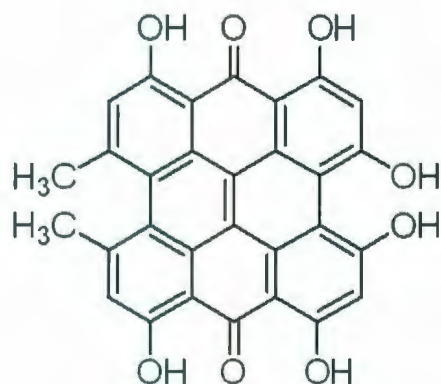


Figure 5.1. Structure of hypericin (MW = 504.44 g/mol).

Figure 5.2 shows the mass spectrum obtained by MALDI-TOF-MS when hypericin is mixed with CHCA matrix at a typical mole mixing ratio of about 500: 1 matrix/analyte. Although hypericin used was a standard purchased from Sigma-Aldrich, one could extrapolate that a simple solvent extraction of St. John's Wort would also be analyzed in a similar manner. As was demonstrated throughout this thesis, there are many matrix-related ions in the low mass region of the spectrum (<600 Da) that can obscure the analyte signal (Figure 5.2).

Analysis of hypericin can be improved with the addition of surfactant CTAB to the mixture. Matrix-related ions are successfully suppressed and hypericin's  $[M+H]^+$  ion is readily identified at  $m/z$  505, as observed in Figure 5.3.

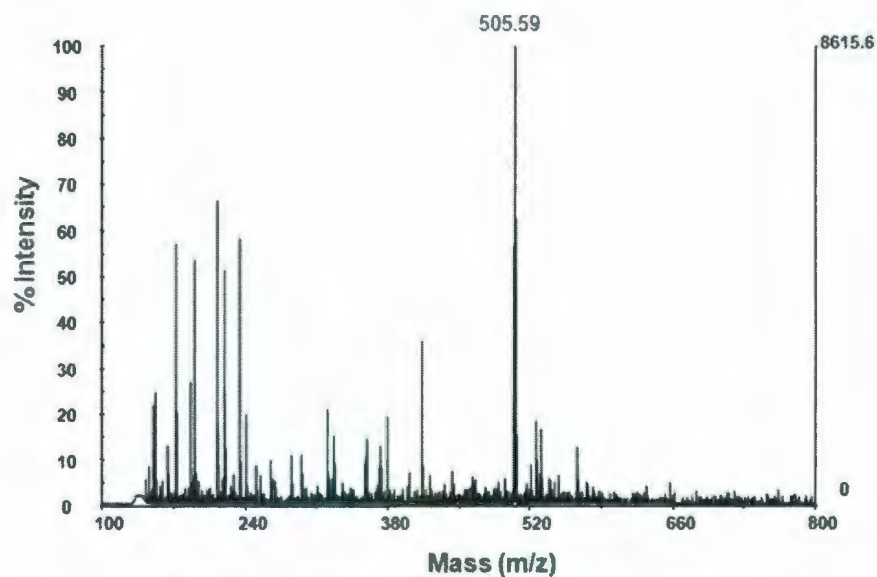


Figure 5.2. MALDI mass spectra of hypericin with CHCA matrix. The  $[M+H]^+$  ion of hypericin is present at  $m/z$  505.59.

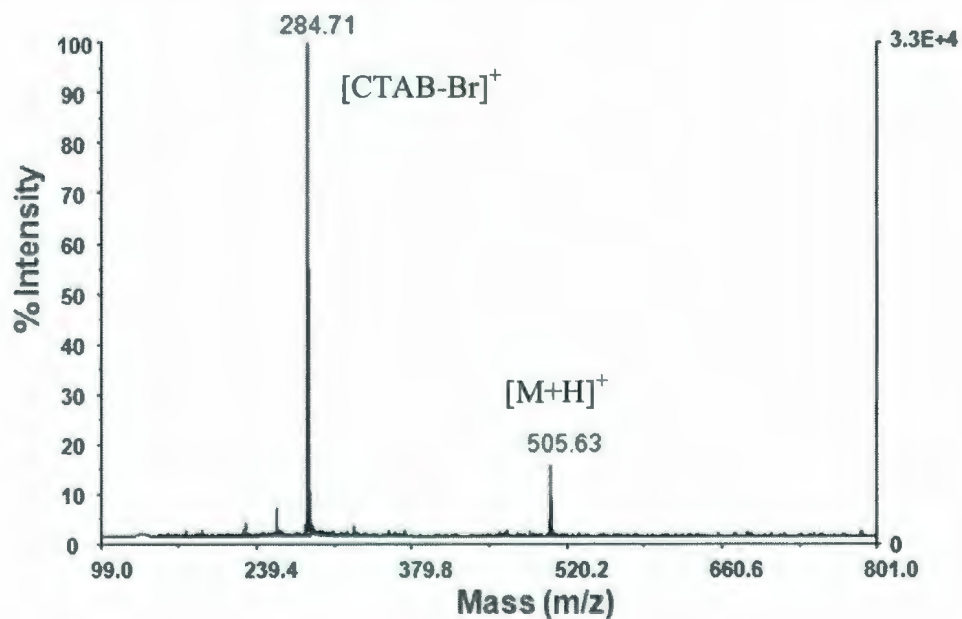


Figure 5.3. Surfactant-mediated MALDI mass spectra of hypericin with CHCA matrix and added surfactant CTAB.

Another possible research project involving the screening of important biomolecules using surfactant-mediated MALDI deals with the tremendous high-throughput capability that the instrument provides. The standard stainless steel target plate provided with the instrument (Applied Biosystems) has 100 individual spots for samples to be deposited. If MALDI-TOF-MS can displace the use of chromatography, it can lead to substantial savings in terms of analysis time. For example, imagine being able to rapidly screen 50 athletes at the Olympic Games for various drugs of abuse whereby duplicate spots per athlete are analyzed. The traditional LC-MS approach that is used is more time-consuming and this is one of the main reasons that not all athletes are tested.

To highlight another surfactant-mediated MALDI advantage, a preliminary analysis was completed on this author's urine on two occasions; one about 2 hours after several large coffees were consumed and another on a day when no coffee was consumed. The mass spectral results using surfactant-mediated MALDI showed the appearance of several known metabolites, some being easily identified. Figure 5.4 illustrates the mass spectrum of a urine sample obtained without the use of surfactant.

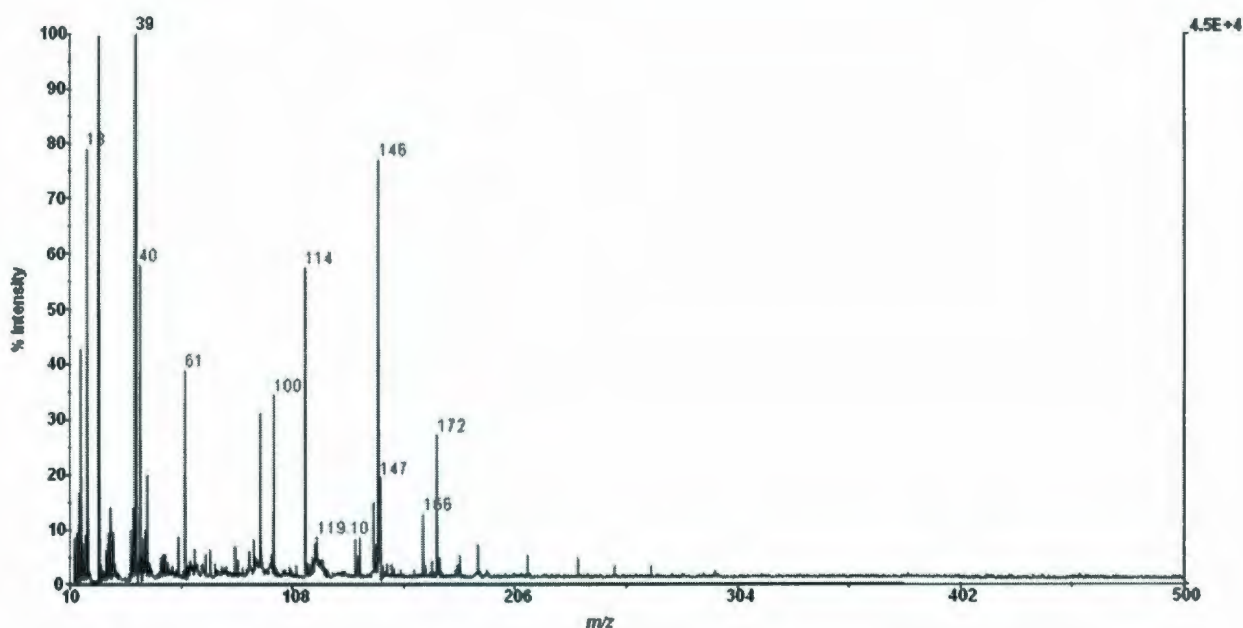


Figure 5.4. MALDI mass spectrum obtained from urine analysis after coffee consumption with use of CHCA matrix.

As could be expected, many CHCA-related ions are present in the mass spectrum. However, the surfactant-mediated analysis of the same urine sample, using CTAB as surfactant, led to a dramatic improvement of analyte signal. The corresponding mass spectrum, shown in Figure 5.5, illustrates that some caffeine was not fully metabolized ( $m/z$  195) while other biomarkers such as urea and creatinine, a degradation product of creatine phosphate in muscle, are present at  $m/z$  61 and 114, respectively. All these ions are suspected to be the protonated species. The ion observed at  $m/z$  152 may be due to creatinine as its potassium adduct. Thus, although this example demonstrates only caffeine analysis as the drug of interest, it can be imagined that, with additional research, that surfactant-mediated MALDI can be applied to other drugs of abuse that are banned in professional sports.

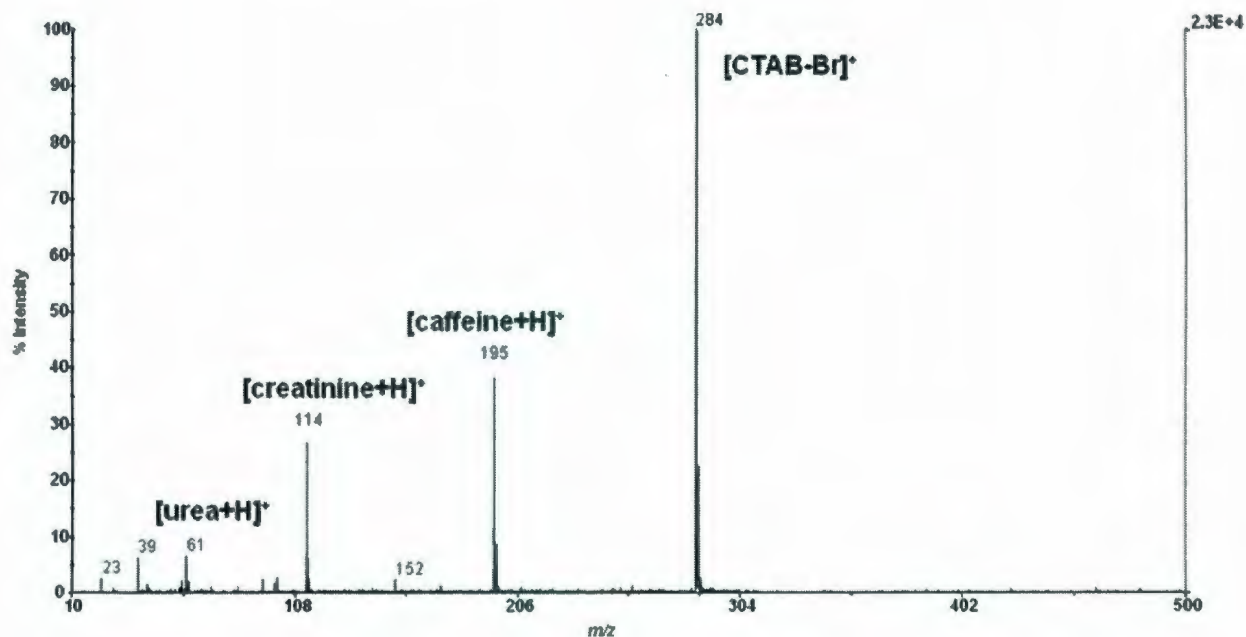


Figure 5.5. Surfactant-mediated MALDI mass spectrum obtained when urine sample was analyzed with CHCA matrix and CTAB surfactant.

Another area of interest would be to further understand the chemical and physical mechanism of this method. Secondary-ion mass spectrometry (SIMS) is a surface analysis technique which analyzes the composition of a solid surface by sputtering a primary ion beam across a surface and collecting the ejected secondary ions [9,10]. These secondary ions are then analyzed via a mass spectrometer for their elemental, molecular or isotopic composition.

SIMS is an interesting additional tool to MALDI in the fact that one can acquire mass spectra from a given sample over a period of time which could lead to a useful “depth profile” [11-14]. Chapter 2 presented a depth profile experiment (Figure 2.11) that was generated by varying the number of laser shots on one location from the MALDI laser. This work proposed that the surfactant was concentrated near the top of the droplet

and thus it yielded a high ion intensity with a low number of laser shots. The analyte caffeine was also monitored and it seemed to be preferentially located near the top of the droplet. This is despite the fact both surfactant and analyte were in the presence of large excess of matrix.

Two years after the research in this thesis was started, a SIMS instrument was purchased in Earth Science and made operational at this university. Some very preliminary experiments were carried out at that time to determine if SIMS might be a possible route to explore depth-profiling experiments. First, sample surveys of caffeine, CHCA and CTAB were conducted individually to determine which ions of each molecule would be generated during SIMS. As an example, Figure 5.6 illustrates the mass spectrum obtained by monitoring those ions only due to a caffeine standard.

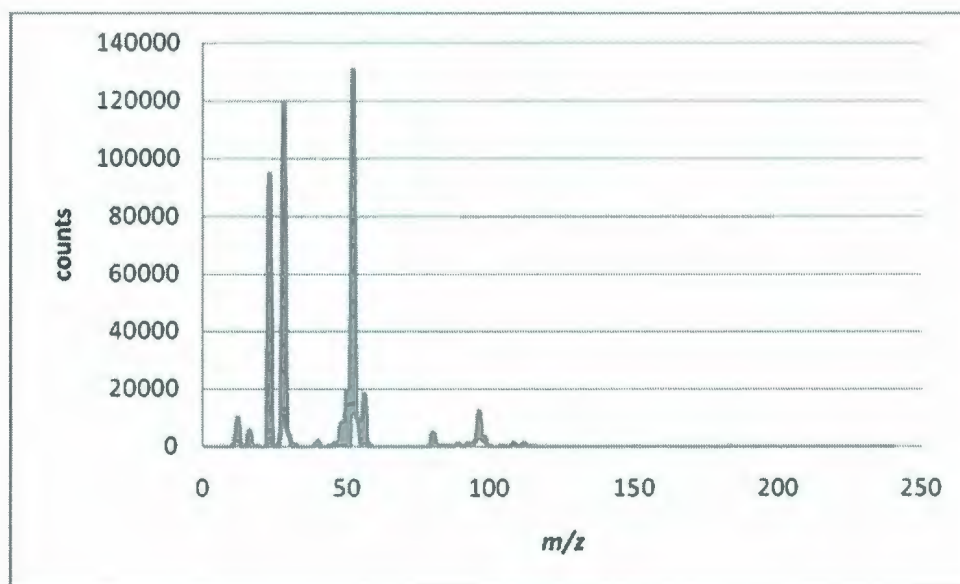


Figure 5.6. SIMS mass spectrum obtained during a survey scan of caffeine standard.

In a similar fashion, scans were completed for CHCA and CTAB and then desirable ions that were produced uniquely from each standard were monitored for mixed samples; ie. caffeine at  $m/z$  96, CHCA at  $m/z$  100 and CTAB at  $m/z$  225.

A real sample spot was deposited on a SIMS sample target and allowed to dry in the same fashion as samples on a MALDI target. The matrix : surfactant mole ratio was 500:1. This sample spot was then probed over a period of time to develop what is analogous to a depth profile. The results are given in Figure 5.7.

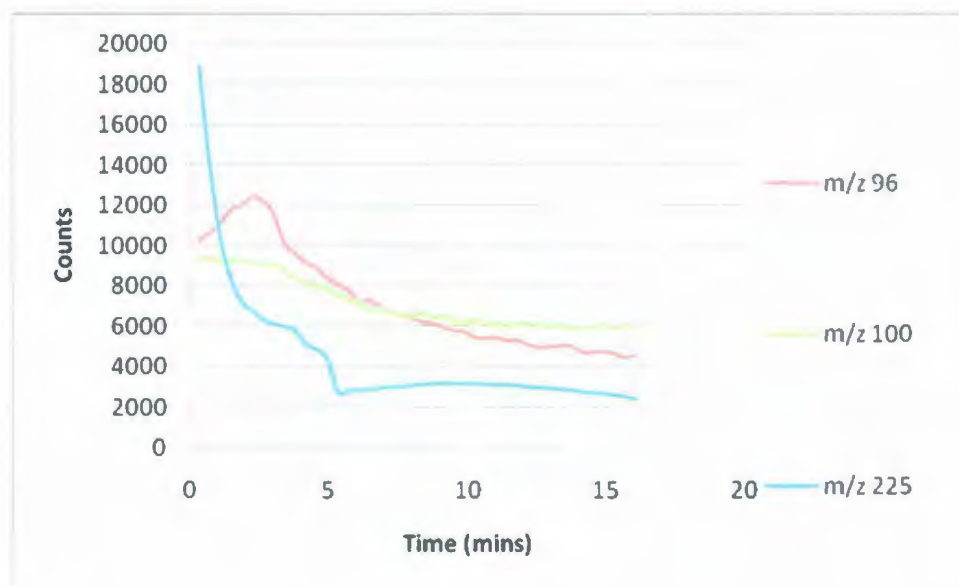


Figure 5.7. SIMS depth profile obtained by monitoring ions for caffeine, CHCA, and CTAB at  $m/z$  96, 100 and 225, respectively.

It appears that the CTAB ion at  $m/z$  225 yields the highest count within the first few minutes which indicates that it is more highly concentrated in the top of the droplet. The caffeine ion ( $m/z$  96), however, peaks in its ion count at about 3 minutes and then

drops off slowly in intensity. It is noted that for the first 5 minutes of this profile, the ion count for the caffeine ion is more intense than that of the matrix. These initial SIMS results support those of the depth profile experiment of this thesis (Chapter 2) which proposed that the surfactant and analyte were concentrated near the top of a droplet. Although preliminary, future research in this area should yield chemical information that is not possible by MALDI analysis alone. SIMS analysis could also assist in understanding sample proportioning and how surfactant-mediated MALDI functions.

It is believed that surfactant-mediated MALDI represents a major step forward for more easily (and routinely) analyzing small molecules. This phenomenon is not yet fully understood but major steps have been made with this thesis. Future applications will be beneficial to the scientific community and further research is likely to make this possible.

## 5.2 REFERENCES

1. Guo Z, Zhang Q, Zou H, Guo B, Ni J. *Anal. Chem.* 2002; **74**: 1637.
2. Grant DC, Helleur RJ. *Rapid Commun. Mass Spectrom.* 2007; **21**: 837.
3. Grant DC, Helleur RJ. *Rapid Commun. Mass Spectrom.* 2008; **22**: 156.
4. Grant DC, Helleur RJ. *Anal. Bio. Chem.* 2008; **391**:2811-2818.
5. Butterweck V, Schmidt M. *Wiener Medizinische Wochenschrift.* 2007; **157**: 356.
6. Ozen KP, Sahin F, Avci CB, Hisil Y, Gunduz C, Saydam G. *Turkish Journal of Hematology.* 2007; **24**: 127.
7. Sarris J. *Phytotherapy Research.* 2007; **21**: 703.
8. Jacobson JM, Feinman L, Liebes L, Ostrow N, Koslowski V, Tobia A, Cabana BE, Lee DH, Spritzler J, Prince AM. *Antimicrobial Agents and Chemotherapy.* 2001; **45**: 517.
9. Wittmaack K. *Vacuum.* 1982; **2**: 65.
10. Aoyagi S. *Surface and Interface Analysis.* 2009; **41**: 136.
11. Lee JW, Kim KJ, Kim HK, Moon DW. *Surface and Interface Analysis.* 2005; **37**: 176.
12. Fares B, Gautier B, Dupuy JC, Prudon G, Holliger P. *Applied Surface Science.* 2006; **252**: 7038.
13. Yamamoto Y, Shimodaira N. *Applied Surface Science.* 2008; **255**: 1479.
14. Kudriavtsev Y, Gallardo S, Villegas A, Ramirez G, Asomoza R. *Bulletin of the Russian Academy of Sciences: Physics.* 2008; **72**: 895.





